Use of Depth Perception for the Improved Understanding of Hydrographic Data

by

Runar Ostnes

A thesis submitted to the University of Plymouth

in partial fulfilment for the degree of

DOCTOR OF PHILOSOPHY

School of Earth, Ocean and Environmental Sciences

Faculty of Science

December 2005

Copyright Statement

This copy of the thesis has been supplied on condition that anyone who consults it, is understood to recognise, that its copyright rests with the author, and that no quotation from the thesis, and no information derived from it may be published without the author's prior consent.

Abstract

Use of Depth Perception
for the
Improved Understanding of
Hydrographic Data

by

Runar Ostnes

This thesis has reviewed how increased depth perception can be used to increase the understanding of hydrographic data. First visual cues and various visual displays and techniques were investigated. From this investigation 3D stereoscopic techniques prove to be superior in improving the depth perception and understanding of spatially related data and a further investigation on current 3D stereoscopic visualisation techniques was carried out. After reviewing how hydrographic data is currently visualised it was decided that the chromo stereoscopic visualisation technique is preferred to be used for further research on selected hydrographic data models. A novel chromo stereoscopic application was developed and the results from the evaluation on selected hydrographic data models clearly show an improved depth perception and understanding of the data models.

Table of Contents

List of Tables

List of Figures

Author's Declaration

At no time during the registration for the degree of Doctor of Philosophy has the author been registered for any other University award.

This study was financed through a Norwegian State Government grant governed through Ålesund University College

Relevant scientific seminars and conferences were attended. External institutions were visited for consultation purposes.

Peer Reviewed publications:

> Ostnes, R., Abbott, V., Lavender, S. (2004). **Visualisation Techniques: An Overview – Part 1.** The Hydrographic Journal. No. 113, July 2004.
>
> Ostnes, R., Abbott, V., Lavender, S. (2004). **Visualisation Techniques and Applications to Hydrographic Data – Part 2.** The Hydrographic Journal. No. 114, October 2004.

Submitted paper for peer review:

> Ostnes, R., Abbott, V., Lavender, S. (2005). **3D Hydrographic data presented by means of the Chromo stereoscopic technique.** World Maritime Technology Conference. London, March 2006.

Conferences attended:

> Hydro4, the 14th Biennial Conference of the International Federation of Hydrographic Societies held from 2 – 4 November 2004 Galway, Ireland

External contacts:

Kolbjørn Sæther, Head of Topographic Department, Norwegian Shell
Stein Wendel, Project Manager, Norwegian Hydro

Word Count: 37924

Signed *Kumar Okhro*

Date *10. FEB 2006*

Chapter 1: Introduction

Practically unchanged for several hundreds of years, hydrographic and nautical information has been presented on a 2 dimensional (2D) paper chart. With the advances in computer- and information technology, new techniques of presenting spatial data have emerged. In the "nautical world" electronic charts have revolutionised navigation and the collection of digital hydrographic data is increasingly efficient.

The International Hydrographic Organization (IHO) defines hydrography as (IHO, 1994);

> "The branch of applied science which deals with the measurement and description of the physical features of the navigable portion of the Earth's surface and the adjoining coastal areas, with special reference to their use for the purpose of navigation."

Computerised visualisation techniques are now developed in several fields, the aim of this research is to analyse their application to hydrography. The authors experience in navigation and hydrography led me to investigate visualisation of data in the water column and seabed, with particular reference to the resource exploration industry and bathymetric charting. Thus, the project will investigate visualisation techniques especially suited to improve the image depth perception and thus the presentation of hydrographic data, as for example coastal navigation, offshore subsea operations and analysis of complex datasets or other scientific purposes requiring improved spatial perception of the data. An accurate digital terrain model will be used to present depth information.

1.1 Aim and Objectives

The aim of the project is to investigate opportunities and benefits of improved visualisation of hydrographic data and develop a new technique founded on these.

The objectives are:

- To determine appropriate hydrographic datasets for a broad approach to marine navigation and other activities (e.g. electronic charting, interpretation and analysis

of a wider hydrographic dataset; tidal streams; fishery sonar or sounding) suitable for assimilation into available software.

- To compare available visualisation methods for suitability and opportunities (with due regard to digital stereoscopic viewing techniques such as auto-stereoscopy (free viewing); complimentary filters; alternating images and chromo stereoscopy).

- To discuss the results and select a sub dataset and scenario of particular interest to focus the project.

- To develop a novel visualisation technique for hydrographic data and analyse the effectiveness of the technique.

- To conclude with a discussion of developments in current techniques and future areas of development.

1.2 Thesis Overview

Chapter 2 investigates and discusses monocular and binocular visual cues and their effect on the perception of depth in an image. In chapter 3 visual displays and techniques are investigated. The advantages and disadvantages of 2D, three dimensional (3D) perspective and 3D stereoscopic displays are evaluated. In chapter 4 the 3D stereoscopic display techniques are explored and a possible technique for further work is identified. Current trends in the presentation and visualisation of hydrographic data is investigated in chapter 5 and based on this investigation the hydrographic data are classified into 5 different classes. The findings of chapter 4 and chapter 5 concludes that the chromo stereoscopic technique is a suitable and interesting technique for the further developmental and experimental work of this study and chapter 6 presents current colour theory and gives an in depth study of the chromo stereoscopic technique. Chapter 7 gives a detailed description of the chromo stereoscopic application development and in chapter 8 the chromo stereoscopic application is tested on hydrographic data models from each of the classes identified in chapter 5. The generated chromo stereoscopic effect and the amount of

increase in depth perception are then evaluated. Finally chapter 9 concludes the work and

gives recommendations for further work.

Chapter 2: Depth Perception and Visual Cues

Having established the ground for the investigation, this chapter reviews depth perception, and the visual cues used to enhance depth perception.

2.1 Depth Perception

A basic limitation of a conventional visual display is that the surface of the display screen is 2D whereas the natural world is 3D. In order to improve the visualisation of hydrographic data amongst other, it is necessary to represent depth or distance perception as a third dimension along the line of sight. Therefore, this section discusses the characteristics of human visual perception of depth and distance.

Depth and distance perception is achieved through the combination of several depth cues. The term, cues, has been utilized to formalize the specification of stimulus conditions for space perception (Carr, 1935). To distinguish between perceived and physical space the relation between distal stimuli and proximal stimuli is important. Any physical objects and scenes are distal stimuli where distal stimuli rouse our nervous system by patterns of energy (e.g. light energy, sound waves). Patterns of energy that reach and affect our sense organs are termed proximal stimuli and by projecting the energy patterns from distal stimuli onto a surface (e.g. a screen or retinal surface) the proximal stimulus patterns can be observed.

Hochberg (1978) defined a depth cue as a pattern of proximal stimulation that contains information about the spatial location of distal objects. Depth cues can be classified into two types: monocular and binocular. Monocular depth cues require the activity of a single eye; binocular depth cues require the use of both eyes. Pictorial depth cues are a subset of monocular depth cues and include linear perspective, relative size, known size, interposition, shadow distribution, aerial perspective, height in picture plane and gradient of texture-density (Hochberg, 1978; Hershenson, 1999). Motion parallax is also described

as a monocular depth cue and is also relevant in this review. Binocular depth cues include

accommodation, convergence and stereopsis (Hershenson, 1999).
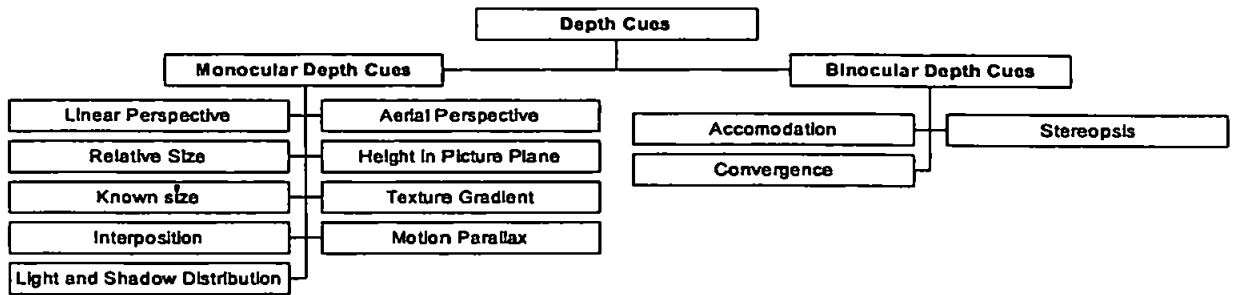
Figure 2.1: Block Diagram portraying the different Depth Cues in two classes, Monocular and Binocular Depth Cues.

2.1.1 Monocular Depth Cues

This section describes each of the monocular depth cues:

2.1.1.1 Linear Perspective

If the size of a distal object is fixed, the visual angle will be inversely proportional to the

distance from the object: this is called linear perspective or outline shape (Kantowitz and

Sorkin, 1983). A constant distance between points subtends a smaller and smaller angle at

the eyes as the points withdraw from the eye. For example, railway tracks appear to

approach each other (i.e., the retinal images of the lines converge) as the distance from the

eyes increases although they are parallel. Therefore, converging lines are a cue that they

are parallel and receding in depth (Wickens, 1992). Figure 2.2 shows the linear perspective

of a cube in relation to the horizon.
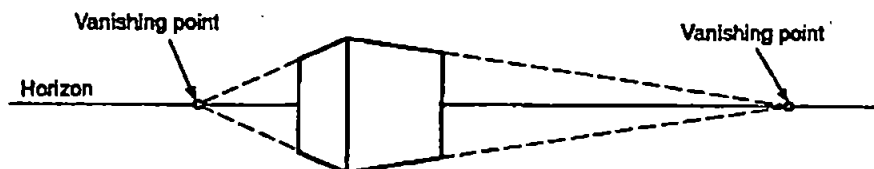
Figure 2.2: Linear Perspective of a Cube (Source: Hershenson 1999)

2.1.1.2 Relative size

Two similar shaped objects with different size will affect the relative perceived distance to the objects. The larger object will appear closer than the smaller. By comparing the apparent size of a distant object with that of a similar, much closer object, the relative distance of the distant object can be approximated (Hershenson, 1999). Relative size is also tied directly to linear perspective. In figure 2.2 the more distant side of the cube can be observed as relatively shorter than the nearest side.

2.1.1.3 Known size

We can use an object's known size to deduce relative depth. Figure 2.3 shows that if the object has known size (S) the distance (d) can be determined as (Coren, S., Ward, L.M., Enns, J.T., 1993):

$$d = \frac{S}{\tan \alpha} \qquad (2.1)$$

For example, a man is taller than a boy. However, if they produce the same size of retinal image, then the brain deduce the man is located farther away than the boy. This is often a weak or ineffective cue because cognitive factors influence the perceived distance.
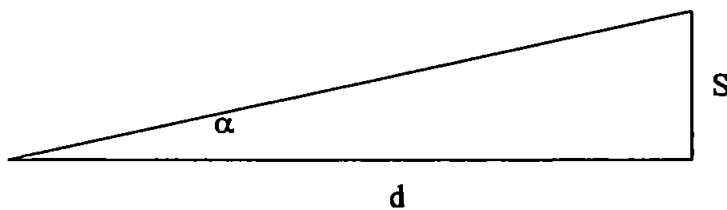
Figure 2.3: Distance from known size

2.1.1.4 Interposition

When a closer object (B in figure 2.4) interrupts the outline of a farther (overlapped) object (A in figure 2.4) it appears to be closer to the viewer. This is an effective depth cue, but it can only indicate which object is in front, not the distance separating them (Hershenson, 1999).
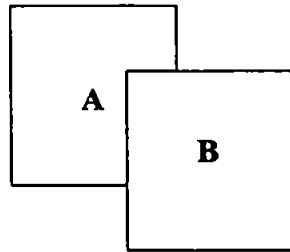
Figure 2.4: Interposition of Objects

2.1.1.5 Light and shadow distribution

Shadows provide some information about the orientation of the objects and their three-dimensional shapes (Ramachandran, 1988). Objects may appear to lie at different distances and have different dimensions as combinations of shadow and highlight change (Graham, 1965). If objects have a light source from one direction, they will have shadows unique to their shape and orientation.

2.1.1.6 Aerial Perspective

Atmospheric scattering of light by molecules (also termed Rayleigh scattering) causes de-saturation of an object's colour, resulting in a more bluish colour and less contrast. This affects the perceived depth of an object (Hershenson, 1999). Hence a more distant object will appear in a more bluish colour and have less contrast. Underwater this would be termed veiling light and is caused by the light scattering from water molecules.

2.1.1.7 Height in picture plane

An object's vertical position in the display can act as a depth cue. Farther away objects appear higher on the display. It is assumed that the ground plane is extended outwards horizontally to the horizon. An object on the same vertical height on the display is perceived to be at the same distance from the observer (Berbaum, K., Tharp, D., Mroczek, K., 1983).

2.1.1.8 Gradient of texture-density

A gradient is the rate of some measured property changing over a continuous, extended stimulus. The surface of most objects is likely to be covered with a reasonably uniform texture or pattern. When looking straight ahead at a textured surface, the gradient of texture-density is zero; as the slant increases, the gradient increases. The gradient of texture-density can provide precise and relatively unambiguous information about the distances and sizes of surfaces and objects in the world (Hochberg, 1978). The crossed squares in the front in figure 2.5 have the same dimensions as the ones placed in the back in the figure, but as they are located farther away from the observer they appear smaller, hence giving a finer texture.
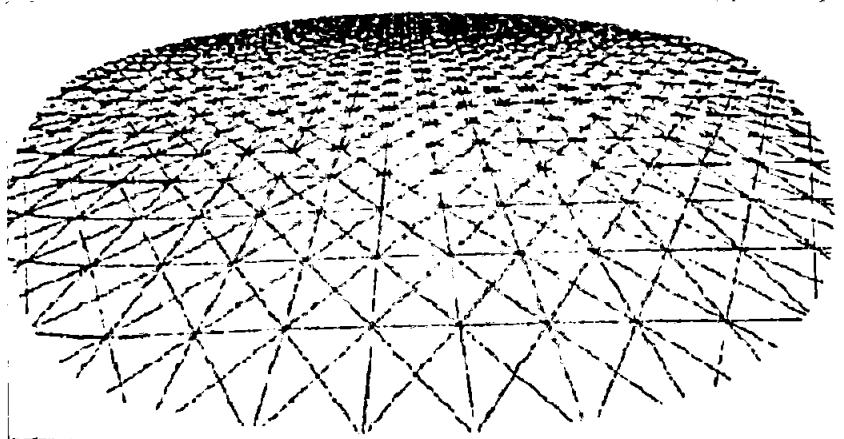
Figure 2.5: Texture density variation as function of distance (Source: Brassard, 1998).

2.1.1.9 Motion parallax

When a subject's eye moves with respect to the environment, or vice versa, there exists a differential angular velocity between the line of sight to an object (fixated) and the line of sight to any other objects. This relative lateral movement of objects at varying distances from the viewer is called motion parallax (Hershenson, 1999). By observing the amount and relative direction that a given image moves on the retina, its distance can be approximated (Clark, M., Jackson, P.L., Cohen, H.H., 1996).

2.1.2 Binocular Depth Cues

This section describes each of the binocular depth cues:

2.1.2.1 Accommodation

When adjusting the focal length of the eyes lens to bring objects at different distances into focus, a muscular strain is present in the ciliary body. This strain is called accommodation, and is effective up to a range of up to two metres (Coren et. al. 1993).

2.1.2.2 Convergence

The eyes are capable of convergence, in which both eyes turn inward toward the medial plane (Brown, 1965). The convergence is proportional to the convergence angle, γ in figure 2.6).
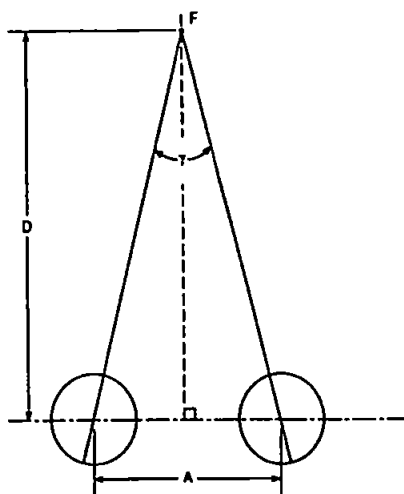
Figure 2.6: Convergence angle. γ = convergence angle, A = inter pupillary distance and D = distance to fixation point (Source: Hershenson 1999)

A large convergence corresponds to near objects and a slight convergence corresponds to far objects. The convergence angle γ varies with the distance to fixation point. The ocular muscles control the angle of convergence. The brain receives messages from the ocular muscles about the degree of convergence. By analysing the information received, the brain can approximate the angle of convergence (Hershenson, 1999). In this way, convergence may serve as a depth cue. A large convergence may lead to the response "nearer", while a

slight convergence may lead to the response "far-off".

2.1.2.3 Stereopsis

The human brain only interprets the monoscopic picture as 3D space (Kim, W. S., Ellis, S.

R., Tyler, M.E., Hannaford, B., Stark, L.W., 1987), and does not provide true depth

perception. Patterson and Martin (1992), reviewing the basic literature on stereopsis,

presented functional factors important for the design of stereoscopic display systems.

These factors include the geometry of stereoscopic depth perception, visual persistence,

perceptual interaction among stereoscopic stimuli, and the neurophysiology of stereopsis.

For the purpose of understanding the ability of humans to perceive stereoscopic depth,

section 2.1.2 reviews the geometry of stereoscopic depth perception presented by Patterson

and Martin (1992) and Chapter 3.2 further discusses stereopsis with regard to visual

displays.

2.1.2.4 Retinal Disparity and Horopter

Stereopsis is produced by horizontal retinal disparity, which results from an inter ocular

difference in the relative position of corresponding monocular images. Figure 2.7 shows

the concept of retinal disparity. F is the fixation point in figure 2.7. Object A produces

corresponding retinal points; point a in the left eye and point a' in the right eye. These two

points are equally distant from f and f' on the retina, respectively. Therefore, A has zero

disparity with respect to F. Object B in front of the horopter (described in the next

paragraph), however, produces non-corresponding retinal points; point b in the left eye and

point b' in the right eye. These two points are not equally distant from f and f',

respectively. Therefore, B has a certain amount of disparity with respect to F (Patterson

and Martin, 1992).

The horopter in figure 2.7, represented by the line through F (fixating point) can be formed

by connecting points, which give zero disparity. Any images from objects on the horopter

stimulate corresponding retinal points in the two eyes (Patterson and Martin, 1992). In other words, for every point on the retina of the left eye, there is a corresponding point on the right eye. Therefore, the horopter can be defined as the locus of all points, which have zero disparity (Hershenson, 1999).
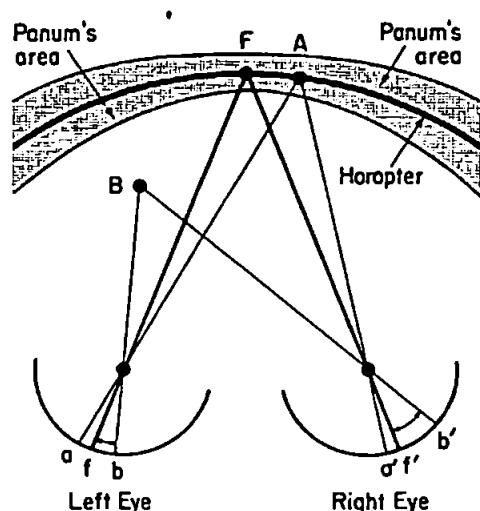
Figure 2.7: Longitudinal Horopter and Panums Fusion Area (Source: Patterson and Martin, 1992)

2.1.2.5 Crossed and Uncrossed Stereopsis

Disparity ahead of the horopter is "uncrossed" when an object falls in front of the horopter (point B in figure 2.7), and disparity behind the horopter is termed "crossed". From Figure 2.7, considering the spatial relationships of images within each eye's view (monocular), it is possible to make geometrical distinction between the crossed disparity and the uncrossed disparity. For crossed disparity, the disparate image is right of the fixation (i.e., b' is right of the b) in the left eye and left of fixation (i.e., b is left of b') in the right eye. For uncrossed disparity, the disparate image falls to left of fixation in the left eye and right of fixation in the right eye (Hochberg, 1978; Patterson and Martin, 1992).

Some people do not show good stereopsis for the crossed or uncrossed direction with brief exposure. Therefore, to improve the visual perception, it is necessary to provide prolonged exposure of stereoscopic stimuli (Patterson and Martin, 1992).

The crossed and uncrossed disparity above is defined based on the corresponding retinal points and horopter. Considering design applications, Patterson and Martin (1992) noted an important factor about the definition. In many applications, the horopter is considered to be placed on the surface of the display screen, then the disparity is defined based on the screen. This definition may create problems in designing accurate stereoscopic displays, because, if the viewer converges to a depth plane other than the defined horopter (i.e., the surface of the screen), the intended relevant disparities become inaccurate.

2.1.2.6 Panum's Fusional Area

Fusion is the perceptual process of blending the two corresponding images into a single image. The range in which the resulting disparity can be fusible (i.e. the area surrounded by the boundary of the limit of the disparity fusion) is called Panum's fusional area (see Figure 2.7). Diner and Fender (1993) explained this extended fusional area as:

> "There is a range of locations on the left retina such that an image formed anywhere within the range will fuse with an approximately matching image formed on a fixed location on the right retina. This process is reciprocal between the retinae".

Objects within Panum's area result in small disparities, which are fusible. Objects outside Panum's area result in large disparities, which are not fusible, producing double images. The limit of disparity fusion is the largest disparity that is fusible. Factors affecting the limit include stimulus size, spatial frequency, eccentricity, and temporal modulation of disparity information (Patterson and Martin, 1992). The disparity limit for fusion increases as the stimulus size increases (e.g. large disparity can be fused with large stimuli), and decreases as the spatial frequency increases. The disparity limit increases with eccentricity (i.e. degrees away from the fovea). The fovea is the most light sensitive area of the retina near its centre. This is the focal point of the retina, and vision is optimal in this part of the retina. The disparity limit also increases as the temporal frequencies of modulation decrease. These factors must be carefully manipulated in order to improve the binocular

fusion in designing stereoscopic displays.

2.1.3 Effects of Depth Cues

Figure 2.8 illustrates the effectiveness of the different depth cues depending on the distance

from the viewer. It is clear that the interposition, described as occlusion in the figure, is the

most powerful depth cue at any distance. Retinal disparity (binocular disparity in the

figure) is one of the most important depth cues at close ranges, gradually decreasing in

effect up to approximately 800 metres. The convergence and accommodation depth cues

have medium effect at close ranges and are reduced up to approximately 10 metres. The

binocular depth cues are most effective in the personal space (up to approximately 2

metres). The motion parallax depth cue is also powerful in the personal space.
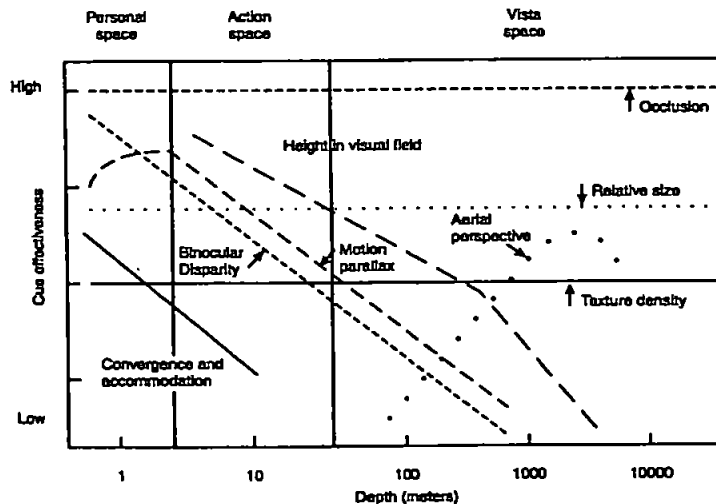
Figure 2.8: Depth Cue effectiveness as a function of distance (Source: Wickens and Hollands, 2000)

2.1.4 Discussion on Depth Cues

It is interesting to note that, except for interposition and stereopsis, most of the depth cues

discussed can not be applied to an orthogonal (i.e. parallel projection) 2D display format

(e.g., a plan-view) that conveys information in two dimensions at once. A perspective

display format can utilize most of the depth cues except for binocular disparity, which can

only be provided by using a stereoscopic display. Pictorial depth cues are patterns that can

occur not only in the picture plane but also in the proximal stimulation at the eye when

objects are scattered around in a three-dimensional landscape. Consequently, such indications of three-dimensional space are necessarily ambiguous. Therefore, any theory that bases our perception of space on pictorial depth cues must consider space perception to be ambiguous. Any pattern in the optic array is much more ambiguous than that. A number of different three-dimensional arrangements can produce the same proximal stimulus pattern at the eye (Hochberg, 1978). Binocular disparity in itself can be a powerful depth cue. However, it cannot be the basis of all space perception. Interestingly, it has been known that one-eyed individuals may show good depth perception, even at a very early age (Hochberg, 1978). At distances of less than 2 metres the binocular depth cue is one of the most effective depth cues.

Chapter 3: Visual Displays and Techniques

A visual display system with appropriate format can provide an efficient Man-Machine-Interface (MMI). Many applications of visual displays and their evaluations are reported in the literature about advanced teleoperation, aircraft cockpit display, and air traffic control displays as for example the different aircraft cockpit displays illustrated in the squares in figure 3.1 . There have been various types of information displays. These include traditional 2D plan-view, 3D perspective, and stereoscopic displays with or without visual enhancements.

This section reviews the basic literature related to 2D, 3D perspective (monoscopic) and stereoscopic displays. First, the basic geometry of 2D, 3D perspective, and stereoscopic displays is reviewed; factors that are considered to be important for the design of these displays are also reviewed. Second, for the purpose of evaluating 2D, 3D perspective, and stereoscopic displays, various experimental studies related to the application of 2D, 3D perspective, and stereoscopic displays are reviewed. Based on this review, a comparison of 2D, 3D perspective- and stereoscopic displays is presented.

3.1 Geometry of 2D and 3D Perspective displays

In order to understand the mechanism of visual spatial judgments, it is necessary to define relevant coordinate systems. Howard (1993) listed the basic frames of reference as:

> "An egocentric frame of reference is defined with respect to some part of
> the observer. Four major egocentric frames of reference include: a
> station-point frame associate with the nodal point of the eye, a
> retinocentric frame associate with the retina, a head centric frame
> associated with head, and a bodycentric frame associate with the torso.
> An exocentric frame of reference is external to the observer" (p. 338).

The evaluation of an egocentric display and three different exocentric displays in pilot navigational performance has been discussed by Prevett and Wickens (1994). Figure 3.1 illustrates the four different displays. The results of this study are presented in Section 3.3.
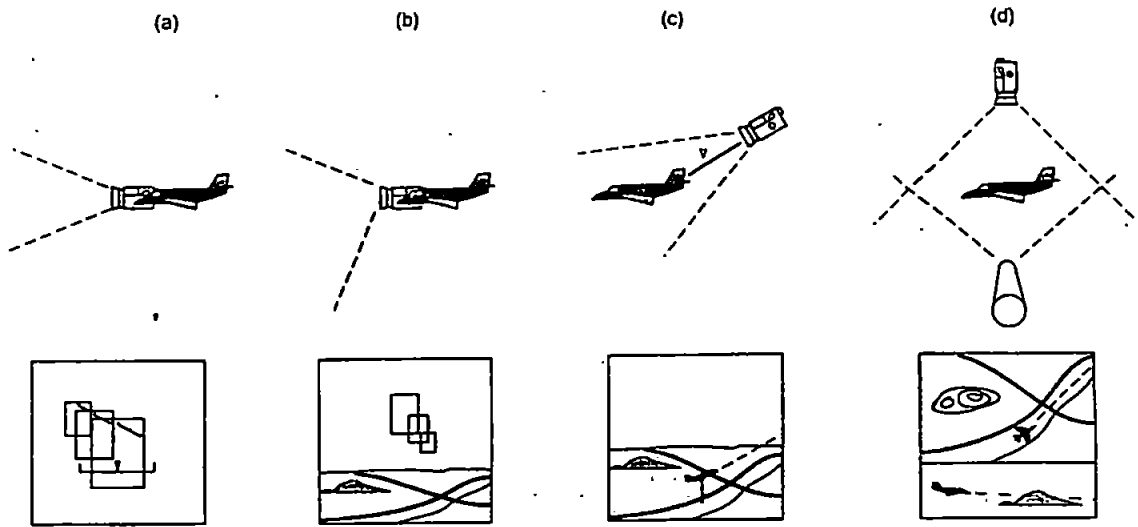
Figure 3.1: Four different display viewpoints from a pilot's point of view. (a) is fully ego referenced, (b) is ego referenced with expanded geometric field of view, (c) is an exocentric presentation (camera above and behind) the aircraft and (d) is a split display 2D co planar presentation. (Source: Wickens at. al, 1996).

3.1.1 Dimensionality

In addition to the choice of reference frame, the choice of dimensionality (2D vs. 3D) is important when presenting data on visual displays. A 3D perspective display can be achieved by projecting an object onto the view plane (projection plane) and then mapping the view plane onto the display screen. There are two methods to generate the perspective projection: the viewpoint-transformation and the object-transformation (Kim et al. 1993). In central projection, projection lines emanate from the centre of the projection (viewpoint). The intersection of the projection line with the view plane forms a projected image of an object. If the viewpoint is set at a infinite distance, a parallel projection is obtained.

A perspective projection can be obtained by setting the viewpoint at a finite distance. In general, two processes are performed to generate a perspective display:

(1)   Perspective projection onto the view planes and

(2)   Mapping of the view plane window onto the display screen.

Basic parameters specifying the view plane include the view reference plane, the view-plane normal, and the view-plane distance. The view reference plane is set near the object to be viewed (Ellis, 2000).

Wickens et. al. (1994, a) examined the effectiveness of 2D versus 3D perspective displays, which were designed to present a series of 3D data sets. In Wickens et. al.'s study, subjects required focused attention or integrative attention to complete the tasks. Focused attention requires low information integration, focusing in one dimension on only one object. Integrative attention, in contrast, requires high information integration, focusing on several objects across more than one dimension. Results showed that 3D perspective displays were superior to 2D displays for the task that required integrative attention.

Wickens et. al. (1994, b) presented a study that contrasted a 2D display, a 3D egocentric display (i.e. the display is presented from the perspective of the pilot sitting in the cockpit) and a 3D exocentric display (i.e. presented from the perspective of the pilot viewing the aircraft from a certain distance from the aircraft) for terminal area navigation.

They discussed the benefits and costs of 3D perspective displays, as compared to 2D displays. Based on this discussion, the use of 3D perspective displays requires less visual scanning effort than that of two (or three) orthogonal plan-view displays. Furthermore, a 3D ego-referenced display is capable of providing visual information that is congruent both with the pilot's view and control axes.

Costs associated with these benefits include "position distortion", "display resolution inconsistency", and "ambiguity along with line-of-sight" (Wickens et. al. 1994, b).

Figure 3.2 shows the geometry of a perspective display. The left figure is referenced to XYZ world coordinate system with the field of view (fov) from COP (Centre Of Projection). Q is projected into Q_p in the picture plane. If EYE is not located at COP, Qp is observed to be originating from somewhere along LOS (Line Of Sight). VRP: View Reference Point, VUP: View Up Vector, VPN: View Plane Normal, VPD: View Plane

Distance, D: Distance. The right figure is referenced to a left-handed $X_v Y_v Z_v$ coordinate system where Θ, Φ and Ψ are pitch, roll and yaw respectively.

Figure 3.2: The geometry of perspective displays (Source: Ellis, 2000).

Comparing 3D perspective displays and 2D displays, these costs will be presented in detail in Section 3.3.

3.1.2 Geometric, Symbolic, and Dynamic Enhancements

To understand how spatial information can be communicated, it is necessary to know the difference between spatial displays and spatial instruments. A spatial display can be considered as any dynamic, synthetic, or schematic mapping of one space onto another. A picture or a photograph is an example of spatial displays. A spatial instrument, however, is a special form of spatial display, which is enhanced by three different techniques: geometric, symbolic, and dynamic techniques (Ellis, 1993).

3.1.3 Geometric Enhancement

Manipulating the choice of projection can enhance the communicative purpose of a

- 18 -

display. Geometric enhancements, in general, are achieved through an appropriate transformation of the metrics of either the displayed space or of the objects (i.e., projection). The projection is chosen depending on the spatial property of importance. A typical factor for assuring geometric enhancement includes the choice of the position and orientation of the eye coordinate system used to generate perspective projection. Here, the selection of azimuth, elevation, field of view angle, and object distance is important (Ellis, 1993; Kim et al., 1987; Kim et al., 1993; Prevett and Wickens, 1994).

For example, Kim, et al., (1993) investigated the effects of varying visual parameters on a three-axis tracking task. The results showed that excessive elevation angle (near 0 degree or -90 degree), and azimuth angle (outside -45 degree to 45 degree) appeared to degrade the tracking performance (see Section 3.3 for details).

3.1.4 Symbolic Enhancement

Symbolic enhancements, in general, consist of objects, scale, or metrics combined into a spatial display to improve the communicated information (Ellis, 1993). A symbol itself is not an actual object. The overlaying of latitude and longitude lines on a map are good examples of symbolic enhancements. Using symbolic enhancements, for example, a target aircraft's position relative to pilot's own aircraft on a perspective display can be presented by drawing a horizontal grid at a fixed altitude below an aircraft symbol and vertical reference lines from the aircraft symbol to the grid (Bemis, S. V., Leeds, J. L., Winer, E. A., 1988; Ellis, 1993; Ellis and Hannaford, 1987; Endsley, 1995; Kim et al., 1993). In addition, if predictor lines showing future position are given, a second vertical reference line can be drawn from the ends of the predictor lines (Ellis et al., 1987). In these examples, the grid, vertical reference lines, and predictor lines are not actual objects. These lines are utilized to enhance the communicative purpose of displays.

3.1.5 Dynamic Enhancement

Dynamic enhancements are achieved through computational enhancements in shaping and

placing objects in interactive spatial instruments. Due to limited computational resources, the resources should be allocated to ensure that the image is computed in a timely and appropriate manner (Ellis, 1993). An example of dynamic enhancements can be found in the study of the interactive, proximity-operations and orbital-planning tools (Grunwald and Ellis, 1993). In this study, they noted that long delays could occur when the orbital dynamics were continuously updated while the operator manipulated the cursor to a new waypoint. The unworkable long delays associated with constant changes in waypoints were eliminated by computationally setting a waypoint.

3.2 Stereoscopic Displays

Utilizing the human stereoscopic vision capability of fusing two retinal images into one image, the stereoscopic display generates the powerful additional depth cue called stereopsis described in chapter 2.1.2. However, it should be noted that stereopsis has its limitation as discussed by Clark et al. (1996):

(1)   Stereopsis is effective only within short distances, about 200 metres or less;

(2)   Stereopsis provides information about distance between objects but cannot provide information about the distance between any objects and the observer; and

(3)   Using stereopsis, people tend to underestimate depth at close distance, and overestimate at far distance.

The stereoscopic display presents two slightly different views of an object on the display. In the 3D world, the view each eye receives is somewhat different because the two eyes see the object from slightly different positions. Differences in these views give two possible depth cues: double image (each eye contributes a different image of the far object when viewing near, and vice versa) and binocular disparity (Hochberg, 1978). The disparity is the difference between where a target falls on the right eye and the left eye and is discussed in detail in section 2.1.2.

The disparity can generate a powerful depth cue (Hochberg, 1978). This depth cue can be

obtained by taking two photographs of a scene (a stereoscopic picture pair, a "stereogram"), one from the position of each eye (65 mm apart on average), and presenting each picture to its appropriate eye, and then viewing such photographs with special devices called stereoscopes. The stereoscope is composed of two converging lenses and a supporting frame that simply separates right and left views. Different stereoscopic techniques will be reviewed in chapter 4.

Patterson and Martin (1992) discussed the geometry of binocular vision applied to stereoscopic displays. Figure 3.3 shows two drawings, one presented to the left eye and the other to the right eye, and their geometrical relationship to binocular vision.
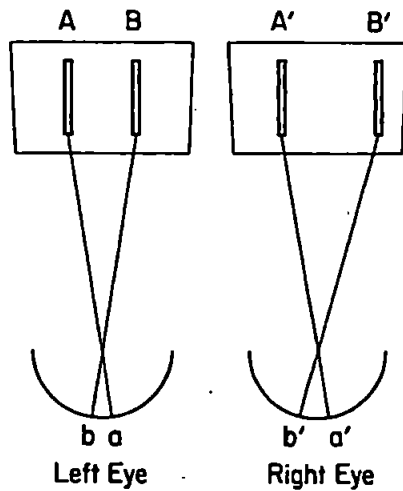
Figure 3.3: Top view depicting two drawings, one presented to each eye (Source: Patterson and Martin,1992)

In this figure, A and A' result in corresponding retinal points (a and a') while B and B' result in disparate retinal points. This difference between the two eyes and the binocular fusion cause depth perception (i.e. B appears behind A).

The magnitude of disparity in stereoscopic displays can be computed as:

$$r \text{ (degree)} = 57.3 * S/D \qquad (3.1)$$

where r is the disparity of visual angle (degrees), S is the separation between half-images (A and A' in Figure 3.3), and D is the viewing distance.

The magnitude of depth can be predicted as (Cormack and Fox, 1985):

$$d = S * D/(I + S) \text{ for crossed disparity} \qquad (3.2)$$

$$d = S * D/(I - S) \text{ for uncrossed disparity} \qquad (3.3)$$

where d = depth interval of the object predicted from the display, and

I = inter pupillary distance (average is 65 mm).

Patterson et al., (1992) performed a study to investigate several factors that affect depth

perception in stereoscopic displays. These factors include:

(1)   half-image separation magnitude (i.e., the magnitude of separation between the

         stimuli, one for the left eye and the other for the right eye),

(2)   direction of separation (crossed or uncrossed),

(3)   viewing distance,

(4)   stimulus size

(5)   extended versus brief stimuli: exposure.

Results showed that perceived depth in the crossed separation direction was frequently

close to the prediction, while that in the uncrossed direction was frequently less than the

prediction. The perceived depth was close to predictions for both the crossed and

uncrossed direction only for large stimuli for a long duration.

Other experimental studies regarding the applications of stereoscopic display and their

effectiveness (Kim, et. al., 1987; Kim, et. al., 1993; Yeh, 1992; Barfield and Rosenberg,

1995) are presented in section 3.3.

3.3 Evaluation of 2D, 3D perspective, and 3D stereoscopic displays

Chapter 3.3 will first evaluate 2D versus 3D perspective displays, then 3D perspective displays are evaluated against 3D stereoscopic displays.

3.3.1 2D versus 3D Perspective Displays

Ellis et al. (1987) conducted an experiment to compare a conventional 2D plan view with a 3D perspective air traffic information display for an identical traffic situation. The subject's task was to decide if an avoidance manoeuvre was needed while monitoring the traffic display. He or she was then to select an avoidance manoeuvre if needed. In this study, no significant difference in manoeuvre decision time between the conventional and the perspective display was found, except in a head on traffic situation where decision time with the perspective display was much shorter. The mean number of selecting avoidance manoeuvres between the two display situations was not significantly different; however, more manoeuvres with a vertical component were found using the perspective display. Bemis et. al. (1988) performed a similar experiment to evaluate operator performance on a perspective and a conventional naval tactical display. The display provided the operator with relative position information on both enemy and own aircraft. Results showed that operators had fewer errors and shorter response times for selecting a closest interceptor when using the perspective display. However, no significant difference in detection latency was found, although the errors in detection were reduced using the perspective display. Prevett and Wickens (1994) compared pilot navigational performance using a 2D planar display (consisting of a 2D map and profile view) with four 3D perspective displays. The four perspective displays included an egocentric and three exocentric displays which were varied with viewpoint location distances (near distance exocentric, middle distance exocentric and far distance exocentric; see Section 3.1). The results showed that the egocentric perspective display was better in a tracking task than the others including the

planar display, while the middle distance exocentric display resulted in better performance in the global awareness tasks than the others. This advantage of the perspective displays was varied with the viewpoint location distances. However, these results support the advantage of perspective displays over planar displays. In these studies, the use of 3D perspective displays resulted in relatively better performance than for 2D displays. Forty aviators were tested and the results were measured by statistically evaluating data from questionnaires for the global awareness performance and vertical and lateral deviation from flight path was recorded to measure the tracking performance.

However, this superiority of perspective displays can be degraded by the following factors as discussed by Wickens et. al. (1994, b):

(1)   Position distortion - The perspective display presents the world from a non-orthogonal angle (e.g., views other than looking straight forward or down). Therefore, certain portions of the world will be covered more predominant than others. The potential remedy of this problem is to widen the field of view. However, such a technique produces the distortion of the real position;

(2)   Display resolution inconsistency - Distances not orthogonal to the line of sight will be presented with less resolution than those orthogonal to the line of sight; and

(3)   Ambiguity along with line of sight - The representation of a 3D world (or objects) on a 2D display surface is inherently ambiguous.

In another study, Nemire et al., (1994) performed an experiment to investigate the effect of a pitched optic array on the perception of gravity-referenced eye level (GREL; the eye level is decided by the reference plane perpendicular to the direction of gravity, Stoper and Cohen (1993)) in a virtual environment display. In this experiment, subjects were asked to indicate GREL while viewing three-dimensional boxes which were generated by different independent measures including box pitch angles (5 levels) and optic structures (simple box with no grid, transverse partial grid, longitudinal partial grid, and full grid). They

found that the judgment of eye level was biased significantly by the longitudinal, but not the transverse structure. The result indicates that the longitudinal information is actually more functional than others in the perspective displays.

3.3.2 3D Perspective versus 3D Stereoscopic Displays

A comparison of 3D perspective and 3D stereoscopic displays in a simulated tracking task has been presented by Kim et. al. (1987). Kim et. al.(1993) performed two experiments to investigate the effects of varying visual parameters on a three-axis tracking task. In the perspective parameter experiment, four perspective parameters were manipulated using a monoscopic perspective display. These parameters were azimuth, elevation, field of view angle and object distance. In the visual enhancement experiment, three visual enhancement depth cues (horizontal grids, vertical reference lines and stereoscopic disparity) were used with both perspective and stereoscopic displays. Independent measures were normalized root mean square (rms) tracking errors.

The results showed that excessive elevation angle (near 0° or -90°), and azimuth angle (outside -45 ° to 45 °) appeared to degrade tracking performance. The vertical reference lines resulted in significantly improved tracking performance with the perspective display. However, this was not the case for the horizontal grid. The stereoscopic display resulted in lower tracking error over all visual conditions. However, the perspective display with appropriate visual perspective parameters (such as 0° to 45 ° azimuth angle, -45 ° elevation angle) and visual enhancement depth cues (such as vertical reference lines) resulted in equivalent performance as compared with the stereoscopic display.

Kim et al., (1993) also reported the results of a similar experiment performed for a three-axis pick-and-place task. The effects of varying visual parameters reported for this pick-and-place task were identical to three-axis tracking task experiments (Kim et al., 1987). Yeh (1992) investigated spatial judgments (relative depth and altitude) with monoscopic and stereoscopic presentation of perspective displays. The results showed that the presence

- 25 -

of binocular disparity in the stereoscopic view improved the spatial judgment. In another study, McLean et al., (1994) compared a 3D perspective video display (one camera view without visual enhancement) with a stereoscopic video display for a peg in a hollow task. The results showed that the stereoscopic video was superior to the 3D perspective video. In these studies, visual enhancement cues such as vertical reference lines were not provided. Therefore, the performance benefits of stereoscopic displays may be decreased with such enhancement cues as presented by Kim et al.(1993). However, Yeh (1992) argued that such enhancement cues are not natural in perspective display formats and may cause unacceptable display clutter. He also discussed the problem associated with perceptual distortions in perspective projection resulting from the enhancement cues.

The benefit associated with using stereoscopic displays was further reported by Barfield and Rosenberg (1995). They performed an experiment to evaluate judgments of relative elevation and azimuth angle between the reference and target cubes using either a perspective or stereoscopic display. Results showed that the stereoscopic display was superior to the perspective display (monoscopic) in judging the relative elevation. However, the judgments of relative azimuth angle were not improved by the use of the stereoscopic display.

3.4 Discussion on visual displays

Studies performed in the mid 1990's comparing 3D perspective with 2D displays show that the use of 3D perspective displays results in relatively better performance than that of 2D displays. More recent and relevant studies are not found in literature searches.

However, Prevett and Wickens (1994) note that previous studies comparing 2D with 3D formats have not provided 2D displays with a fair comparison, presenting vertical information (e.g., altitude data) in 2D display symbolically or digitally (e.g., data tag), rather than in analogue form. The perspective display, in general, provides poor control in the vertical dimension, while providing better control in lateral dimensions, as compared to

2D displays (Wickens et al., 1994).

Other studies comparing 3D perspective with stereoscopic displays show that monoscopic displays, if provided with appropriate visual perspective parameters (such as 0 to 45 deg. azimuth angle and -45 deg. elevation angle) and visual enhancement depth cues (such as vertical reference lines) are nearly equivalent to stereoscopic displays (Kim, Tendick and Stark, 1993). In addition, the advantage of stereoscopic displays over 3D perspective displays may be reduced by disruption (vibration and poor viewing conditions) and the cost associated with implementing the stereoscopic displays (Wickens, 1992). However, the enhancement cues added in perspective displays may be unnatural and cause unacceptable display clutter. Furthermore, the problem associated with perceptual distortions in perspective projection resulting from the enhancement cues remains unproved (Yeh, 1992; Wickens et al., 1994). Chapter 2.1 3 establishes that the binocular depth cue is one of the most effective clues at close ranges. Including this stereoscopic depth cue in the presentation on a computer display is hence of significant value as the display is part of the personal space.

Chapter 4: 3D Stereoscopic Display Techniques

3D effects and depth perception in a display system can be achieved in a number of different ways. The simplest method is to apply one or several of the monocular depth cues discussed in section 2.1.2. In order to establish stereoscopic effects, to further enhance the depth perception, a binocular depth cue has to be applied. The left eye image and the right eye image of the stereo pair have to be channelled to the respective eye. An exception is the chromo stereoscopic technique described in 4.1.7 that only needs one colour-coded image. A large number of stereoscopic display techniques have been developed over the years, the principal ones reviewed in this chapter. They can generally be classified as stereoscopic and auto-stereoscopic techniques. The major distinction between stereoscopic and auto-stereoscopic display techniques is that the former requires the observer to use some form of viewing aid whereas the latter provides free viewing.

The advancement in stereoscopic display technology continues as a result of both computer power and display technology which have evolved by orders of magnitude over the last decades. The latest stereoscopic display techniques include virtual retinal displays, which project the stereo pair directly onto the eye's retina and the latest auto stereoscopic techniques include electro holography and complete virtual environments with immersive large format environments like the CAVE (CAVE Automatic Virtual Environment). The scope of this section is to give a short description of the current and most accepted stereoscopic and auto stereoscopic techniques, and a brief discussion on different display characteristics. Finally a technique suitable for further work will be selected. This technique will be selected based upon the novelty of the method, the feasibility to implement and the usability in an operational environment. The suitability of the method will be further examined in the discussion of how digital hydrographic data is presently presented at the end of chapter 5, and a final decision on which method is best suited for further work will be made.

4.1 Stereoscopic Display Techniques (Aided Viewing)

While viewing stereoscopic displays the observer normally wears glasses that may have near complimentary colour filtered lenses, polarised lenses or lenses that occlude one eye sequentially in order to channel each of the images in the stereo pair to their respective eyes. Figure 4.1 gives an overview of the stereoscopic techniques described in this text.
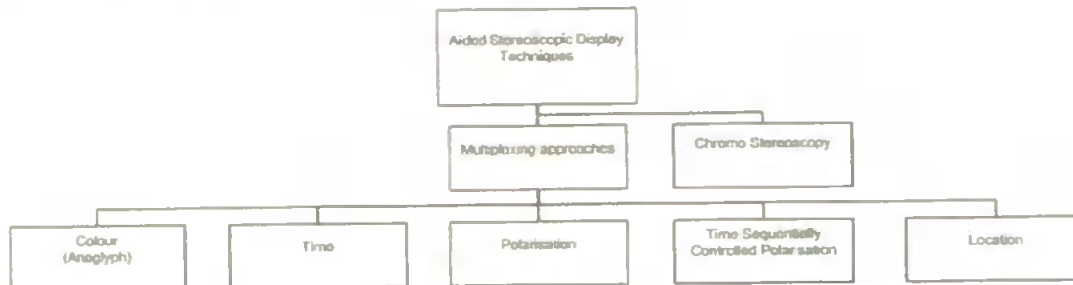
Figure 4.1: Block diagram describing stereoscopic display techniques

4.1.1 Colour Multiplexed (Anaglyph)

Colour multiplexing or anaglyph is perhaps the most familiar stereoscopic technique. The technique is widely used to display stereoscopic images in books, movies and on the Internet. The anaglyph consists of a stereo pair with near complimentary colours, red and green or blue are the most commonly used. The two images in the stereo pair are transparent. The observer views the stereoscopic image through a pair of near complimentary filters corresponding to the colours used in the stereo image. Each filter will exclude the corresponding image in the stereo pair and in that way give the required separation of the left and right image for stereoscopic viewing (Diner and Fender, 1993).
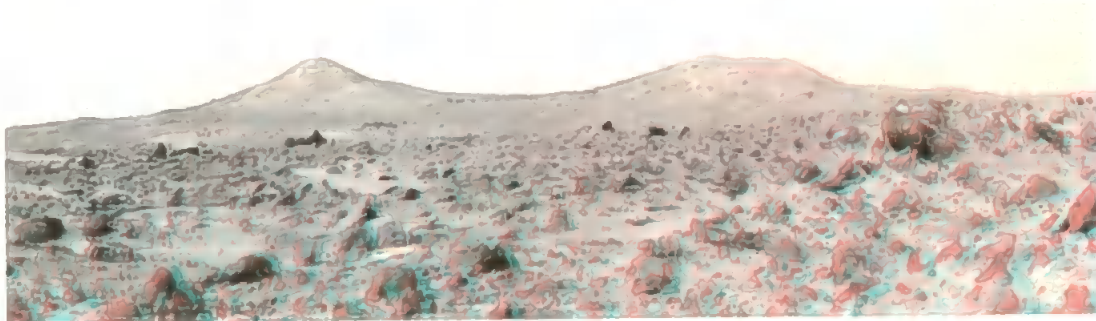
Figure 4.2: A typical anaglyph of the Terrain on Mars, where the near complimentary images are merged.
(Source: National Aeronautics and Space Administration (NASA))

The advantages of this method are that it is inexpensive to implement, it can accommodate for multiple observers and the stereo image will be of the same resolution as the display. Translation of the anaglyph onto hard copy (e.g. paper) is also an uncomplicated process. The method has been limited to produce monochrome (black and white) images, however resent developments have shown that a limited colour rendition in the stereo image is possible (Wei et al., 1998).

Colour rivalry occurs under some instances when an illuminated area of one colour presented to one eye appears to rival a similar area of another colour presented to the other eye. Colour rivalry limits the application of the anaglyph method. Another restrictive phenomenon is transitory shifts in the chromatic adaptation. The viewer will experience unpleasant after effects such as headaches and nausea from wearing the anaglyph filters. The hue of a perceived colour is dependent on the adaptation of the viewer. If the viewer has been subjected to high intensity red light (e.g. anaglyph filter) the effect on the viewer will be that red colours will appear to shift in hue towards the complimentary colour cyan. (Pastoor and Wöpking, 1997). Stereo crosstalk is a significant problem; this is when the image meant for one eye is faintly visible to the other eye. The image becomes blurred as a phenomenon called ghosting is created. Crosstalk can create difficulty in fusing the two images together. Viewed without the colour coated glasses, the image will appear blurred and interpretation is impeded.

4.1.2 Polarisation Multiplexed

In order to separate the left and right image this method applies linear or circular polarization techniques. Polarization glasses are used in combination with orthogonally polarised images presented on two displays. In the two display setup, the displays are covered with orthogonal polarisation filters and arranged at a 90 degrees angle. A beam splitter (semi reflector) is used to channel the left and right images to the observer. The observer is wearing appropriate polarisation glasses to separate the images. This

stereoscopic technique is still widely in use, however the hardware requirement makes the technique more expensive compared to comparable techniques (Lipton, 1997). An alternative method to combine the stereo images is to interlace the images on the display by row or column; this method will only require a single display. Cross polarization of alternating areas of the display will separate the images. Common to the multiplexing techniques in general is that the observer is able to view the stereo image at full colour and full resolution, the technology is becoming fairly inexpensive and the technique provides for multiple viewers, each with their own headset. The multiplexing methods are also compatible with non-stereoscopic presentations, unlike anaglyphs, which distort the colour perception of other presentations. Polarisation multiplexing has the disadvantage that the efficiency or transmission is poor; the intensity of the light emitted from the display is low. With a light intensity loss of up to 70% the image will appear dark. The interlacing techniques will reduce the resolution by 50%. To maintain an acceptable, flicker free presentation, the frame rate should not decrease below 120 Hz (Macdonald and Lowe, 1997).
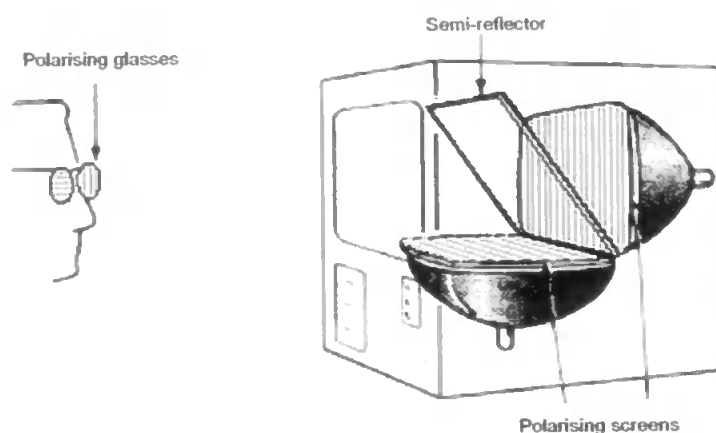
Figure 4.3: A two–display polarisation multiplexed arrangement (Petrie, G., 2001)

4.1.3 Time Multiplexed

By displaying the left and right eye images alternately at high speed (50-60 Hz / image) on a single display it is possible to obtain stereoscopic effect. The observer must wear electro-

optical shutters, one for each eye, the shutters are synchronised with the alternating images on the display. When the left eye image is displayed, the left eye shutter is open allowing the left eye to observe the image; the right eye shutter is closed.

It is the human visual system's ability to store and merge stereo pairs with a time lag of up to 50 ms. that makes this technique possible (Hershenson, 1999). To avoid display flicker, the technique requires that the display refresh rate is relatively high, more than 60Hz (Diner and Fender, 1993), and closer to 120Hz for reasonable quality, similar to the requirements of the interlacing polarisation multiplexed method.

Figure 4.4:   A typical time multiplex stereo kit with shutter glasses, synchronisation cable and software (Source: Stereographics Corporation)

The temporal resolution will be halved, as each eye only perceives the image half the time. This results in a reduction in the display brightness. The relatively heavy glasses may be cumbersome to wear. More advanced work bench systems such as the Fakespace Immersadesk R2 (Fakespace Labs Inc.) are also available. These systems are portable and equipped with active shutter glasses, however the cost of obtaining such systems is a major disadvantage.

4.1.4 Time Sequentially Controlled Polarisation

This method combines the polarisation - and time multiplexing techniques by displaying

alternating polarised images to the viewer. The display screen is covered with a Liquid Crystal (LC) layer, which functions as a polarizer. The alternating left-eye and right-eye images on the display have different polarisation patterns (clockwise / anti-clockwise). The observer wearing glasses with appropriate polarisation for each eye is able to separate the left and right image. The key advantage of this method is that the observer only needs simple, inexpensive and lightweight polarising glasses that require no extra synchronisation devises (Pastoor and Wöpking, 1997). The main disadvantage of this technique is also display flicker and reduction of display brightness due to halved temporal resolution.

4.1.5 Location Multiplexed

In photogrammetry, analytical stereo plotters have been widely used. These instruments are very complex, expensive and require special skills to operate. A photographic stereo pair is placed on the workbench and the left and right images are separately channelled to the viewer's corresponding eyes through a complex arrangement of optics.
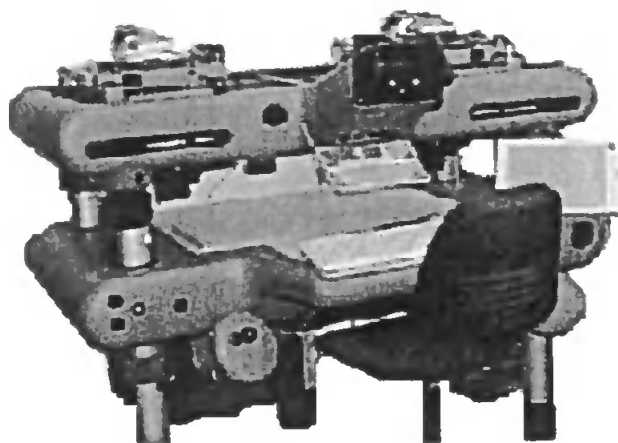
Figure 4.5: The LH Systems AM 2000 analytical stereo plotter (Source: LH Systems)

These systems provide high precision and high resolution stereo images, however they are cumbersome to use and provide only a fixed perspective image.

A more familiar and simple location multiplexed technique is used by the View-Master®
stereoscope that many children have used as a toy for decades.
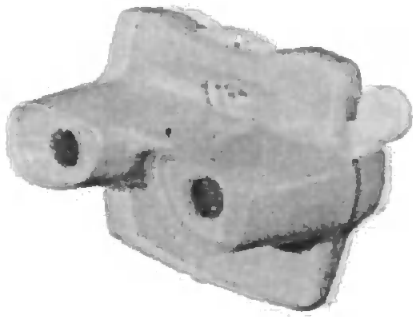
Figure 4.6: The View-Master® stereoscope (anaglyphic presentation)

4.1.6 Head Mounted Displays

Head Mounted Displays (HMD) which is a further development of the location
multiplexed technique is increasingly used in Virtual Reality (VR) and stereoscopic
visualisation. An HMD consists of a miniature display system, (two displays, one in front
of each eye) and optics to focus the display at a comfortable distance in front of the eyes.

Figure 4.7: A typical Head Mounted Display. (Source: Wearcam)

The HMD can simply be a pair of goggles or a full helmet. The viewer's immediate

surroundings are usually occluded by the HMD, giving a feeling of total immersion in the displayed scene. A head-tracking device is included in the system allowing the system to respond to head movements. This function is particularly important when the observer is immersed in a VR environment where changes in viewing direction will alter the picture displayed (Shibata, 2002). One of the major constraints of HMDs is their limited volume of activity due to cabling, and overall weight. The considerable amount of computing power required for the displayed image to be updated in accordance with the head movement may introduce a delay in the displayed image, this delay has a tendency to cause motion sickness in HMDs. "See-through" HMDs are also developed, to free the observer from immersion, and is particularly suited for augmented reality applications where the stereoscopic image is merged with the real world. The disadvantage of see-through HMDs is that when the observer focus on the displayed image the background will be diffused. To free the observer from wearing HMDs, a further development of the location multiplexed technique, Binocular-Omni-Orientation-Monitor (BOOM) display, was developed in the late 1980's. Two miniature displays are installed in a casing attached to an arm.

Figure 4.8: BOOM Display on arm with 6 degrees of freedom.
(Source: Fakespace Labs Inc.)

4.1.7 Chromo Stereoscopy

Einthofen (1885) found that it is possible to place objects with different colours at different depths of view when the objects are placed at the same distance (chromo stereopsis). In the early 1990s researchers found renewed interest in this method to create a stereoscopic effect from colour coding images. However, later the interest for this method has diminished. The principle of chromo stereoscopy is relatively simple. As white light is refracted through a glass prism, it is separated into the colours of the visible spectrum; the different colours have different refraction angles (Figure 4.9).
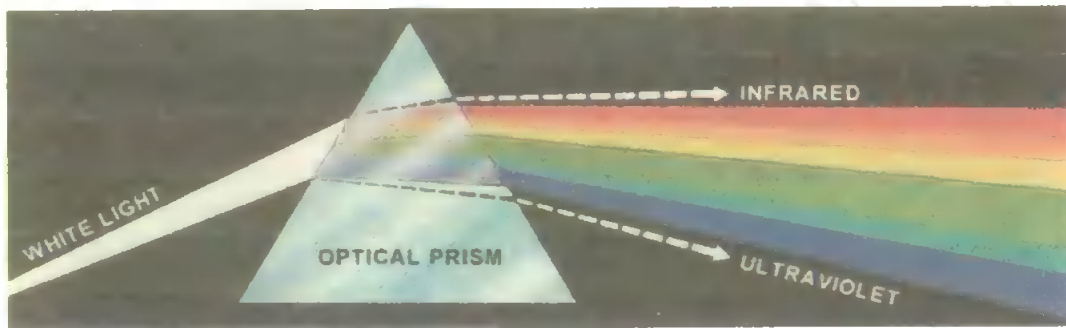
Figure 4.9: White light refracted through a glass prism. (Source: University of Toronto)

A red object has positive chromo stereopsis and will appear closer than a blue object at the same distance. By viewing a colour coded image with double prism eyeglasses to enhance the chromo stereopsis effect, the required depth perception is achieved. Figure 4.10 illustrates the effect. When the observer is wearing single prism glasses the object appears closer to the observer than desired, double prism glasses has been developed to place the image at the correct distance from the observer (Toutin, 1997). The main disadvantage by using the chromo stereoscopic technique is that it is not possible to view the image in its true colours. However, the chromo stereoscopic image is easy to translate to different mediums such as paper, overhead projectors, and to non-stereographic presentations. This is the only stereoscopic technique where only one image is required for stereoscopic effect; this will increase the readability of the image in non-stereoscopic presentations, increase

resolution and decrease the need for extra computer power and advanced display technology.
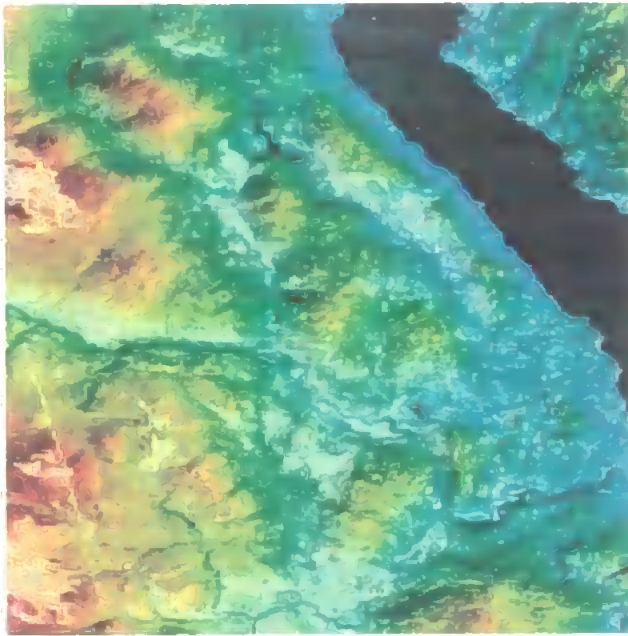
Figure 4.10: An example of a Colour Coded Image prepared for Chromo Stereoscopic viewing using Chromadepth^{TM} spectacles (Source: Toutin, 1997)

4.2 Autostereoscopic Display Techniques (Free Viewing)

As stated earlier, the research and development of different auto stereoscopic techniques are proceeding at an ever-increasing speed. Figure 4.11 summarizes the more common current techniques in autostereoscopy. Pastoor and Wöpking (1997), Börner (1999) or Okoshi (1976) give more detailed descriptions.
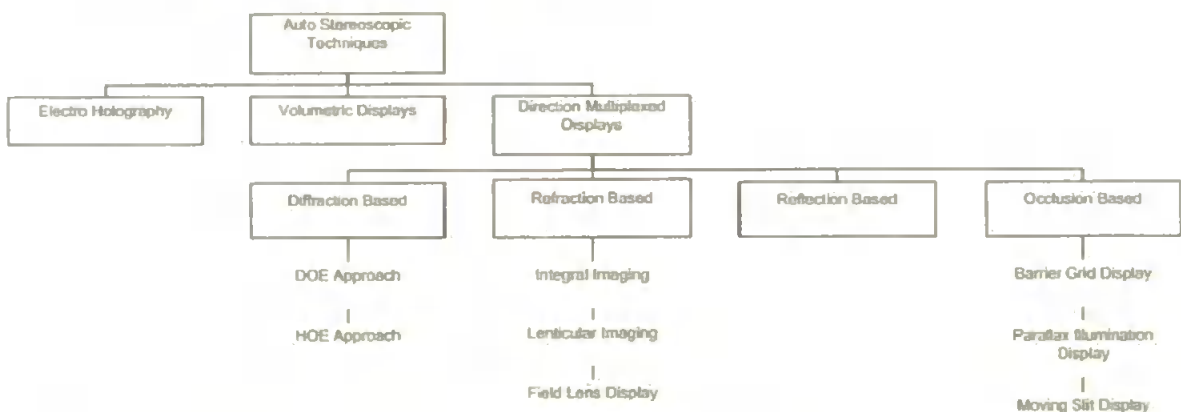
Figure 4.11: Block diagram summarizing current auto stereoscopic techniques

4.2.1 Direction Multiplexed Displays

Direction multiplexed displays are the most common auto stereoscopic displays and are most compatible with computer graphics. The observer directly views the same display area with both eyes. The left eye image is presented only to the left eye and the right eye image is presented only to the right eye. The difference in viewing angle is caused by the separation of the eyes, and vertical bars or lenses are built into the display, permitting or blocking certain parts of the underlying display from view of certain angles from the display. The images are interlaced in a way comparable with lenticular or barrier strip stereograms.

Several techniques based on the physical principles of diffraction, refraction, reflection and occlusion have been developed (Pastoor and Wöpking, 1997). The most established refraction based method is lenticular imaging.
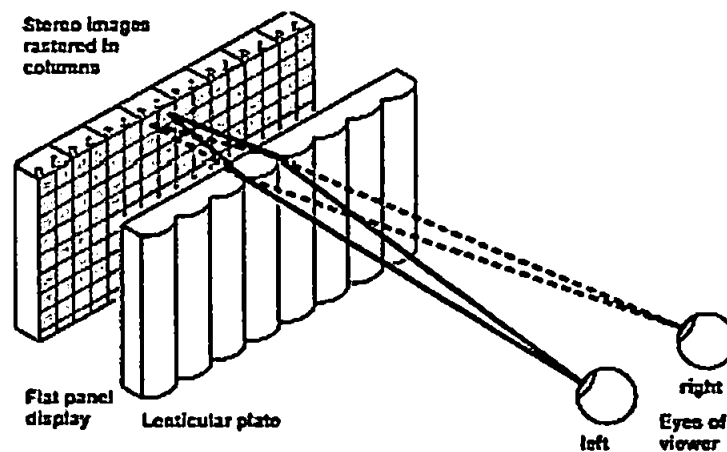
Figure 4.12: Principle of the lenticular imaging technique. (Source: Börner, 1999)

An array of long narrow lenses (lenticules) is built into the display screen as shown in figure 4.12. Each lens focuses on the image information located behind it and directs the light in different directions (Börner, 1999). In order to view the stereo image, the observer must be located in particular locations relative to the display (stereo zones). If not the stereo image may be blurred or the stereoscopic effect may be lost. However, certain lens arrays will allow more than one observer to view the stereo image. The main disadvantage

of this technique is that the display resolution is effectively halved. Interpretation of the image without the lenticular plate is also inhibited.

Figure 4.13: Lenticular image interlaced stereo pair (Source: Börner, 1999)

4.2.2 Electro-Holography

Electro Holograms store wave front information about an object as microscopic interference fringes during the holographic exposure process. When the developed hologram is illuminated the interference fringe pattern acts as a complex diffractive lens that reconstructs the object light's direction and intensity (Benton, 1985).

Progress in electronics, electro optics and computers has renewed the interest in holographic techniques to present stereographic images. However, the extremely high display resolution requirement and the enormous amount of information needed to represent a holographic image is a major challenge for the research establishments, regarding display technology and data transfer, for this technique to develop further (Trayner and Orr, 1996). Sato (2001) gives an overview of recent research development on the topic of electro-holography.

4.2.3 Volumetric Displays

Volumetric displays work by filling a volume of space with image points, effectively a 3D pixel (Voxel) display. The image points originate at a real point in space and hence take up a three-dimensional volume. A large variety of volumetric display techniques such as fibre optics, lasers, oscillating screens or stacking transparent LCD screens have been developed. The volumetric display image is visible from a wide range of viewpoints, even permitting a viewer to walk around the display. However, the volumetric displays are non-occluding, i.e. they have an appearance of transparency (Favalora, G. E., Napoli, J., Hall, D. M., Dorval, R. K., Giovinco, M. G., Richmond, M. J., Chun, W. S., 2002). Occlusion is an important depth cue, often stronger than even stereopsis. Consequently volumetric displays are not a suited technique to display photo realistic images. The amount of information these images are able to represent is also limited because the viewer is confused by the absence of hidden surface elimination. Another disadvantage has been that the plotting of the images are not sufficiently fast to produce the points on an 3D object. Hence volumetric displays have been limited to wire frame rendering presentation.

Figure 4.14: An example of a volumetric spherical display. A pink fighter airplane is visualised above the green terrain. In the right picture the fighter plane is visualised in side view. (Source: Actuality Systems Inc.)

4.3 Discussion on 3D stereoscopic display techniques

The majority of the auto stereoscopic techniques are still at a developmental stage; they are expensive and require a vast amount of computer power to produce a 3D image (Javidi and Okano, 2002). The lenticular imaging technique is currently the most accessible. This technique does however have limitations, the most significant being the reduction of the display resolution by 50%, and interpretation of the image without the lenticular display is inhibited.

The aided viewing techniques are as earlier described more established and is presently, to some extent, employed in fields of scientific visualisation such as medical imaging, photogrammetry and geological imaging in the petroleum exploration industry. The polarisation and time multiplexing techniques are most common (Macdonald and Lowe, 1997). The major disadvantages such as, the light intensity loss, flicker and loss in resolution will improve as display technology and computing power develops, making these techniques well accepted for scientific visualisation. The further development of HMDs will also gain from increased computer power and display technology, eliminating most of the present disadvantages in this technique. The technique will probably be less expensive over time and thereby more available. Despite its simplicity and economical advantage, the anaglyph technique's major disadvantages make it less probable as a contender in the further development of stereoscopic visualisation techniques (Javidi and Okano, 2002).

The chromo stereoscopic technique has several advantages that can be advantageous when visualising scientific data, although except for Toutin's application to remote sensing data, it has not been possible to find examples where this technique is applied. Thus,

- the easy translation into different mediums,
- only the single image required for stereoscopic effect,
- the inexpensive glasses,

- no reduction in resolution,

- low demand on computer power,

are all desirable qualities, especially in a semi-operational environment such as

hydrography.

The major disadvantage, a non realistic colour scheme, can simply be overcome by present

display technology that allows switching between different 3D model textures. For the

purpose of selecting a technique for this project the chromo stereoscopic method appears

intriguing because of the advantages described above. The novelty of the technique and the

relatively low cost of equipment makes this stereoscopic display technique advantageous

for further investigation. After investigating the presentation of digital hydrographic data in

chapter 5, the best-suited technique for the experimental work of this thesis will be

selected.

Chapter 5: Presentation of Digital Hydrographic Data

As described in chapter 2, depth perception increases with an increasing number of visual depth cues. The effect of the binocular depth cues is powerful and beneficial to include in the presentation of spatial data to increase the comprehension of the dataset. This is especially true concerning complex datasets with a number of spatially interrelated objects. As explained in chapter 3 the powerful binocular depth cue stereopsis is presented in a 2D display by using stereoscopic display techniques. Despite the large number of stereoscopic techniques available, surprisingly few are employed in scientific visualisation today. However some scientific branches such as medicine, chemistry, the petroleum exploration industry and complex mechanical engineering include stereoscopic techniques to a greater extent to gain increased perception and understanding (Hearn and Baker, 1997).

This chapter will give an overview of the current trends in scientific visualisation with respect to stereoscopic techniques and examine how digital hydrographic data is currently presented. Further it will investigate how suitable this data is to visualise using stereoscopic techniques. Hydrographic datasets for a broad approach will be examined; however the focus will be on digital hydrographic data that are three dimensional in nature. In essence data that is volumetric in nature, or data, where position is determined in a volumetric model. The datasets will be classified, and appropriate datasets representing each of the established classes will be selected for the visualisation presentations including the stereoscopic depth cue, these presentations are part of the data analyses chapter.

In general, hydrographic data is presented as 2D images with few or no visual depth cues, or as 3D perspective models including several, of the monocular visual cues to increase depth perception. Presently, to the author's knowledge, only one software developer with a

- 43 -

base in an academic establishment specialising in hydrography has developed hydrographic software applications where stereoscopic display techniques are available (Interactive Visualization Systems, 2004). However the stereoscopic display techniques are limited to anaglyphs and time polarizing multiplexing explained in chapter 4.

In compliance with the definition of hydrography (chapter 1) the data investigated will be limited to the volume between the water surface and the seabed. Further only data that can be spatially referenced in the volume or constitute the limiting surfaces of the volume will be investigated.

5.1 Current trends in Scientific Visualisation data presentation

As a result of the computer revolution, visualisation of data has evolved at an ever increasing rate and in areas like advanced engineering and medical science advanced visualisation techniques including stereoscopic viewing is included. The computer gaming industry has vastly contributed to the development of computer visualisation. One of the major models of the visualisation process was introduced by Haber and McNabb (1990). The model represents a general classification of data that comes from numerical simulations; however it is more generally applicable to computer visualisation. Figure 5.1 show that the model identifies three major processes, data preparation, visualisation mapping and presentation.

The first process, data preparation, creates a model of the raw data. Based on the derived data, a visualisation mapping process is conducted, and an Abstract Visualisation Object (AVO) is created. Each quantity of the derived data is mapped to an attribute of the AVO such as space, time and colour. The third process, presentation, produces a picture on an output device, in most cases on a computer screen.
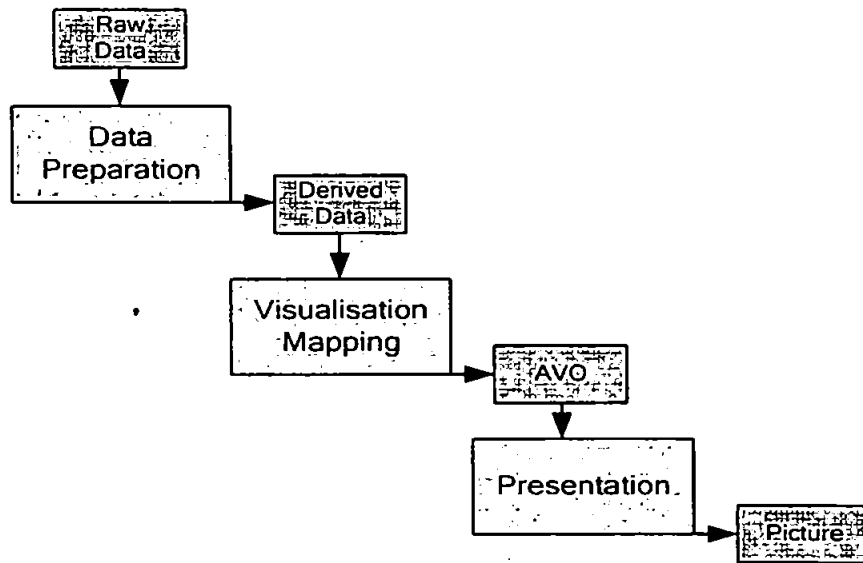
Figure 5.1: The Haber McNabb visualisation model (Source: Haber and McNabb, 1990)

When investigating the developments of the presentation process of the model it is evident

that scientific branches dealing with complex spatially related data are including

stereoscopic viewing to enhance the presentation process. As discussed in the chapter 4

multiplexing techniques are still most accepted with a growing interest in advanced Virtual

Reality (VR) presentations, however the cost and computer power required for the

advanced VR systems are still a limiting factor.

As earlier mentioned scientific fields such as medicine, advanced engineering, the

petroleum exploitation industry and meteorology where high volume and complex datasets

are analyzed presently applies stereoscopic presentations to enhance the data perception.

Suthau et. al. (2002) have developed an application, ARION (Augmented Reality for Intra

Operative Navigation), to assist medical surgeons during liver transplantations. The real

scene viewed by the user is combined with a virtual scene generated by the computer

where additional information is augmented (figure 5.2). Optical, see-through, head

mounted displays as described in chapter 4.1.6 are used to stereoscopically enhance the

presentation.
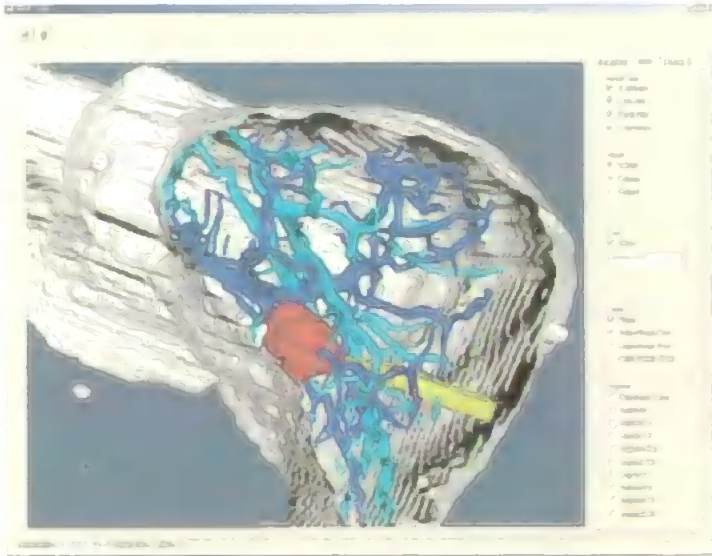
Figure 5.2: The Arion computer application is developed to enhance visualisation during liver transplantations (Source: Suthau et. al., 2002)

Figure 5.3 illustrates a numerically 3D modelled severe storm animation which was developed at the National Centre for Super Computing at the University of Illinois. The model is stereoscopically presented using the time multiplexing technique described in chapter 4.1.3
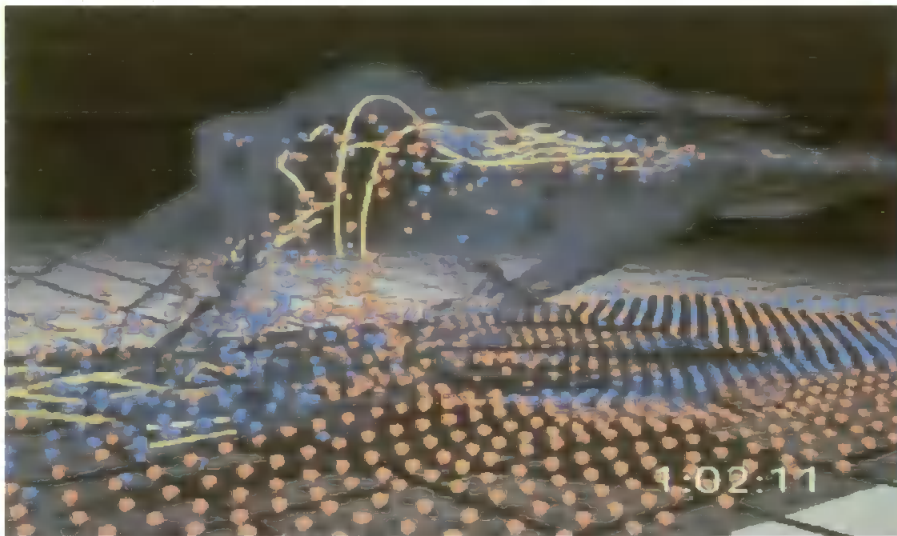
Figure 5.3: Scientific visualisation of a numerically modelled severe storm (Source: University of Illinois, 2004)

Photogrammetry and remote sensing have applied stereoscopic presentation techniques to increase the depth perception of images to extract height information. In state of the art

computer applications such as the Erdas Stereo Analyst (Erdas, 2004) it is possible to add stereoscopic depth to the image data. However, only anaglyph and time multiplexing techniques are available. The advanced 3D Visualisation system, Fledermaus from IVS can generate a wide range of impressive data presentations of hydrographic data, where colour stratification along the vertical axis is widely applied, stereoscopic viewing is available through the time multiplexing techniques (Interactive Visualization Systems, 2004).
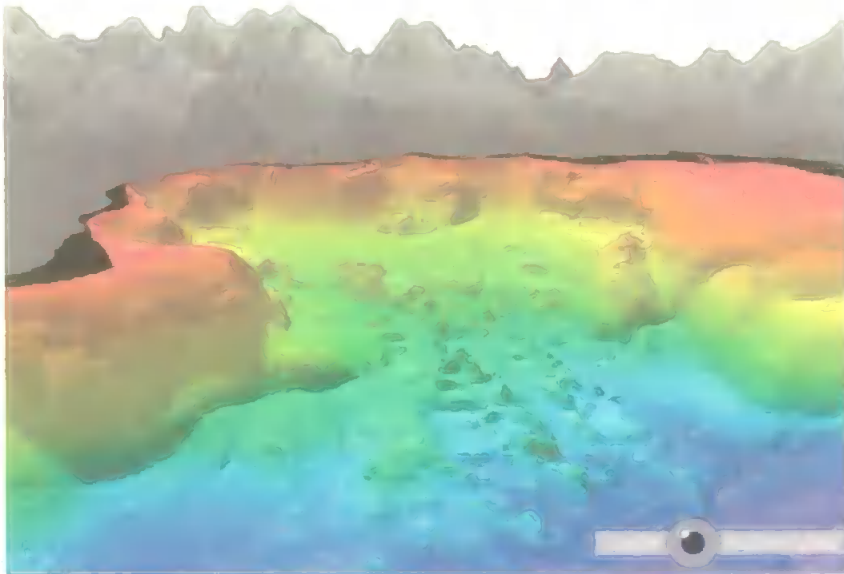
Figure 5.4: A typical presentation output from the Fledermaus application. A visualisation of Lake Tahoe seabed colour stratified along the z axis, with monochrome mountains in the background. (Source: Interactive Visualization Systems, 2004).

5.2 Sonar Sensor data

Sonar (SOund Navigation And Ranging) was used for the first time in Germany in 1912. Technological development has brought enormous improvement in transducer and signal processing technology. According to Kjerstad (2002) the technology has branched into 3 main groups of sonar systems.

- Offshore industry and survey related systems employed for accurate relative positioning and to gather bathymetric data,

- Military systems that consist of both active and passive systems used for submarine

detection navigation and underwater communication,

- Fishery systems employed for fish finding, navigation, biomass measurements and acoustic sensors on fishery tools.

In active sonar systems the returned acoustic signal determines the range from the transducer to the detected object. The object's location in the sonar beam can be determined, and the shape and direction of the sonar beam is manipulated to get desired information on the object's relative location, shape and size (Kjerstad, 2002). The surface texture of the object can also be classified by some of the systems. Passive sonar systems record and analyse the received sound by transducers or hydrophone arrangements. Using advanced signal correlation techniques, both bearing and distance to registered targets is calculated. The passive systems are also capable of classifying targets; these systems are primarily used in military systems where stealth is often a requirement. Military systems used in submarine warfare and similar operations will not be discussed further in this text because of the difficulties involved in obtaining information on the latest developments in relevant technologies.

The following sections of chapter 5.2 will describe how hydrographic sounding data are currently presented and what visual cues are used in the current presentation of sounding data. First, the data from offshore surveying and mapping systems are investigated; thereafter the sounding data from today's advanced fishery sounding systems is examined.

5.2.1 Offshore survey and mapping systems

The main objective of a bathymetric survey is to produce a terrain model or relief of the seabed. This can be accomplished by correlating a position with a depth measurement in a regular grid, or a Triangulated Irregular Network (TIN) giving x, y, z coordinate sets, where x and y refer to the horizontal position and z to the depth measurement (sounding) (Brouns et. al., 2001). Until the early 1980s hydrographic originals were edited and hand drawn (figure 5.5) by hydrographers from echograms and the depth contours were

extrapolated from the dataset.
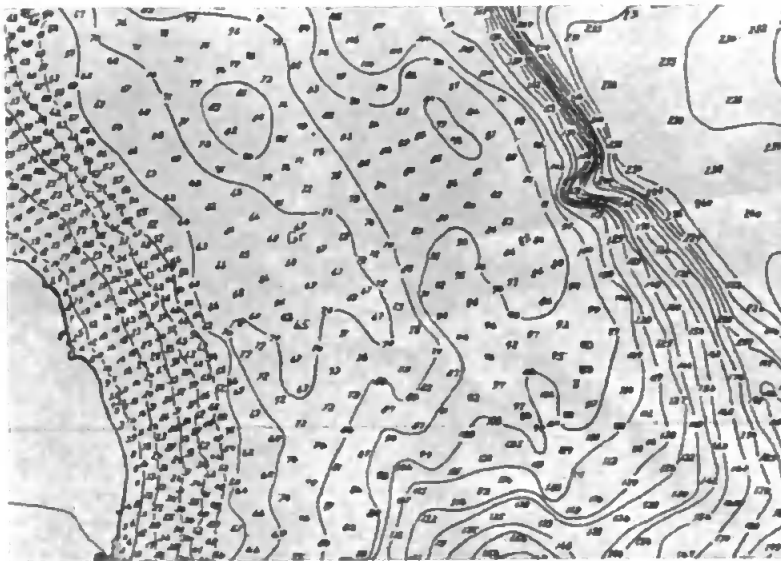
Figure 5.5: Hand drawn hydrographic original in scale 1:20000 (Source: Kjerstad, 2002).

Today this process is automated and positional data is merged with depth soundings to create a Digital Terrain Model (DTM) of the seabed. In recent years multibeam sounders have improved the hydrographic survey of an area by producing a relatively high resolution DTM in a corridor extending each side of the survey ship's track.

The traditional way of presenting the seabed and its features in an operational nautical context is still in 2 dimensions on a paper chart, or electronic charts digitised or scanned from paper charts. The bathymetric details are still presented as spot depth numbers and contour lines. Figure 5.6 shows a computer display presenting an electronic navigation chart (ENC) (IHO, 2000). Contour lines and spot depths deeper than the set safety depth are excluded from the presentation to improve the readability of the chart, however areas with depths less than the safety depth is colour coded (shades of blue in figure 5.6). With the underlying DTM a perspective view of the seabed is easily computed and several commercial software packages are capable of presenting a perspective view of the seabed in a selected area to give the viewer better perception of the bathymetric data (figure 5.7).
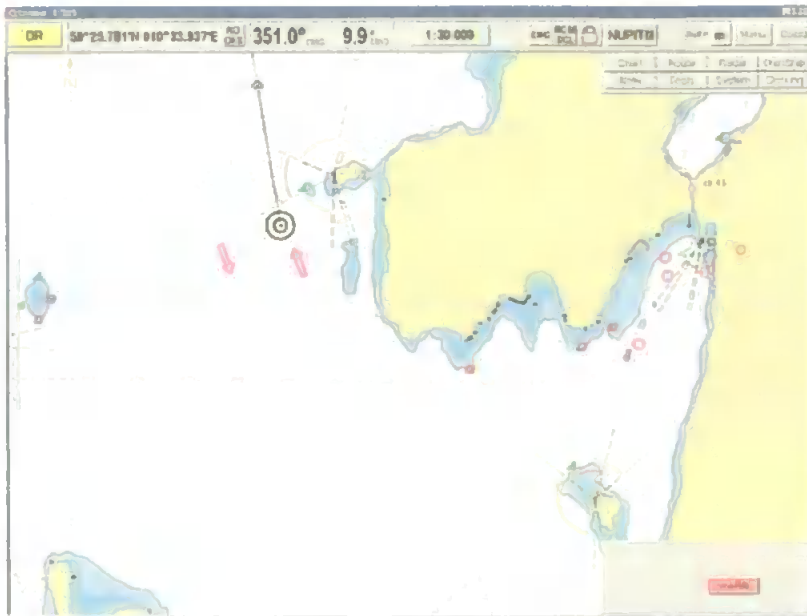
Figure 5.6: Computer display presenting a electronic vector chart (Source: Kongsberg Norcontrol AS)

By including a perspective model and shading most of the monocular depth cues are included. In order to increase the depth perception even further, stereoscopic depth cues can be integrated. Figure 5.7 gives an example of a presentation including a perspective model. Contour lines, spot depths and colour coding are also included to increase perception of the local bathymetry.

Figure 5.7: Perspective view of selected area as presented in an electronic chart software package (Source: Chartwork Ltd.)

In the offshore industry and other areas requiring a high-resolution presentation of a smaller area of the seabed with its features, high resolution multibeam sounders and Side Scan Sonars (SSS) are common data sensors today. By attaching the SSS to a towed fish, a ROV or an autonomous underwater vehicle (AUV) the sonar frequency can be increased to enhance the resolution. By bringing the side scanning sonar close to the seabed and with the sonar beams radiating more horizontally across the seabed it is also possible to get a side view of the seabed features. This increases the detection of features pointing upwards from the seabed and will provide better classification of the roughness of the seabed like stones and sand waves, and as shown in figure 5.8 it is possible to get perspective images of ship wrecks and other features. Note that figure 5.8 also includes the light and shadow distribution monocular depth cue to increase perception.

Figure 5.8: Typical SSS image (500 kHz) of a shipwreck on a 75-metre range collected with a Klein Side Scan Sonar System 3000.
(Source: Klein Associates Inc.)

Several specialised hydrographic software packages such as Eiva Navipack, Reson Navisoft and Trimble HYDROpro are available and a product survey was presented in Hydro International (2002). These software packages are often comprehensive, in the sense that they are used in the planning of hydrographic operations, collecting the hydrographic

data from multiple sensors and processing and presenting the data output. The most sophisticated software manufacturers such as QPS QINSy provide specialised 3D visualisation tools to improve presentation of data even further. The visualisation tools are capable of generating 3D surface models or 3D contour models presented in perspective view. Depth colour coding is also available by most of the visualisation tools and is to an increasing degree used to enhance the perception of depth along the vertical axis. Figure 5.9 gives an example of a typical presentation of a hydrographic dataset, a colour coded DTM where the colour coding is a function of depth (z-axis).
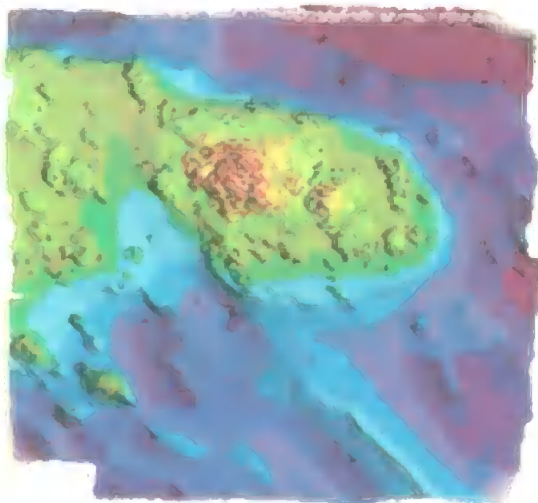
Figure 5.9: A typical example of multibeam bathymetry data presentation, including colour stratification of the data combined with sun-illumination shading. The shading shows added relief detail and texture, both of which are valuable for increased perception of the dataset. (Lockhart et al., 2001).

The QPS QINSy software also includes a Virtual desktop environment with a perspective model of a DTM and objects such as ROVs, divers, SSS fish and structures are presented in real time. Several of the monocular depth cues listed in chapter 2 are included in the presentations; however only one of the software packages presently available provides stereoscopic display techniques to further enhance the depth perception. Figure 5.10 gives an example of a presentation from one of the most sophisticated commercial software packages currently available on the market.
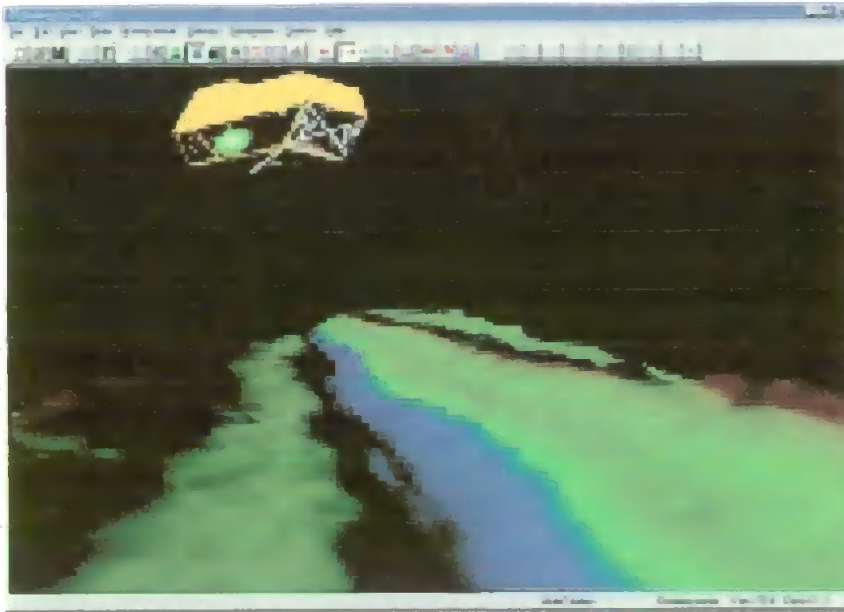
Figure 5.10: QINSy 6 hydrographic software package contains a virtual environment manager. This figure displays an extract from a ROV flying over a colour-coded seabed DTM in real time (Source: Quality Positioning Services BV (QPS)).

Hydrographic applications such as RoxAnn GD (Sonavision, 2005) also classify the properties of the seabed, but this property is not of great concern for 3D presentation, rather a matter of the texture or colour you place on the bathymetric surface.

5.2.2 Fishery systems

This section investigates how data from acoustic systems related to fisheries are visualised. Fish finding sonars and echo sounders have a wide range of purposes depending on the type of fishery. In general the differences are in presentation of data, signal range and resolution of data. The fishery system technology has also developed rapidly during the last decades. Current data visualisation is developed mainly by the sonar system manufacturers and is in general limited to traditional 2D sonar images with colour coding as illustrated in figure 5.11.
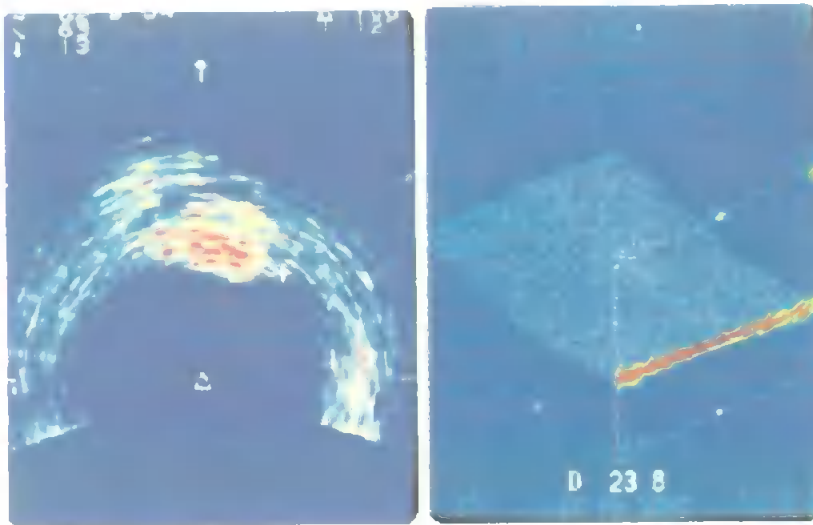
Figure 5.11: Two presentations of data on the Furuno CH-37 colour sector scanning sonar. The left hand picture shows a more traditional sonar display of a horizontal sweep, colour coded to enhance the interpretation. The right hand picture contains an oblique perspective presentation of the seabed from the vertical fan beam mode. The perspective image is overlaid with real time fish and bottom echoes (Source: Furuno Norge AS).

However one innovative software provider (ICAN) is presently developing a software package that presents the fishing vessel and fishing gear in a 3D perspective model with a bathymetric DTM to visualise the seafloor (figure 5.12). The model is colour coded along the z-axis (depth) as can bee seen in figure 5.12.
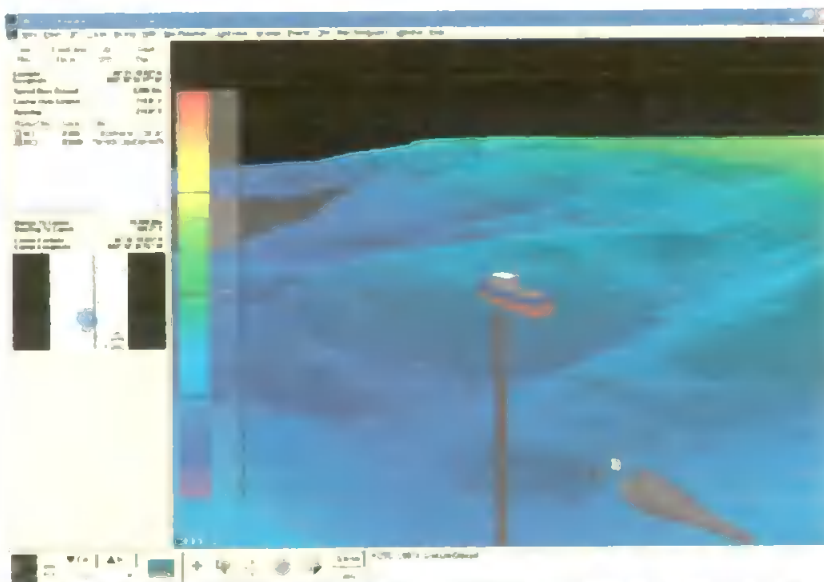
Figure 5.12: The Fishing Information Navigation System (FINS) is currently under development by the Canadian company ICAN. The vessel and the trawl "float" over the colour coded surface model of the seabed (Source: International Communications and Navigation Ltd. (ICAN)).

5.3 Remote Sensing data

Stereoscopic display techniques described in chapter 4.1 have been used by other sciences and technologies to enhance the display of digital geo-referenced models such as DTMs. Software packages used in remote sensing (Lillesand and Kiefer, 2000) and in photogrammetry (Wolf and Dewitt, 2000) such as Erdas Imagine Stereoanalyst (Leica Geosystems, 2004) can easily generate stereoscopic models from DTMs or stereo images. The stereoscopic display techniques used are mainly anaglyphs or time-polarisation multiplexing.

The remote sensing contribution to hydrography is summarised in Lavender (2001). Section 5.3 reviews the different remote sensing systems and techniques available to collect hydrographic data where remote sensing includes systems mounted on airborne or satellite platforms. The systems can be categorised in two main groups, active and passive.

5.3.1 Active systems

The active systems include radar systems and LIDAR (LIght Detection And Ranging) systems and Synthetic Aperture Radar (SAR). Several of the spaceborne platforms are equipped with accurate radar altimeters.

Along the platform footprint the radar altimeters are able to measure the sea surface height to a maximum accuracy of approximately 2 cm provided an ideal reference ellipsoid is available. Radar altimeter systems collect point measurements; these are then interpolated to produce a global map as shown in figure 5.13.
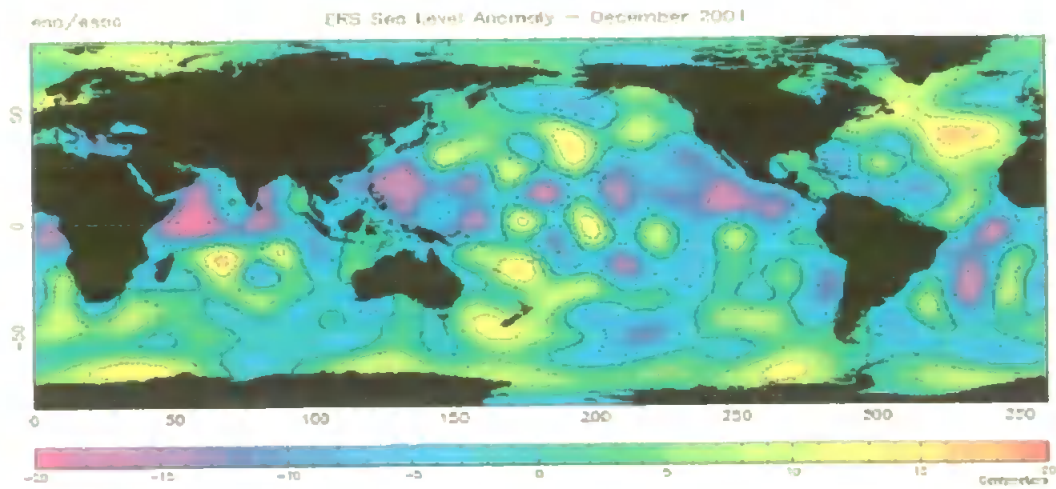
Figure 5.13: Radar altimeter data from the ERS satellite showing sea surface height anomalies from an average anomaly map on a global scale. The anomalies are colour coded using the visual spectrum. (Source: European Space Agency (ESA) Earthnet Online)

The minute vertical variation over a relatively large area makes the data well suited for a 2D presentation with elevation variations indicated as elevation contour lines or as coloured areas of equal elevation (figure 5.13), however less suited for 3D presentations unless the dataset is of a local area. The sea surface height will frequently constitute one of the vertical limiting surfaces, and in a local area model the vertical variations in sea surface height may be of such magnitude that a 3D presentation is favourable.

In order to increase performance of the radar systems on space-borne platforms SAR technology is generally used (Lillesand and Kiefer, 2000). Through modified processing techniques the characteristics of a very long radar antenna is synthesised. By recording the signal travel time and the strength of the returned signal it is possible to measure the sea surface roughness (Lavender, 2001). By analysing the sea surface roughness data it is also possible to detect oil spills (Tromsø Satellite station, 2003).
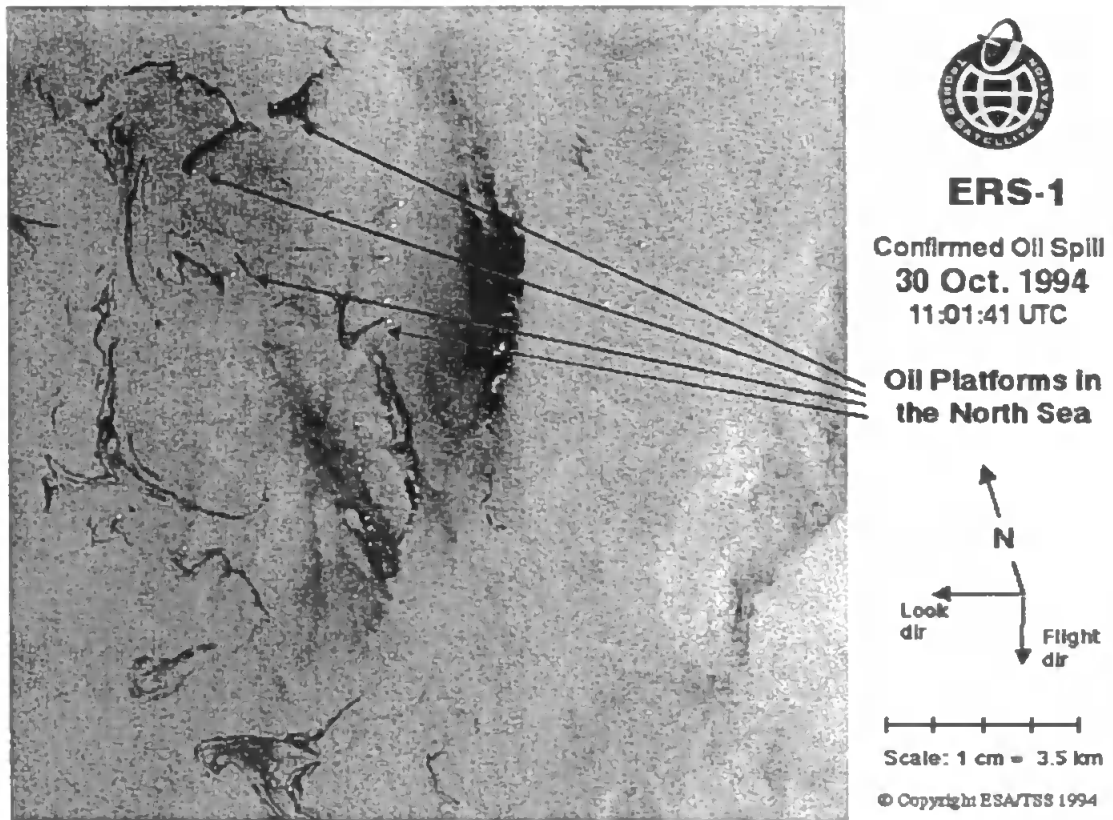
Figure 5.14: SAR image illustrating oil spills from oil platforms in the North Sea. The sea surface roughness increases from dark to light colour in the picture. (Source: European Space Agency / Tromsø Satellite Station (ESA/TSS)).

SAR images from several platforms, e.g. Radarsat and ERS are employed to detect, map and classify icebergs, measure the ice concentration in an area and to monitor the extent of the ice border (Lillesand and Kiefer, 2000). Figure 5.15 shows the arctic ice cover limit with colour coding to categorize different types of ice.

By developing ship detection software algorithms and applications it is possible to use SAR images to detect and track ship traffic in an area for instance for fisheries enforcement activities (Wahl, 1998).
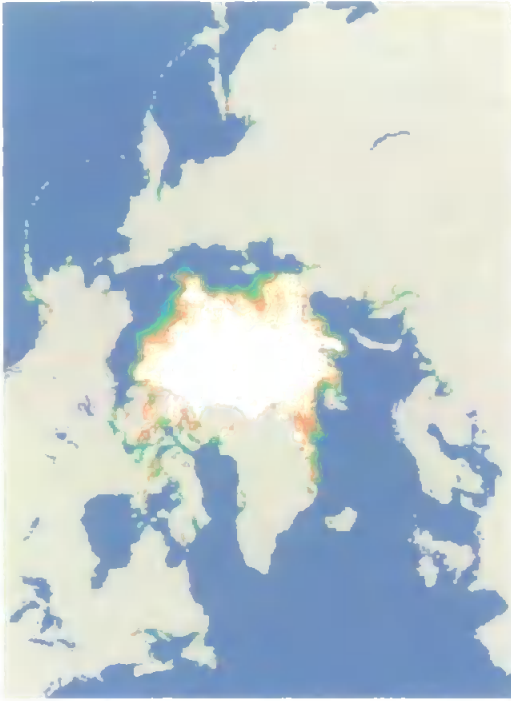
Figure 5.15: Image illustrating the Arctic ice cover in March 1993. The ice cover (in %) is colour coded from blue (ocean) to white 100% solid ice. (Source: Nansen Environmental and Remote Sensing Center (NERSC)).

LIDAR systems are mounted on airborne platforms and are able to produce a high resolution bathymetric DTM of the covered area. The systems are limited to maximum depth measurements of approximately 50 metres depending on water turbidity (de Jong et al., 2002). Several national hydrographic offices are using this method to collect bathymetric data in shallow and less accessible coastal areas. Sinclair (1999) provides an overview of the capabilities and performance of the Australian LIDAR system, Laser Airborne Depth Sounder (LADS). Figure 5.16 shows a LIDAR data generated digital bathymetric model. The model includes surface rendering with colour coding of the z-axis.
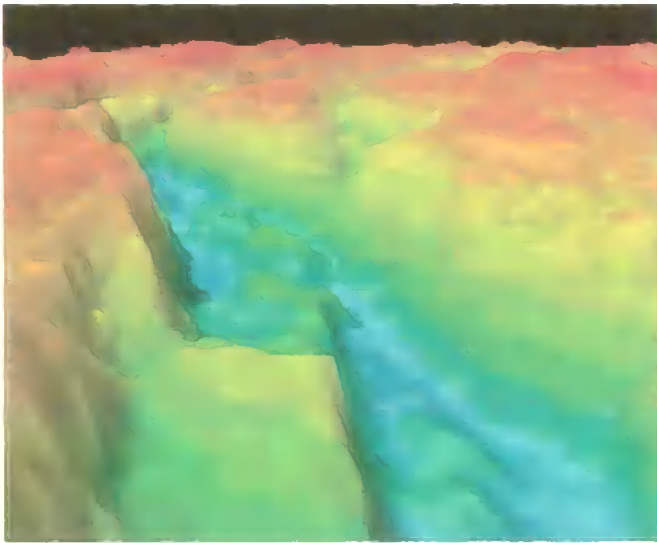
Figure 5.16: High accuracy and high-resolution bathymetric model from LIDAR data collected by LADS in Norwegian waters. The model is colour coded using the visible spectrum (Source: Sinclair, 1999).

5.3.2 Passive systems

The passive remote sensing systems used to collect hydrographic data are optical sensors mainly on airborne platforms; however optical imagery from space borne platforms such as Landsat is also used (Lavender, 2001). The optical data collection finds a place primarily in the transition zone between land and sea. To include stereoscopic visual clues to the optical images traditional photogrammetric techniques are used to create 3D stereo models. Digital photogrammetry software packages make it possible to produce DTMs from scanned optical imagery (Wolf and Dewitt, 2000), and to drape orthophotos on top the DTM to get a terrain model that includes the surface details.

Remote sensing data from passive sensors on space borne platforms are used to collect a variety of marine biological data in the surface layers of the oceans (Lavender, 2001). However with reference to the IHO definition of hydrography these data will not be discussed in this text.

5.4 Tidal model data

High-resolution tidal models based on mathematical tidal dynamics computations and tidal

gauge observations are available (Moe et. al., 2002). Tidal data are traditionally presented in a tabular format and on charts containing bathymetric features overlaid with a grid of isolines connecting spots with equal sea surface elevation (figure 5.17).
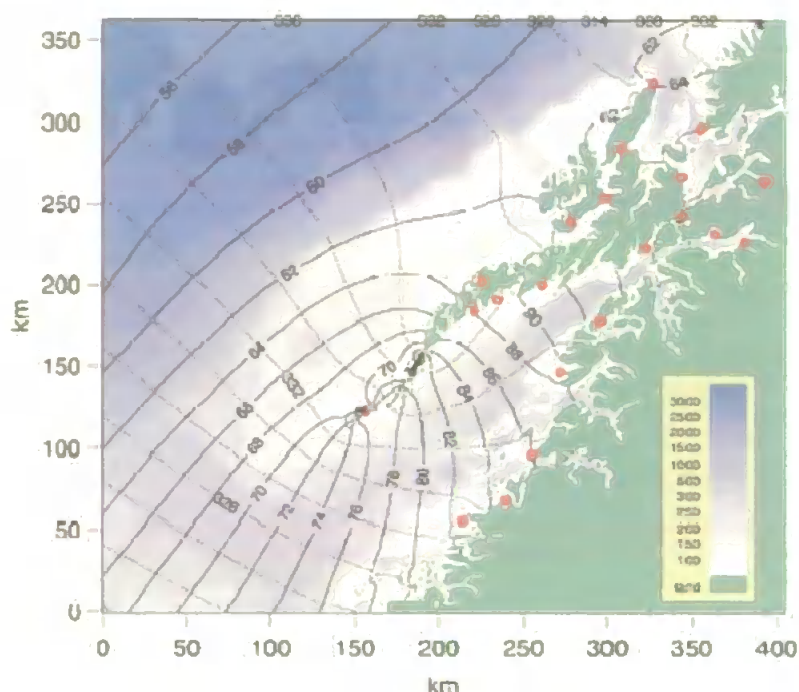
Figure 5.17: Isolines for amplitude (2 cm separation) and phase (2 degrees separation). Tidal stations marked with red dots. Colour shading depicts water depth. (Source: Moe et. al., 2002).

Today computerised modelling techniques provide for animations of the propagation of tides. Figure 5.18 shows a picture from an animation of sea level changes associated with the M2-tide in the Nordic Seas. The light blue area depicts the areas of high sea level and during the animation the area changes according to the mathematical model. The tidal height will constitute the limiting surface of the hydrographic model in many circumstances and, particularly for local models where the vertical and horizontal scale is more similar, it can be of value to present it in 3D.

Figure 5.18: Figure from Animation of the sea level change in the Nordic seas (2 frames). Light blue colour depicts area of higher elevation (Source: University of Oslo, Department of Mathematics)

5.5 Ocean and tidal current data

Ocean and tidal current data is traditionally presented as 2D vector charts where each vector represents the local direction of the current and local current velocity is depicted by the length of the vector. These presentations are often based on a combination of current measurements from current meters or Acoustic Doppler Current Profilers (ADCP) and mathematical models. The models are frequently layered, each layer containing a vector chart representing the currents at different depths. Computer modelling has supplemented animations and perspective views to the presentations. Figure 5.19 shows a presentation of the tidal current in the Drøbak Sound, in the Oslo fjord in southern Norway.

This presentation is an animation showing the temporal variations of the tidal currents in the sound. By presenting the current layers at different depths in a model volume in 3D an increased perception of the water movement can be achieved. It is possible to visualise models of temperature layers and variations of salinity in the hydrographic model in a similar fashion.
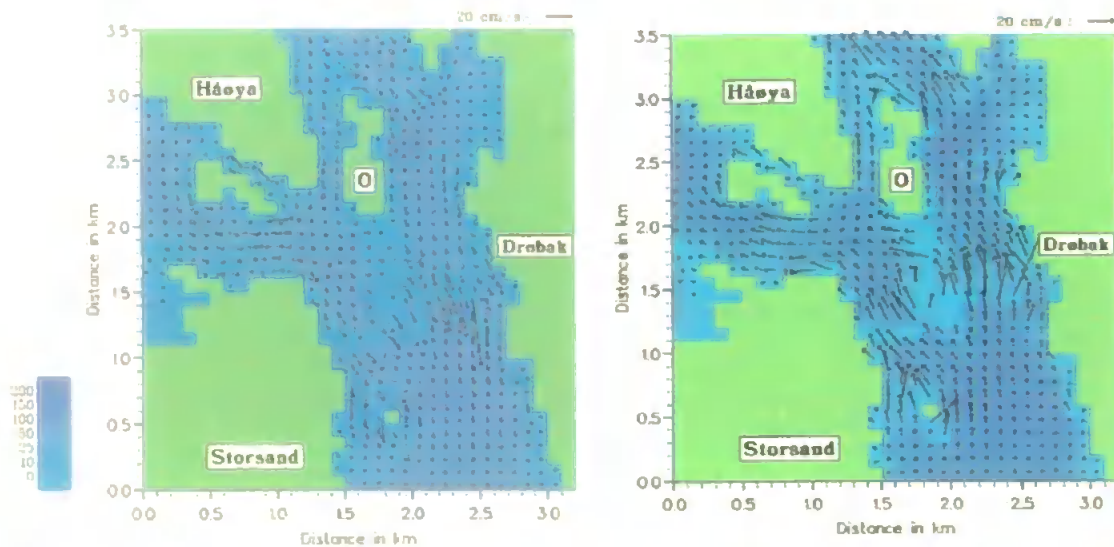
Figure 5.19: Computer model presentation of tidal currents in the Oslo Fjord. Picture is based on animation that shows the temporal changes of the currents (2 frames). (Source: University of Oslo, Department of Mathematics).

Figure 5.20 presents an animation of a 2D (only one layer) tidal current vector field model. By introducing more layers at different depths the tidal current variations as a result of the ship and the bathymetry can be visualised and a stereoscopic presentation would increase the perception of the model.

Figure 5.20: This picture is a snapshot of an animation that demonstrates the results from a 2D tidal current model in the vicinity of an unloading dock on the east coast of Canada. It also provides a demonstration of the ability to fly through a transparent water surface for another perspective of the surrounding bathymetry (Source: Baird Software).

5.6 Man-made Object data

Man-made objects constructed or operated subsurface are mainly positioned in the water volume by hydro acoustic systems. An object's attitude and movement can, in many instances, be determined by sensors mounted on the object (e.g. gyro and Doppler log on a ROV (Remotely Operated Vehicle)) or by tracking the objects. This will allow for a dynamic presentation. The size and shape of the object can either be known, as is the case for an ROV, or it can be unknown, as is the case for an unidentified sonar target. If the object size and shape is known it can be modelled using a CAD software package or similar.

An example of this is a ROV positioned by a Super Short Base Line (SSBL) Hydro-acoustic Positioning Reference (HPR) system. The relative position of the ROV is determined by using a composite transducer consisting of a multitude of transducer elements. By measuring the phase difference of the received signal at the receiving transducer elements, the ROV's position can be determined. If the absolute position and attitude of the transducer is known, the ROV's absolute position can be derived. The object shape, size, attitude and 3D position in the water volume can be included in the visual presentation. Underwater positioning principles are further discussed in Ingham and Abbott (1992).

Today the visual presentation of man made objects is generally presented in a 2 dimensional Computer Aided Design (CAD) fashion as a situational display with the altitude of the dynamically positioned object above the seabed terrain numerically displayed. However the visual presentation is evolving towards 3D perspective models, and the most advanced software packages such as QINSy and MakaiLay includes this form of presentation. Figure 5.21 illustrates a 3D presentation of a cable laying operation.
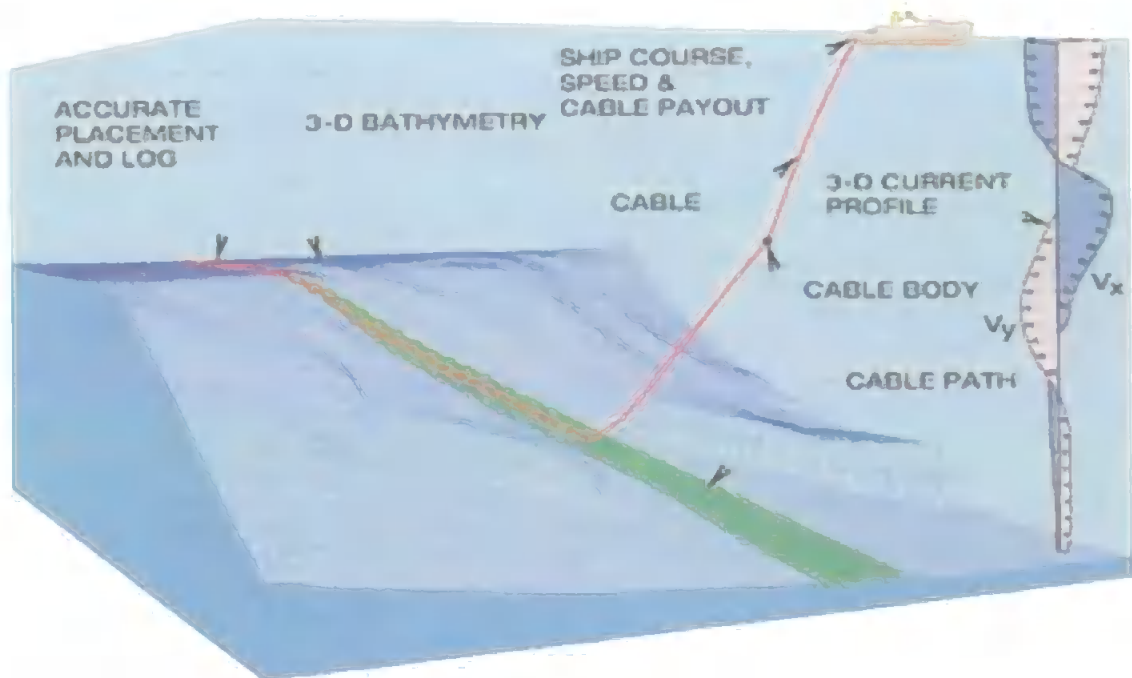
Figure 5.21: 3D presentation of a cable laying operation, including water volume, bathymetry, cable, surface vessel and also a 3D current profile. (Source: Makai Ocean Engineering Inc.)

5.7 Discussion on Digital Hydrographic Data

The hydrographic data presented in this chapter can be classified into 5 different classes.

- Bathymetric data

- Biological/organic data in water volume

- Sea Surface data

- Ocean and Tidal Current data

- Man-made Objects data

Data that has been labelled to be 2D in nature and not well suited for stereoscopic presentation can in some instances be modified by employing vertical exaggeration (expanding the z-axis). This will create more volume in the model and may make the model more appropriate for stereoscopic presentation, but the spatial relations will not be correct and can either lead to increased perception for the viewer, or if not carefully implemented, to misperception of the data.

This review of hydrographic datasets reveals that the bathymetric data from Sonar or Lidar systems are suitable for stereoscopic viewing; the data is 3D in nature and in general available as computer models (i.e. DTMs). However it is important to have some variations and features in the bathymetry to get the effect of the stereoscopic techniques. Especially when combined with datasets of man made objects in a more complex model, a better perception of the model can be achieved. In general the more spatially complex the model is, the greater is the benefit of the stereoscopic presentation. Operating vessels in confined waters or an ROV manoeuvring around subsea structures are examples of suitable operations where stereoscopic presentation of the increasingly complex datasets would be valuable.

Biological or organic features can be modelled as closed volumes inside the data model. In figure 5.12 the fishing vessel and the trawl is located in the computer model. If the fishery sonar data (e.g. a shoal of fish) is implemented in the model, a stereoscopic presentation will increase the perception of the trawls location relative to the shoal of fish. An increased perception of the trawls location relative to the seabed features is also accomplished. Biological matters (such as algae) in the upper layers of the water column identified by a remote sensing system can be presented in the same fashion, though this data is generally more 2D in nature and not suited for stereoscopic presentation.

The Sea Surface height data is composed from remote sensing radar altimetry and tidal models. The data is in general less suitable for stereoscopic presentations due to the 2D nature of the data. However by increasing the scale along the z-axis (vertical exaggeration) the data model becomes more 3D and a stereoscopic presentation can be valuable). Sea surface height data at a local scale would be useful as in many cases it would constitute one of the limiting surfaces of the model. The remote sensing detection of oil spills by analysing the texture of sea surface roughness (figure 5.14) will not be appropriate for stereoscopic viewing as it only describes the surface characteristics of the sea. The

detection of icebergs and the ice border from remote sensing systems supplies data that can be used to find a vessel's relative position to these surrounding features. A stereoscopic presentation will however not be valuable. A 2D radar picture would give a better representation.

Ocean or tidal current data at a specific depth is generally 2D in nature, however if data from several layers of depth is merged into the water volume a 3D vector field is formed. An example where this would be the case, is in a presentation of the water flow passing a feature in the water volume. By employing stereoscopic techniques to the 3D vector field of the currents, an increased perception of the variations in the dataset would be gained. Man-made Objects such as subsea structures in a port or in an offshore oilfield are currently modelled in Computer Aided Design (CAD) and 3D modelling applications. Some of these applications already include stereoscopic presentations using the multiplexing techniques. These objects are often well suited for stereoscopic visualisation due to the often complex nature of these data objects.

5.8 Conclusions

It is well established that stereoscopic depth cues will increase the perception of 3D datasets, in particular more complex datasets. In chapter 4 the currently most accepted stereoscopic techniques were reviewed. The multiplexing techniques are the most widespread and accepted techniques. These techniques are relatively easy to implement but they are rarely used when presenting hydrographic data. The major drawbacks are the loss in light intensity and reduction of resolution. The advances in enhancing the present techniques and developing new techniques are rapid and will surely introduce alternative methods in-the future.

The chromo stereoscopic technique has several advantages as described in the discussion of chapter 4. When presenting hydrographic datasets chromo stereoscopy is an interesting alternative. Colour coding along the vertical axis is widely used on hydrographic datasets

(e.g. bathymetry in figure 5.9). By employing the colour coding scheme along the line of sight axis, instead of along the z-axis as widely used today, and by using appropriate eyewear a stereoscopic effect is produced.

When presenting increasingly detailed and complex digital hydrographic datasets used in increasingly complex operations, the stereoscopic techniques can supply the viewer with the desired enhanced perception. With relatively simple means stereoscopic techniques can be implemented in the software tools currently available to present hydrographic data. Chapter 6 will further investigate the chromo stereoscopic technique and chapter 7 will present a novel and simple application that includes a chromo stereoscopic texture on a hydrographic dataset.

Chapter 6: Further analysis on Chromo Stereoscopy

Chapter 4 concluded that the chromo stereoscopic technique, even though a relatively simple and low cost technique to implement, has several advantages when visualising scientific data. Chapter 5 further concluded that the chromo stereoscopic technique has several qualities that can be advantageous when presenting hydrographic data. Based on these conclusions this project will perform experimental work and develop a novel software application that applies the chromo stereoscopic effect on selected hydrographic data models. These models will cover the classes presented in the previous chapter. First a short introduction to colour theory is given to aid the comprehension of the chromo stereoscopic method and as well to better understand the use of colour in the application development. Then a more in depth discussion on the chromo stereoscopic technique will be performed. In chapter 7 the chromo stereoscopic application development will be described.

6.1 Colour Theory

Colour describes the eye's perception of light at different wave lengths. Visible light is the part of the electromagnetic spectrum with wavelengths between approximately 380 nano metres (nm) (violet) to approximately 730 nm (red), see figure 6.1.
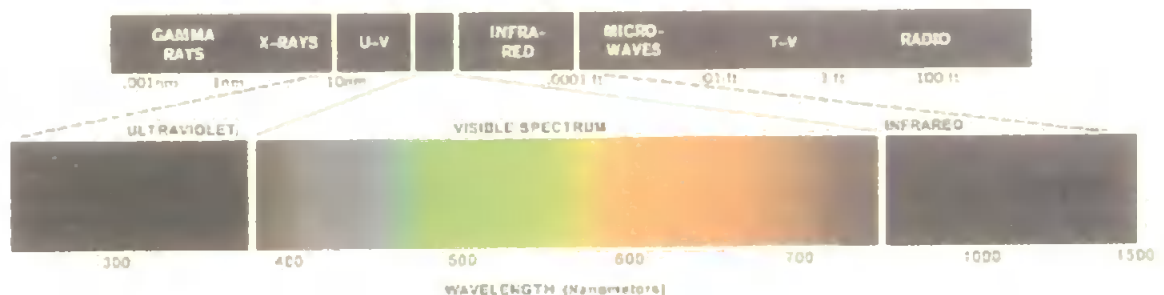
Figure 6.1: **The electromagnetic spectrum comprising the visible range (Source: Gonzales and Woods, 2002)**

The dominant frequency or dominant wavelength of a light source is called the hue or colour of the light. If the dominant wavelength of a light source is 730 nm the viewer will perceive the light as red in colour (Gonzalez and Woods, 2002). Other properties are necessary to describe the properties of light. Saturation or purity of light describes how washed-out the colour is. Pastel colours are less pure. The brightness of a colour is the perceived intensity of the light. Chromaticity is used to describe the colour characteristics, dominant wavelength and saturation. When mixing two or more colours (primary colours) a wide range of other colours (secondary colours) are formed. These three characteristics, dominant wavelength, saturation and brightness are used to describe the properties of a light source. The spectral range for a device describes how much of the visible spectrum the device is capable of representing (Pender, 1998). Figure 6.2 shows a comparison of spectral ranges for different devices, it is obvious that a typical colour monitor only represent a limited amount of the visible spectrum compared with the capabilities of the human eye. It is important to select a proper colour model to optimize the colour representation.

Human eye
Photographic film
RGB monitor
4 colour press
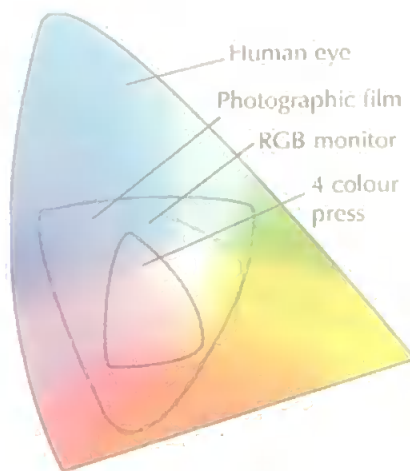
Figure 6.2: The spectral ranges for different applications (Source: Pender, 1998).

Colour models are used to specify colours in a standard, generally accepted way. They represent a method to explain the properties of colours in a particular context. A wide

range of colours are created in each colour model (typically from 3 primary colours), this is termed the colour gamut or colour scale. A multitude of colour models exist, the models are either oriented towards hardware (e.g. colour monitors) which emit light or applications which reflect light, such as all forms of prints. Different models are developed to describe different characteristics of colours. This text will focus on the hardware orientated RGB (Red, Green, Blue) and the HSV (Hue, Saturation, Value) colour models which is used in the development of the chromo stereoscopic application.

The RGB colour model uses three primary colours (red, green and blue) to produce the colour gamut. It is an additive model which means that contributions from each primary colour is added together to get the resulting colour. This colour model is commonly used and corresponds to the input data of a Cathode Ray Tube (CRT) colour monitor where the parameters are the amount of red, green or blue light to emit. Figure 6.3 shows the RGB colour cube.
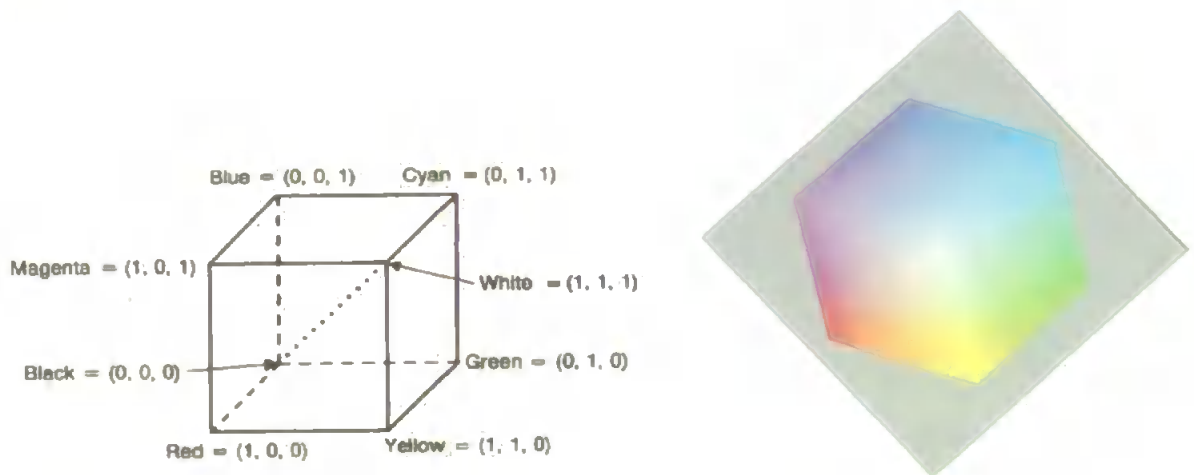
Figure 6.3: **The RGB colour Cube. The left side shows the cube in a Cartesian coordinate system. The right side shows one side of the cube in colours. (Source: Foley, J. D., van Dam, A., Feiner, S. K., Huges, J. F., 1990)**

A strength of the RGB colour model is that the colour space is within a unit cube. This makes the computer programming less complicated, in that range checking is more convenient. It is then easier to link distance from the viewer along the line of sight to a colour in the visible spectrum, this is a valuable property when developing the chromo

stereoscopic application.

A major limitation of the RGB model is that the colours are not perceptually uniform and therefore it is not sensible to measure colour differences in the RGB colour space. Specifying colours in the RGB colour space is more convenient if hue, saturation and brightness are separate parameters. The HSV colour model achieves this (Gonzales and Woods, 2002).

The major diagonal from black at (0,0,0) to white at (1,1,1) in the RGB colour model forms a grey scale (figure 6.3 left). The HSV colour model is created if the cube is rotated so the white corner points towards the viewer and the black corner points away from the viewer, then a hexagon is formed with hues radiating around the Gray scale axis (Foley et. al.). The HSV colour model uses this concept to define a hue angle, saturation and value (the latter corresponds to brightness).
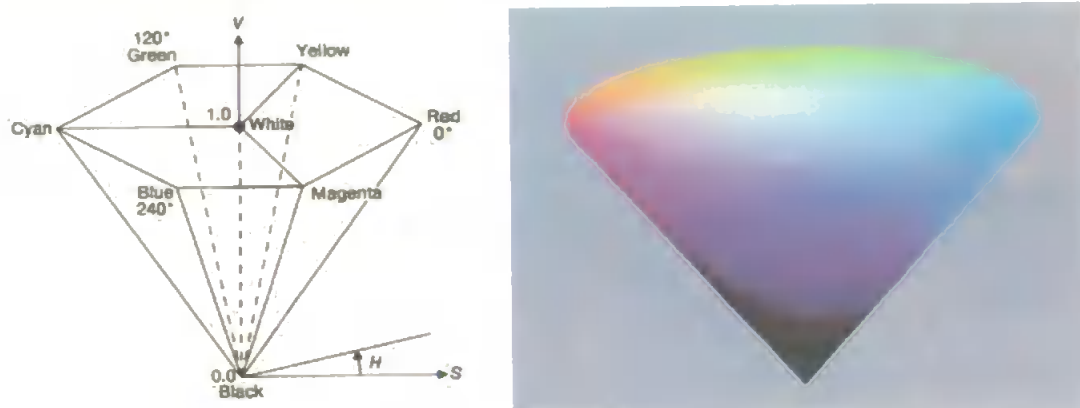
Figure 6.4: **The HSV colour model, at left the model in a polar coordinate system, at right represented in colours (Source: Foley et. al., 1990)**

It is easier to mix colours in the HSV colour model than in the RGB colour model because the three parameters are more closely to perceptual attributes.

6.2 Chromo stereoscopy

Chapter 4.1.7 briefly described how the chromo stereoscopic technique is used to convert colour into a stereoscopic effect. The chromo stereoscopic effect can easily be observed

without any aids in a 2D image with bright red and blue areas scattered against a black background. The effect appears mainly from the natural chromatic dispersion of the eye acting on the off-axis component of the light entering it (Sundet, 1972). In essence light with a short wavelength (e.g. blue) is more refracted than light with a long wavelength (e.g. red). There is a direct relationship between the position of a colour in the spectrum and the perceived depth. The physiological fact that the pupil centre and the visual axis in most cases are non coincidental enhances the chromo stereoscopic effect. These two factors will result in a slight retinal disparity between the red and blue areas. Kishto (1965) found that the chromo stereoscopic effect is affected by the amount of illumination introduced to the model. Most people will get an increased chromo stereoscopic effect if the model is properly illuminated. If the illumination is reduced some people (less than 12%) experience a reversal of the stereoscopic effect.
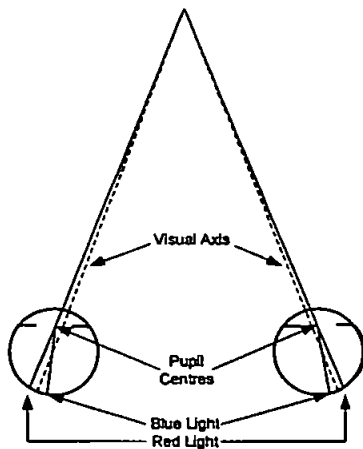
Figure 6.5: The figure shows the offset of the pupil centres and the visual axes (broken line). It also shows how the difference in refraction between red and blue light rays results in retinal disparity. The angles in this figure are exaggerated in order to portray the effect.

Although present, the auto chromo stereoscopic effect can only create a limited amount of depth perception to the viewer. It is necessary to use optical devices to increase the retinal disparity and thereby get a useful depth perception.

6.2.1 Single Prism Glasses

Kohler (1962) and Kishto (1965) experimented with an arrangement of single prisms to enhance the chromo stereoscopic effect. The single prisms are placed in the line of sight of each in order to increase the dispersion of the light reaching the eye's retina (figure 6.6). It is apparent that the prisms in figure 6.6 are converging, bringing the blue colours of the spectrum to the front, and thus reversing the previously described and natural colour scheme.
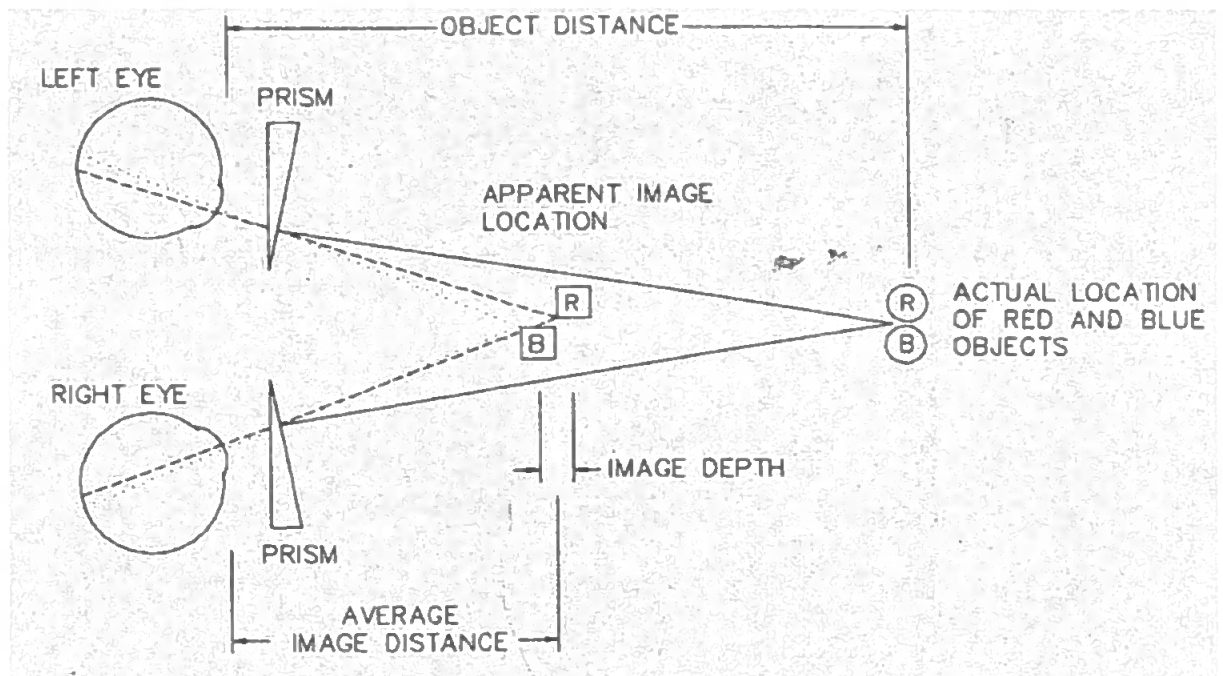
Figure 6.6: Converging single prism arrangement to increase the chromo stereoscopic effect. (Source: Kishto, 1965)

This is an alternative to the natural presentation accomplished by arranging the prisms in such a way that the light rays diverge (figure 6.7). There might be applications where a reversed colour scheme is desired; however this text will focus on the natural colour scheme with the red end of the visual spectrum closer to the viewer which after all is both the natural psychological and physiological colour scheme.
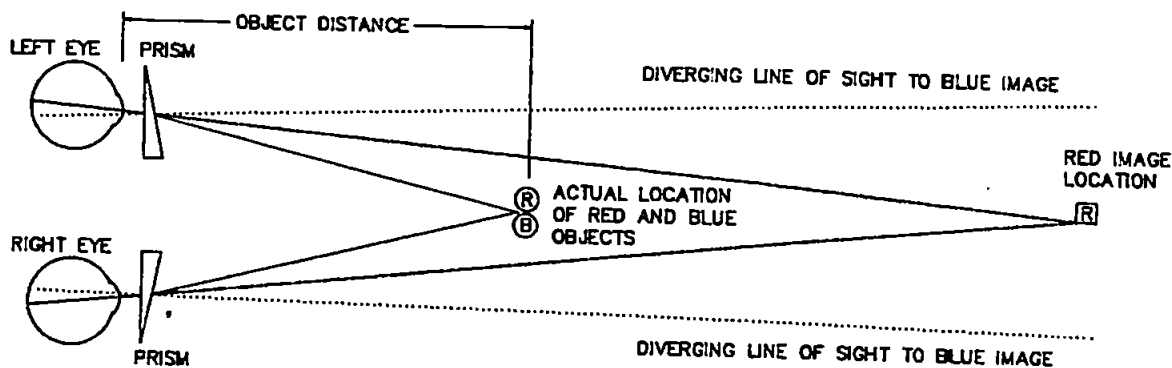
Figure 6.7: Diverging single prism arrangement to increase the chromo stereoscopic effect (Source: Steenblik, 1987)

The use of single prisms causes the line of sight from the viewer to the image to be diverted (figure 6.6 and figure 6.7). This will cause the viewer to adjust the eyes inwards to fuse the image when viewing the object through converging glasses. This will introduce strain to the eyes and visual distress (Steenblik, 1987). The resulting image will appear closer than the object because the lines of sight converge to a point closer in space. However, the focus of the eyes must remain at the distance of the original object. The difference in convergence distance and focal distance causes the visual distress resulting in headaches, vertigo and nausea. As the viewer moves the head the visual distress is increased, the image moves in an unnatural way because it appears closer than it actually is. The optimal effect would be if the image distance is equal to the object distance, if not, the perceived depth is not as great. This can be explained by the fact that when the image distance increases, the angular difference between the red and blue will amount to a much larger perceived depth difference (Kishto, 1965). Increasing the prism angle will not increase the image depth. It will increase the angular separation between the red and blue images; however it will also force the fused image to appear even closer to the viewer. The result is the gain is lost to the increase in angular separation, which acts over a smaller distance. The natural colour scheme with a diverging prism arrangement will not improve the situation. The viewer will need to adjust the eyes outward to fuse the images, resulting in a similar visual pain.

6.2.2 Double Prism Glasses

In order to improve the effectiveness of the chromo stereoscopic technique and to overcome the problems with visual distress, Steenblick (1987) investigated the approach to use a double prism arrangement. By introducing an extra set of prisms, more specifically a super chromatic prism, he found that the image space could be put in the centre of the object plane and at the same time retain the colour dispersion. Super chromatic optics are designed to maximize colour dispersion and minimize other refractive effects. A single colour in the visible spectrum is then selected to correlate with the object plane. This single colour is often yellow as it is located in the middle of the visual spectrum. The other colours of the spectrum are then distributed to place the parts of the image in front or behind the object plane. By employing the double prism two goals were achieved. First the difference between focal distance and convergence distance is greatly reduced, resulting in almost entirely eliminating the visual distress. Secondly the chromo stereoscopic effect was enhanced. The desired properties of the super chromatic prism is to increase the refractive index (i.e. maximize the dispersion of light penetrating the prism). The prisms are assembled as illustrated in figure 6.8.
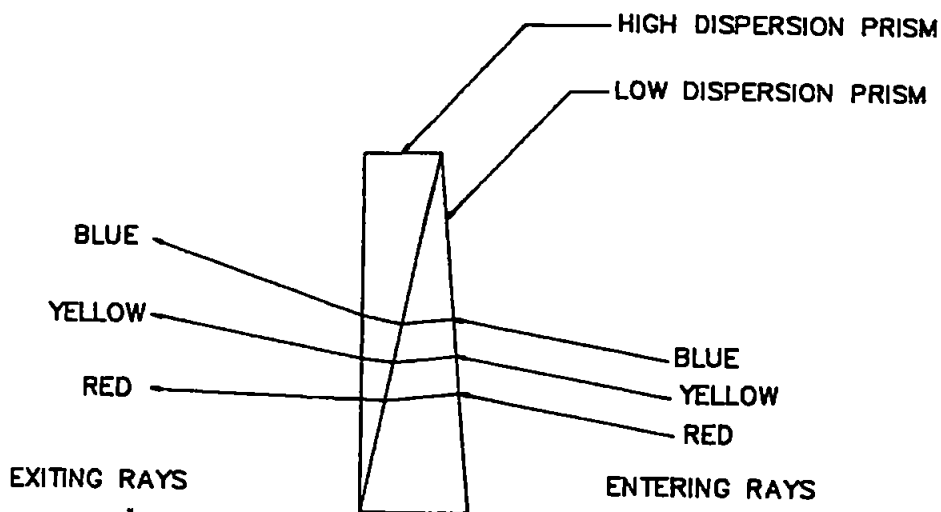
Figure 6.8: **The Super chromatic prism. The prism arrangement in this figure uses a reversed colour scheme with blue colours in front (Source: Steenblik, 1987).**

One of the prisms forming the super chromatic prism has a high refractive index resulting in high dispersion of the light. Further it introduces the undesired deviation of the light rays. The second prism counteracts this undesired deviation by applying an equal deviation of the selected colour in the opposite direction. The result is that the path of the selected colour, yellow in figure 6.8, is parallel before and after penetrating the super chromatic prism. However the path of the light ray is displaced to correlate the object distance and the image distance (figure 6.8). The colours of the light ray on each side of the selected colour are highly dispersed to produce the enhanced chromo stereoscopic effect.

The super chromatic glasses can be made by several optical materials, such as glass, plastics and liquids. The earlier glasses were often made of liquid filled glass cells, because of the high refractive index property. In the early 1990s binary optics (microptic film) were developed at Massachusetts Institute of Technology (MIT). Binary optics can be used to mass produce inexpensive chromo stereoscopic glasses with optical properties that closely match the liquid optics glasses (Steenblik, 1987). Using binary optics, Steenblik produced a very effective plastic blazed grating super chromatic prism that is used in the chromo stereoscopic glasses. Figure 6.9 shows a cross section of the prism from above. The grating has a saw tooth profile.
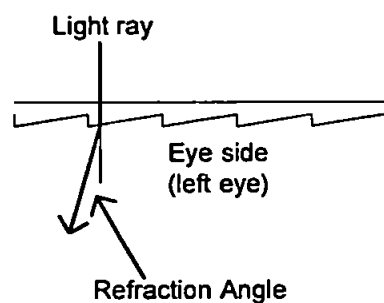
Figure 6.9: Cross section profile of the super chromatic blazed grating prism (Source: Lipson, 1995).

Tuneable depth glasses are also developed. These glasses are made by arranging two super chromatic prisms in front of each other for each eye. The super chromatic lenses are

mechanically linked in such a way that they can counter rotate. By rotating the prisms the viewer can select any desired image depth.

6.2.3 Applications

Chromo stereoscopy is well suited to be applied in several different mediums such as the computer graphic display or hardcopy printed images. After the discovery of the chromo stereoscopic effect by Einthofen (1885) some studies on the effect has been performed by researchers such as Kishto (1965) and Sundet (1972). As Steenblik made it possible to manufacture large quantities of low-cost super chromatic glasses in the early 1990s one should expect that this simple to employ stereoscopic technique would become an alternative to other stereoscopic techniques, especially the more established multiplexing techniques. However, except for Toutin (1997), it has been impossible to find any documentation or examples that this method is used in any scientific work or implemented in any software application that presents scientific data. The only material found is simple demonstrations of the technique.

Toutin (1997) performed some tests using chromo stereoscopic techniques to enhance the depth perception on remote sensing data. Data from multiple remote sensing sources such as aerial photographs, images from Landsat TM-3, ERS-1 and Radarsat was merged with the corresponding Digital Elevation Model (DEM) and colour coded according to the chromo stereoscopic principles. The images were ortho-rectified, the line of sight vertical and hence the colour coding is a direct function of the z-axis of the DTM, (figure 4.10). Toutin concluded that this is an interesting and simple technique to enhance depth perception of remote sensing data.

Chapter 7: Chromo Stereoscopic Application Development

This chapter will initially give a short description of the computer modelling techniques that the chromo stereoscopic (CS) application is developed on, then the actual CS application development is described in detail.

The Haber and McNabb (1990) visualisation model that was briefly discussed in chapter 5.1 describes the data preparation process as the first major process in the scientific visualization pipeline. The raw data is merged and processed to create a model from which new data can be derived. In this project, raw data from the classes defined in chapter 5.7 are employed. Chapter 8 describes, in more detail, the different datasets used to create and evaluate the chromo stereographic application.

The software selected for the data preparation process is the 3ds max 6 (Discreet, 2004) 3D modelling software, which is one of the world's leading professional 3D modelling applications. It has a powerful import function that can supply the upcoming model with raw data from various sources. Among the more popular import formats are AutoCAD (DXF, DWG) files, Initial Graphics Exchange Standard (IGES) files, Adobe Illustrator files and Virtual Reality Modelling Language (VRML) files that make it possible to import files from web browser applications (Murdock, 2003). For the data preparation phase of this project's experimental work the raw data is imported into 3ds max 6, merged and refined to prepare a computer model suitable for the CS application. Some of the objects can, if necessary, be created in the 3ds max 6 application. A man made object can, for example, either be imported from a CAD application, or it can be created directly in the 3ds max 6 application. Figure 7.1 illustrates the data preparation process for this project.

```
┌─────────────────┐   ┌─────────────────┐
│                 │   │   3ds max       │
│                 │   │                 │
│   Raw Data      │   │ - Import data   │                ,
│                 │   │ - Make objects  │
│ - DTM           │   │ - Merge data    │        ┌──────────────────┐
│ - CAD objects   │   │ - Build model   │        │                  │
│ - Sensor data   │   │    - geometry   │        │     Model        │
│ - Mathematical  │──▶│    - surface modelling│──▶│ ready for export to│
│   models  '     │   │ - Refine data   │        │ Chromo Stereoscopic│
│ - Etc.          │   │    - texture    │        │   application    │
│                 │   │    - lighting   │        └──────────────────┘
│                 │   │ - Save model in 3ds│
│                 │   │   format        │
│                 │   │                 │
└─────────────────┘   └─────────────────┘
```
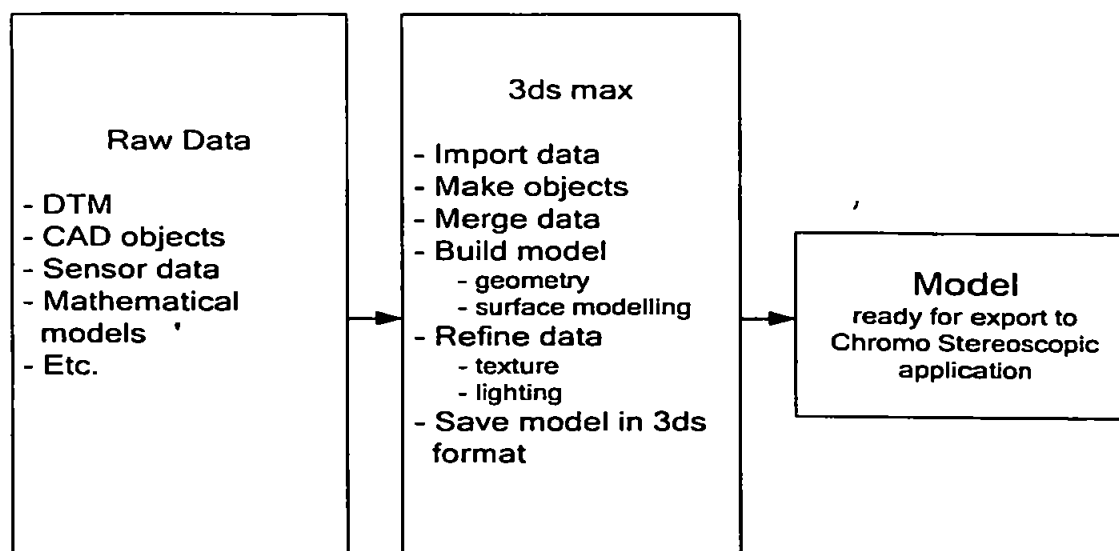
Figure 7.1: Data preparation process for the experimental work

The focus of the experimental work in this project is on the visualisation mapping and

presentation process of the visualisation model. Consequently, the work on the import of

the data will not be covered to the same level of depth. It is possible to make data objects

in the 3ds max application itself and include them in the model, which is a process similar

to building an object in a CAD application and exporting it to 3ds max 6. All the objects

that constitute the model, either imported from external applications or produced in 3ds

max are merged into one complete data model. It is out of the scope of this project to

describe, in detail, the computer modelling techniques used in the 3ds max application

when building the models. Watt (2000) and Hearn & Baker (2004) give a detailed

description of current computer modelling techniques. Murdock (2003) describes how

these stages are implemented using the 3ds max 6 application. This text will only briefly

describe the stages relevant to the CS application. Foley et. al. (1990) and Watt (2000) give

comprehensive descriptions on the general theory of how to create the objects, setting up

the scenes and the rendering process. The 4 major stages in the rendering process of a

computer model are as illustrated in figure 7.2 (Angel, 2000).
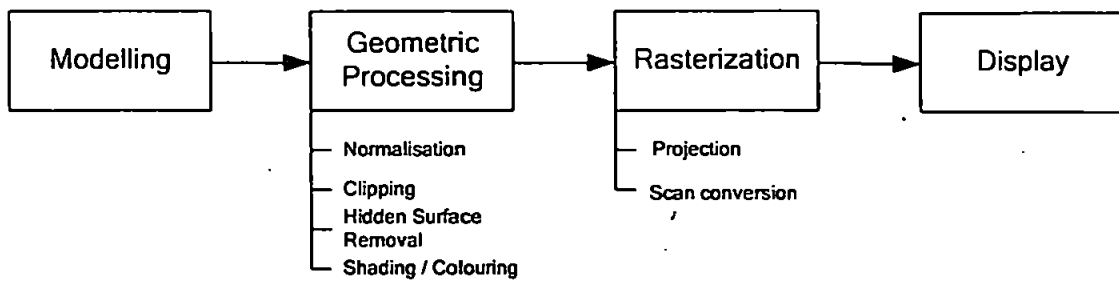
Figure 7.2: Major tasks when rendering geometric objects (Source: Angel, 2000)

The first stage, modelling, includes the creation of objects and building the scene. In this experiment, the modelling stage is completed in the 3ds Max 6 application as described earlier. The three other stages are completed by the developed OpenGL (Open Graphics Library) application described later in this chapter. The second stage, geometric processing, determines which objects appear on the display and also integrate colour and shades to the objects. The first step of geometric processing is to normalize the model projection. This is done in order to make the process of clipping the lines around the viewing volume more calculation efficient. By applying a normalization transformation, the model projection view volume is transformed into a canonical view volume where the x and y boundary planes are equal to -1 and 1, and the z boundary planes are 0 and -1 (Foley, 1990). The clipping process establishes which objects, or parts of the objects, to display. The objects or parts of objects which fall within the specified viewing volume will be accepted, the parts that are rejected in the clipping process will be excluded from the display during the hidden surface removal process. The final stage in the geometric process is the lighting / shading computations. In the rasterisation stage the 3D model is transformed into a 2D picture through the projections. In the scan conversion process each pixel on the display is assigned a characteristic value computed earlier based on geometric shape, lighting / shading colouring and texture. Finally in the display stage the picture is taken from the frame buffer in the computer memory and presented on the computer display.

A parallel process in OpenGL is the pixel (picture element) operation process. This process merges with the geometric rendering process at the rasterisation stage (figure 7.3) and work on the pixel level and not the vertices level as is the case for the geometric rendering process. Several operations are accessible in the pixel operation process, however only the texture mapping process will be addressed here. Vertices are mapped to the texture coordinates and the texture value for each pixel is determined through interpolation. The surface texture is in this way merged with the geometric object.

The refining of the model will however be described to some depth as it has direct influence on the visualisation mapping process. Finally, before the refined model is exported from the 3ds application into the CS application, the data is saved in the 3ds format.

7.1 Application Development

Another advantage of selecting 3ds max 6 in the data preparation process is that it supports the OpenGL hardware acceleration graphics language. The Microsoft Visual C++ programming language and OpenGL are used to develop the chromo stereographic application; these applications are briefly described in chapters 7.1.1 and 7.1.2.
All the work in making the models and developing the CS application is performed on a Dell Precision M60 laptop PC with an Intel Pentium M processor (the internal clock speed is 1.6 MHz). The size of the internal physical memory is 512 MB, the hard disc drive has a storage capacity of 60 GB and the graphics card is a Nvidia Quadro FX Go700 with a memory capacity of 128 MB and hardware supported OpenGL.

7.1.1 Open GL

OpenGL is the leading programming environment for developing graphics applications. It has, since it was introduced in 1992, become the industrial standard 2D and 3D graphics API (Application Programming Interface). OpenGL is a software interface to computers

graphics hardware (Woo et. al., 1999). One of the major advantages of OpenGL is that it is

platform independent (i.e. OpenGL can run on all platforms, laptop, desktop or

workstation) and in a wide range of software environments such as Mac, OS/2, Unix,

Linux and MS Windows. The graphics library consists of several hundred distinct

commands that are called upon by the programming language in use; for this project the

Microsoft Visual C++, described in chapter 7.1.2 is the programming language.

Figure 7.3 shows a schematic diagram of the OpenGL process. The commands are entered

into the graphics library on the left side of the figure. Some of the commands specify

geometric objects to be drawn while others control how the objects are handled by the

various stages. Most of the commands may be accumulated in a display list for processing

by OpenGL later. Otherwise, commands are effectively sent through a processing pipeline.
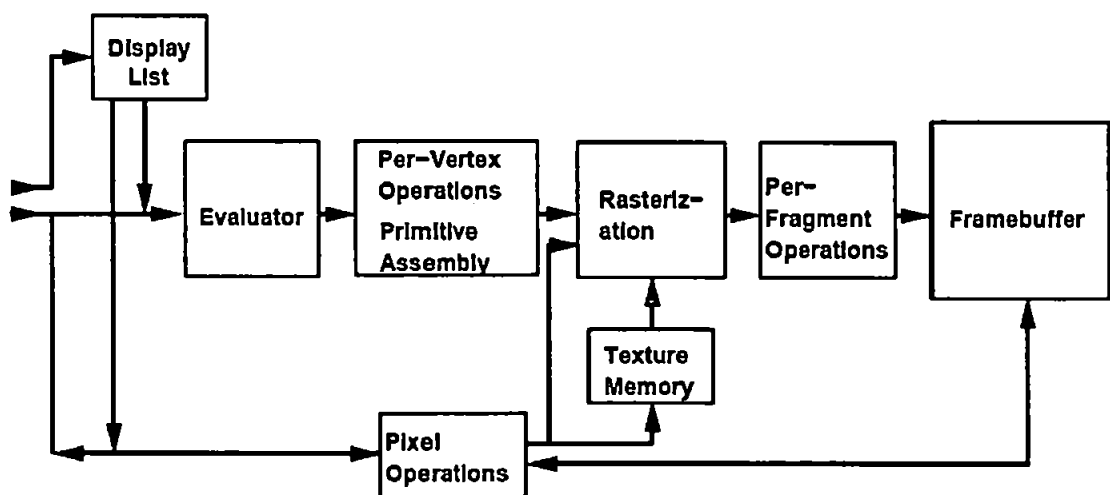
Figure 7.3: Schematic presentation of the OpenGL pipeline (Source: Woo et. al.,
1997)

The first stage provides an efficient way to approximate curve and surface geometry by

evaluating polynomial functions of input values. The next stage operates on geometric

primitives described by vertices: points, line segments and polygons. In this stage, vertices

are transformed and lighting included. The objects are clipped to a viewing volume in

preparation for the next stage, rasterisation. This stage produces a series of frame buffer

addresses and values using a 2D description of a point, line segment or polygon. Each fragment so produced is fed to the next stage that performs operations on individual fragments before they finally alter the frame buffer. These operations include conditional updates into the frame buffer based on incoming and previously stored depth values (to effect depth buffering), blending of incoming fragment colours with stored colours, as well as masking and other logical operations on fragment values (Woo et. al. 1999).

The vertex processing portion of the pipeline, to send a block of fragments directly to the individual fragment operations, can be omitted, to write a block of pixels directly to the frame buffer; values may also be read back from the frame buffer or be copied from one portion of the frame buffer to another. These transfers may include some types of decoding or encoding. This ordering is meant only as a tool for describing the GL, not as a strict rule for how the GL is implemented, and it is presented only as a means to organize the various operations of GL. Objects, such as curved surfaces for instance, may be transformed before they are converted to polygons.

There are several related libraries that are used. When Microsoft Visual C++ was set up for this experiment, the Graphics Library Utility (GLU) and GL Utility Toolkit (GLUT) libraries was also installed. The GLU library only uses the functions contained in the OpenGL library, but contains codes for common objects relieving the programmer from writing standard code repeatedly. The function of GLUT is to provide the minimum functionality required in a windows system. It is designed to hide the complexities of the window system API in use, here Microsoft Windows. In essence, it will create a window on the display screen where the output of the OpenGL application is displayed (OpenGL, 2004).

7.1.2 MS Visual C++

OpenGL is as described in 7.1.1 an API, an interface to the computers graphics hardware. This implies that the software application needs to be developed using a computer

programming language that calls upon the desired GL functions. OpenGL supports a wide range of programming languages, such as Ada, C, C++, Fortran and Java. For this project the Microsoft Visual C++ .NET programming language environment was selected because the author has some previous programming experience in C++. The GLU and GLUT libraries was downloaded from the World wide web (WWW), installed and made available for visual C++ as described in appendix 2 (Taylor University, 2004).

7.2 Application Structure

The model developed in 3ds max 6 is imported to the chromo stereoscopic OpenGL application using a 3ds file format import library. Details about the import library are found in appendix 3. In order to generate a chromo stereoscopic effect, a suitable surface texture has to be draped over the model. The aim is to create a coloured surface texture that distributes the colours in the visible spectrum onto the model, where the part of the model closest to the viewpoint will be red and the part of the model farthest away from the viewpoint will be blue. A colour ramp function for a 1D texture from red to blue was developed, the ramp starts where the closest part of the model crosses the line of sight, the ramp ends where the line of sight vector exits the part of the model farthest away from the model as illustrated in figure 7.4.
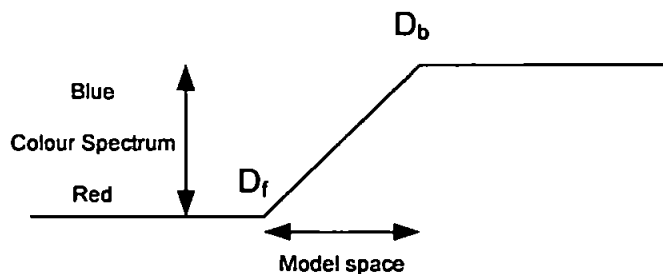
Figure 7.4: **Colour ramp function for one dimensional texture. The visual colour spectrum is distributed along the vertical axis. The model space, front to back of model along the line of sight axis, is distributed from the distances D_f to D_b along the horizontal axis.**

The HSV colour space model is used to create the colour ramp function. One of the

advantages of using the HSV colour model is that by setting the saturation and brightness

values equal to 1 the saturation and brightness of the texture will be fixed (Watt, 2000).

The HSV colour model is then converted to the hardware oriented RGB colour model, and

the hue values from 0° (red) - 240° (blue) are interpolated in the range between D_f and D_b

for an optimal colour distribution. If the start and end point of the ramp function is

improperly set, the chromo stereoscopic effect will not be optimal, as the colour spectrum

does not properly envelope the model.

As the colour of the pixels along the line of sight is established, the texture coordinates

have to be generated. OpenGL has a dedicated automatic function for this operation. As a

texture-mapped scene is drawn, both object coordinates and texture coordinates for each

vertex must be provided. After transformation, the object coordinates determine where on

the screen that particular vertex is rendered. The texture coordinates determine which texel

(texture element) in the texture map is assigned to that vertex. A texel represents the

smallest graphical element in 2D texture mapping to "wallpaper" the rendition of a 3D

object to create the impression of a textured surface. In exactly the same way that colours

are interpolated between two vertices of shaded polygons and lines, texture coordinates are

linearly interpolated between vertices.

Texture coordinates can comprise one, two, three, or four coordinates. They are usually

referred to as the s, t, r, and q coordinates to distinguish them from object coordinates (x, y,

z, and w). For 1D texture the s coordinate is used; for 2D textures, s and t are used.

Equation 7.1 specifies the generated texture coordinate (Hearn and Baker, 2004):

texture coordinate (s) $= p_1 x_0 + p_2 y_0 + p_3 z_0 + p_4$ (7.1)

where p_1 to p_4 are the texture parameters for the coordinate (x_0, y_0, z_0). Usually the texture-

coordinate values range between 0 and 1.

As the chromo stereoscopic texture is 1D, the s texture coordinate is required to be

specified for each coordinate on the model surface; hence the parameters p1 to p4 must be defined. The automatic texture generation function can differentiate between an object model referenced coordinate system or a coordinate system where the z axis (model depth) is defined as the line of sight. For the CS application it is preferable to apply the latter. The generated texture coordinate (s) value at the closest point where the line of sight axis crosses the model surface (D_f) must equal zero (red), and the generated texture coordinate value at D_b must equal one (blue). The one dimensionality of the texture along the z axis results in $p_1 = p_2 = 0$. The following simplified equation is then derived from equation 7.1.

$$s = p_3 z_0 + p_4 \qquad\qquad (7.2)$$

Evaluating the ramp function in figure 7.4 we get the following equation.

$$s = \frac{-z_0}{D_b - D_f} - \frac{D_f}{D_b - D_f} \qquad\qquad (7.3)$$

The parameters for the automatic texture generation function in equation 7.1 can then be derived.

$$p_1 = p_2 = 0$$

$$p_3 = \frac{-1}{D_b - D_f}$$

$$p_4 = \frac{-D_f}{D_b - D_f}$$

How D_f and D_b should be set for optimum performance will be discussed in chapter 8.

7.3 Program description

In the following section each main module in the source code of the CS application will be described in detail. Figure 7.5 describes the main tasks of the modules in the applications and how the modules interact. The modules are developed and programmed by the author using C++ and OpenGL except the HSV2RGB function module which is adapted from Foley et. al. (1990), and the Load3ds model import library (appendix 3) which is downloaded from internet and adapted.
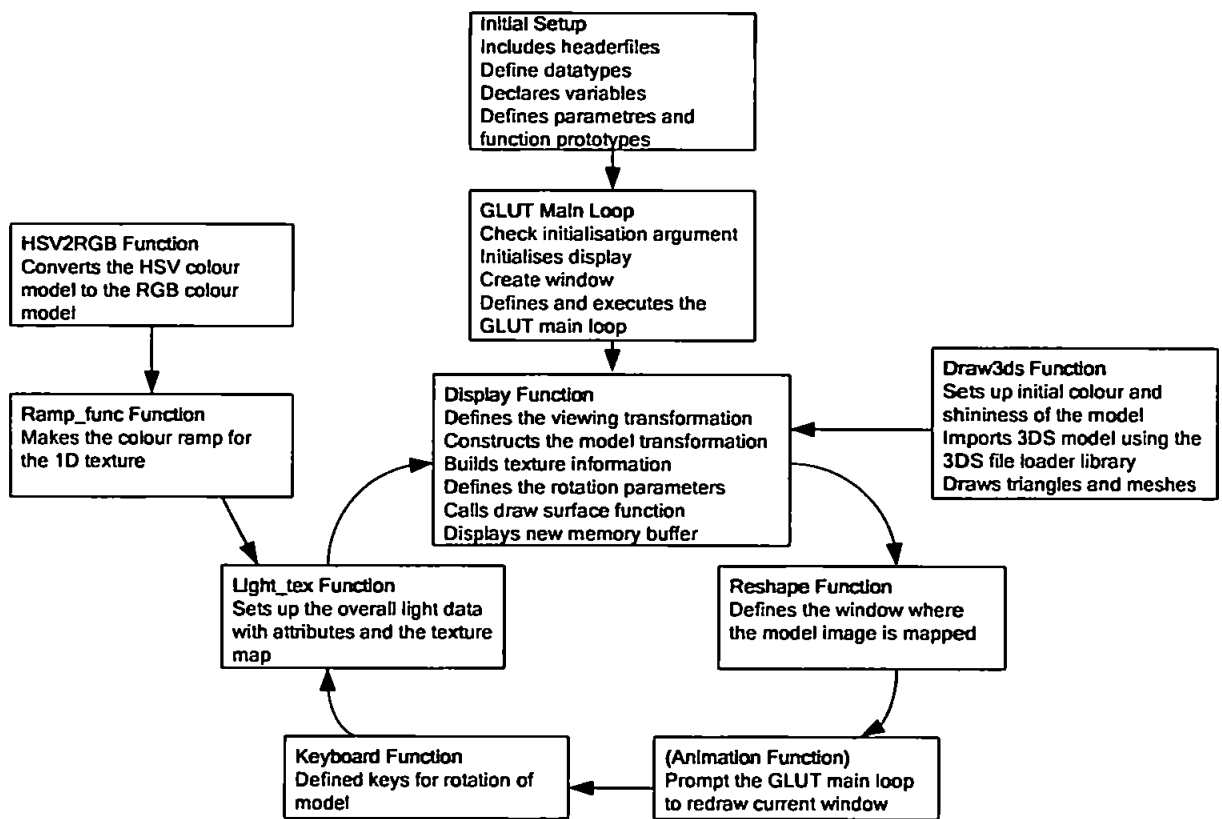
Figure 7.5: Application modules description and interaction.

7.3.1 Initial setup

The initial program setup includes relevant header files, defines data types, declares variables and defines parameters and function prototypes. A header file is used to create *libraries* of code that can be used over and over, the header files can be recognised by the .h extension to the filename (almost all C++ programs require some header files to be

included). When the compiler finds a reference to a header file it writes the contents of that header file into the *executable* code of your program. The **#include** directive tells the pre processor to treat the contents of a specified file as if those contents had appeared in the source program at the point where the directive appears. An overview of the header files for this application is included in appendix 4.

`static char ch;` This code declares a character array called "ch" and initializes it with the filename that is being compiled. The array contains the characters from the keyboard that controls the rotation of the model. When modifying a variable, the `static` keyword specifies that the variable has static duration (it is allocated when the program begins and de-allocated when the program ends) and initializes it to 0 unless another value is specified. Type `char` is an integral type that usually contains members of the execution character set — in Microsoft C++, this is ASCII.

The "1" and "2" keys rotate the model clockwise and counterclockwise around the x-axis. The "3" and "4" keys rotate the model clockwise and counterclockwise around the y-axis. The "5" and "6" keys rotate the model clockwise and counterclockwise around the z axis. The character array is used in both the display function (7.3.6) and the keyboard function (7.3.7).

`static GLfloat saveState[16]` declares the model view matrix that is a 4 by 4 matrix used to specify the viewing, modelling and projection transformations. This matrix is then multiplied by the coordinates of each vertex in the model to accomplish the transformations (Woo et. al. 1999). The `viewProj[16]` declares an array where the original viewing projection is saved and the transformation is held. These two arrays are used in the display function (7.3.6). t= 0 sets the time variable to zero, to initialise the animation function.

The L3DS scene command loads the model file (scene) in 3ds format into the application. The data type `float vp` defines the distance of the viewpoint to the model (figure 7.6). By

changing the data type value the viewpoint is moved closer to or further away from the model (floating data types are capable of specifying values that may have fractional parts). The variables Df and Db defines the front and back limits of the ramp function (i.e. the start and stop points of the colour texture, see figure 7.6). Chapter 8 will demonstrate how important it is that these values are set correctly to get the desired stereoscopic effect.
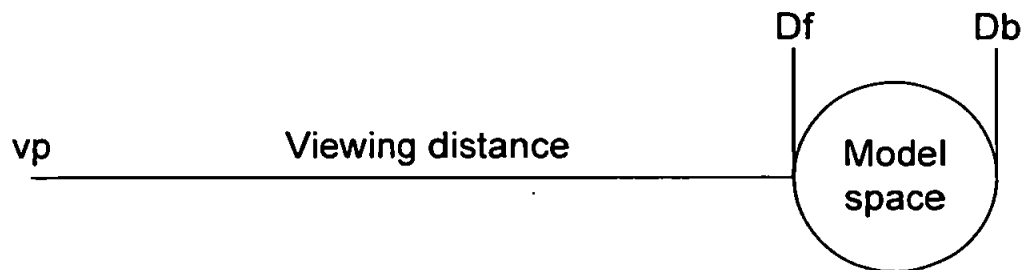
Figure 7.6: Viewing distance and ramp start and endpoint variables.

The 'textureparameters' and 'texturename' data types are defined and later applied in the display function to calculate the colour texture map. GLuint defines texturename as an integer value in OpenGL. The data type ramp is defined with 256 steps and 3 values specified (h,s and v).

The list of function prototypes are defined using the statements of the form format void name ( ). The parenthesis defines the required arguments. If the parenthesis contains void, the function requires no argument and no values are returned from the function. The unsigned character argument in the keyboard function indicates an input argument from the keyboard is expected without a sign extension.

Table 1: Initial Setup

```
#include "stdafx.h"
#include "l3ds.h"

#ifdef _WIN32
#include <windows.h>
#endif

#include <GL/glut.h>
#include <stdlib.h>
#include <stdio.h>
#include <math.h>

static char ch;

static GLfloat saveState[16] = {1.0,0.0,0.0,0.0,
                                 0.0,1.0,0.0,0.0,
                                 0.0,0.0,1.0,0.0,
                                 0.0,0.0,0.0,1.0},
              viewProj[16],
              t=0.0;

L3DS scene;

float vp = 100.0;
float Df, Db;
float textureparametres[4];
static GLuint texturename;
float ramp[256][3];

void ramp_func(void);
void HSV2RGB(float, float, float, float *, float *, float *);
void light_tex( void );
void draw3ds( void );
void display( void );
void reshape( int ,int );
void keyboard(unsigned char, int, int );
void animation ( void );
```

7.3.2 Setup Colour ramp function

In table 2 the ramp_func function makes the colour ramp for the 1D (linear) texture, the ramp values spans from 0 to 240 in 256 steps. Each step is defined by the integer value variable i. Further the hue, saturation, value, red, green and blue variables are defined as floating point values. The 'for loop' processes the hue value for each step (i = 0 to 256). The saturation and value (brightness) are constant and set to 1. The loop then calls the HSV2RGB function and converts the colours from the HSV to the RGB colour model for each ramp step. The ramp is then put together with the computed RGB values corresponding to each ramp step.

Table 2: Ramp function

```
void ramp_func(void)
{
    int i;
    float h, s, v, r, g, b;

    for (i=0; i<256; i++) {
        h = (float)i*240.0/255.0;
        s = 1.0; v = 1.0;
        HSV2RGB( h, s, v, &r, &g, &b );
        ramp[i][0] = r; ramp[i][1] = g; ramp[i][2] = b;
    }
}
```

7.3.3 HSV to RGB colour model conversion function

The function that converts from the HSV colour model to the RGB colour model is

adapted from Foley et. al. (1990) figure 13.34, where the function is fully explained. It is

not of significant value for the reader of this text to understand in detail how the

conversion is performed; the detailed description of this function is thus omitted. The

function is used by the ramp function to output RGB data.

Table 3: HSV to RGB conversion function

```
void HSV2RGB( float h, float s, float v, float *r, float *g, float
*b)
{

    float f, p, q, t;
    int   k;

    h = h/60.0;
    k = (int)h;
    f = h - (float)k;
    p = v * (1.0 - s);
    q = v * (1.0 - (s * f));
    t = v * (1.0 - (s * (1.0 - f)));
    switch (k) {
        case 0: *r = v; *g = t; *b = p; break;
        case 1: *r = q; *g = v; *b = p; break;
        case 2: *r = p; *g = v; *b = t; break;
        case 3: *r = p; *g = q; *b = v; break;
        case 4: *r = t; *g = p; *b = v; break;
        case 5: *r = v; *g = p; *b = q; break;
    }
}
```

7.3.4 Light and texture setup function

Figure 7.7 shows a flow diagram of the main processes of the light and texture setup function.

```
┌─────────────────────────────────────────┐
│        Set GL variables for function     │
└─────────────────────────────────────────┘
                    │
                    ▼
┌─────────────────────────────────────────┐
│           Set up overall lightdata       │
└─────────────────────────────────────────┘
                    │
                    ▼
┌─────────────────────────────────────────┐
│      Enable and define lighting for model│
└─────────────────────────────────────────┘
                    │
                    ▼
┌─────────────────────────────────────────┐
│             Set up texture map           │
└─────────────────────────────────────────┘
```
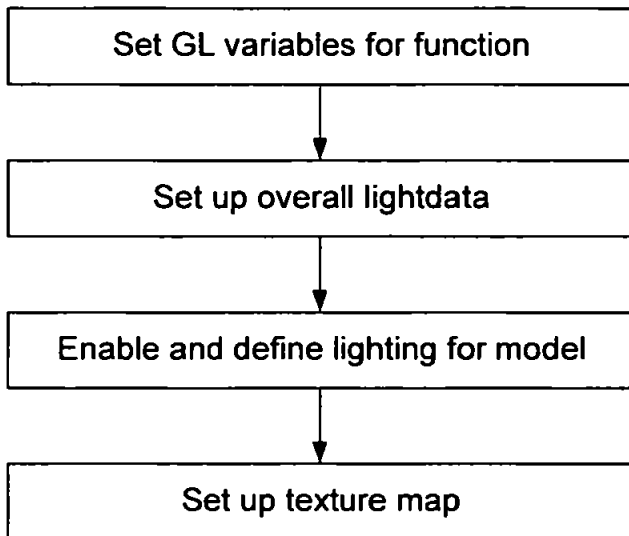
Figure 7.7: Flow diagram of the light and texture setup function.

The light_tex function sets up the overall light data with attributes and the texture map, see table 4. First the variable i is declared and set equal to 1, it is used later as a parameter when establishing two sided lighting on the model. Next, three GL floating point variables are defined. The light_pos0 variable positions the light source and supplies the GL_POSITION parameter with the light source coordinates (x, y, z) and sets the light source to be non directional (value of 1.0). The light_col0 variable supplies the parameters GL_SPECULAR and GL_DIFFUSE with values for the specular and diffuse intensity of the light. GL_SPECULAR affects the specular light effect from an object, which is often the same colour as the light shining on it. To produce a realistic specular effect, the values for the GL_SPECULAR and GL_DIFFUSE parameters should be set equal. GL_DIFFUSE (1.0, 1.0, 1.0, 1.0) produces a bright white light. The four values define the RGBA colour of the light. The A value is not used without effects such as blending or transparency is desired. The amb_col0 variable supplies the GL_AMBIENT parameter with values for the intensity of the ambient light that a light source supplies to the model, with the default value being zero (RGB) meaning no ambient light present (here 0.3). The GL float variable

- 92 -

mat_specular is put into the glMaterialfv command, the four values define the RGBA colour setting. The command glClearColour clears the colour buffer and defines the clearing colour. The command glShadeModel specifies the shading model to be used when drawing lines or filled polygons. The GL_SMOOTH parameter interpolates the colour between the vertex colours resulting in a smooth shaded model. The glMaterialfv specifies the material properties to use for the lighting calculations. The properties are applied to both the front and back of the model. The specular reflection property makes the reflection from the model dependent on the position of the viewer, and the reflection becomes brighter as the viewing angle approaches the direct viewing angle. The glLightfv command define the light source as described by the corresponding variables above. The glLightModeliv command sets up two sided lighting. When using two sided lighting the back facing polygons will also be illuminated. This is important, as in more complex models the back faces can be visible.

The next section, where each line starts with the command glenable, enables and defines the lighting for the application. The attribute GL_LIGHTING enables the lighting, and GL_LIGHT0 enables the light source (in this application only one light source is defined). The attribute GL_DEPTH_TEST enables the depth buffer. The depth buffer (or z-buffer) establishes the distance from the viewpoint to each pixel in the model. This is an important function in this application and will be used later to define the colour coded texture applied to the model. The GL_NORMALIZE attribute will normalize the vectors after transformation. The normalized vectors are perpendicular to the model surfaces and will define the spatial orientation of the surface. It is important to establish this orientation to achieve correct lighting characteristics within the model.

The last section in light_tex function (table 4) sets up the texture map. When an object, or a model, is texture mapped, patterns are added to increase the detail of the object or model. In this case the desired colour coded 1D texture is added to the model. First the ramp_func

function is called. The command glPixelStore specifies the storing mode for the pixels in the memory, with the parameter GL_UNPACK_ALIGNMENT specifying the alignment requirements for the start of each pixel row in memory and value 1 setting the mode to byte alignment. The glTexEnv command sets the texturing function to be applied to the model. The GL_MODULATE parameter multiplies the object colour values with the texture values, in this instance the object colour is set to white resulting in the desired colour coded texture replacing the white colour.

The next three glTexParameter commands are executed, with the GL_TEXTURE_1D parameter defining the model texture as 1D. The first command contains the parameter GL_TEXTURE_WRAP_S with the value GL_CLAMP. The S in the parameter refers to the s-coordinate value in the 1D texture space, which specifies that the RGB colour in the texture is wrapped around the model. The GL_CLAMP value forces the s-coordinate values to range from 0.0 – 1.0, this range is used when wrapping a single (not a repeating) image onto a model. The second and third command contain the GL_TEXTURE MAG_FILTER and the GL_TEXTURE_MIN_FILTER parameters, both with the value GL_LINEAR. These commands will magnify or minimise the texture elements in order to align these elements with the boundaries of the pixel areas. The GL_LINEAR value forces the function to calculate the pixel colour as a linear combination of overlapping texture colours instead of selecting the nearest texture colour to a pixel.

The glTexImage1D command defines the one dimensional texture image. The first parameter defines the texture as a 1D texture, with the four following numbers describing the level of detail (0); the internal format for describing a texture element (3) which is GL_RGB format; the width of the texture image (256); the length of the ramp and the height of the texture image (0) because it is 1D (a straight line). The format parameter GL_RGB defines the texture colour data input format as RBG and the data type is floating point (GL_FLOAT). The description of the texture colours are stored in the parameter

ramp, which is called from the ramp_func function. At last the GL_TEXTURE_GEN__S

parameter turns on texture coordinate generation for the s-coordinate and the

GL_TEXTURE_1D parameter enables 1D texture generation.

Table 4: Light and texture function

```
void light_tex(void)
{
    GLint i = 1;

    GLfloat light_pos0[]={   0.0,  100.0,  100.0,   1.0 };
    GLfloat light_col0[]={   1.0,    1.0,    1.0,   1.0 };
    GLfloat amb_color0[]={   0.3,    0.3,    0.3,   1.0 };

    GLfloat mat_specular[]  =( 0.8,  0.8,  0.8,  1.0 );
    glClearColor( 0.1,  0.1,  0.1,  0.0 );
    glShadeModel(GL_SMOOTH);
    glMaterialfv(GL_FRONT_AND_BACK, GL_SPECULAR, mat_specular );
    glLightfv(GL_LIGHT0, GL_POSITION, light_pos0 );
    glLightfv(GL_LIGHT0, GL_AMBIENT, amb_color0 );
    glLightfv(GL_LIGHT0, GL_SPECULAR, light_col0 );
    glLightfv(GL_LIGHT0, GL_DIFFUSE, light_col0 );
    glLightModeliv(GL_LIGHT_MODEL_TWO_SIDE, &i );

    glEnable(GL_LIGHTING);
    glEnable(GL_LIGHT0);
    glEnable(GL_DEPTH_TEST);
    glEnable(GL_NORMALIZE);

    glPixelStorei( GL_UNPACK_ALIGNMENT, 1 );
    glTexEnvf( GL_TEXTURE_ENV, GL_TEXTURE_ENV_MODE, GL_MODULATE );
    glTexParameterf( GL_TEXTURE_1D, GL_TEXTURE_WRAP_S, GL_CLAMP );
    glTexParameterf( GL_TEXTURE_1D, GL_TEXTURE_MAG_FILTER, GL_LINEAR );
    glTexParameterf( GL_TEXTURE_1D, GL_TEXTURE_MIN_FILTER, GL_LINEAR );
    glTexImage1D( GL_TEXTURE_1D, 0, 3, 256, 0, GL_RGB, GL_FLOAT, ramp );
    glEnable( GL_TEXTURE_GEN_S );
    glEnable( GL_TEXTURE_1D );
}
```

7.3.5 Draw3ds function

The Draw3ds function sets up the initial surface colour and shininess of the model, and

draws the model surface triangle mesh. Figure 7.8 shows a flow diagram of the main

processes of the draw3ds function. The data type used for the drawing of the 3D vertices

was defined as point3 in the initial setup. The integer variables i and j are defined for

calculations within the function. The GL floating variables white[], yellow[] and

mat_shininess[] are defined and specified for later use as parameters in the glMaterialfv

command. The white[] and yellow[] variables are specified with the corresponding RGBA

- 95 -

values. The mat_shininess variable is set to 30, but the value can range from 0 to 128 and it controls the extent and brightness of the light (a higher value results in a brighter and more concentrated highlight).

```
┌─────────────────────────────────────────┐
│        Set GL variables for function      │
└─────────────────────────────────────────┘
                    │
                    ▼
┌─────────────────────────────────────────┐
│      Define model material properties     │
└─────────────────────────────────────────┘
                    │
                    ▼
┌─────────────────────────────────────────┐
│     Draws the triangles and meshes of the │
│                   model                    │
└─────────────────────────────────────────┘
```
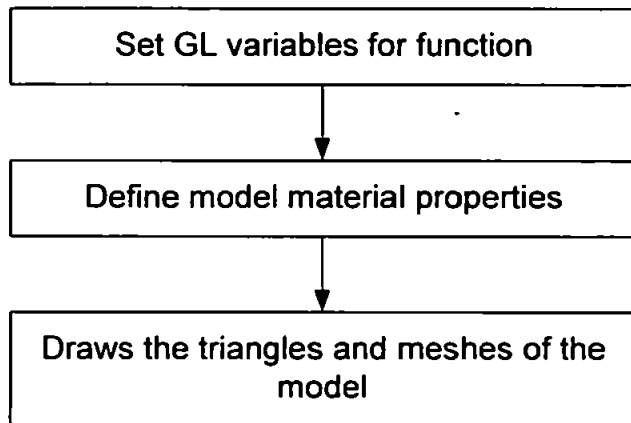
Figure 7.8: Flow diagram of the draw3ds function

The glMaterialfv command defines the properties of the object's material. GL_FRONT, GL_BACK and GL_FRONT_AND_BACK define what faces of the model the material property is applied to. The front face material is attached with a white diffuse colour. The material facing back is attached with a yellow diffuse colour. The diffuse colour property of the material makes the colour of the model a function of the colour and angle of the incoming light. Both front and back faces are attached with a shininess or specular exponent of 30.

The remaining part of this function contains two loops to draw triangles and meshes, which are imported using the L3DS import library (appendix 4). First, the variable j is set equal to the L3ds method GetMeshCount that returns the number of meshes in the loaded 3DS file. The j variable is then set to mesh. GetTriangle Count (), which gets the number of triangles in the model and multiplying by 3 gives the total number of vertices in the model. The next line loads the actual 3DS model triangle mesh. The glBegin function with the GL_POLYGON argument executes a list of glVertex commands that constructs the actual polygons of the model from the vertices. The glNormal3fv command calculates the normal vector of each of the loaded triangles, which is important as explained earlier in

establishing the orientation of the surface of each triangle in the mesh. The glVertex4fv

command specifies the x, y and z coordinates of the vertices of the loaded model. The

function terminates with the glEnd () command.

Table 5: Draw3ds function

```
void draw3ds(void)
{
    int   i, j;

    GLfloat white[] = {1.0, 1.0, 1.0, 1.0};
    GLfloat yellow[]= {1.0, 1.0, 0.0, 1.0};
    GLfloat mat_shininess[]={ 30.0 };

    glMaterialfv(GL_FRONT, GL_DIFFUSE, white );
    glMaterialfv(GL_BACK, GL_DIFFUSE, yellow );
    glMaterialfv(GL_FRONT_AND_BACK, GL_SHININESS, mat_shininess );
    j = scene.GetMeshCount();

    for (uint i= 0; i<scene.GetMeshCount(); i++)
    {
        LMesh &mesh = scene.GetMesh(i);

        j = mesh.GetTriangleCount() * 3;

        for (i = 0; i < mesh.GetTriangleCount(); i++)
        {
            LTriangle tri = mesh.GetTriangle(i);

            glBegin(GL_POLYGON);

            glNormal3fv((const GLfloat*)&mesh.GetNormal(tri.a));
            glVertex4fv((const GLfloat*)&mesh.GetVertex(tri.a));
            glNormal3fv((const GLfloat*)&mesh.GetNormal(tri.b));
            glVertex4fv((const GLfloat*)&mesh.GetVertex(tri.b));
            glNormal3fv((const GLfloat*)&mesh.GetNormal(tri.c));
            glVertex4fv((const GLfloat*)&mesh.GetVertex(tri.c));

            glEnd(); ·
        }
    }
}
```

7.3.6 Display function

The Display function defines the viewing transformation, constructs the model

transformation, builds the texture information and defines the rotation parameters before

calling the draw3ds function and finally displaying the model, figure 7.9 illustrates the

main processes of the display function in a flow diagram.

```
┌─────────────────────────────────────────┐
│       Construct model transformation      │
└─────────────────────────────────────────┘
                     │
                     ▼
┌─────────────────────────────────────────┐
│        Include viewing transformation     │
└─────────────────────────────────────────┘
                     │
                     ▼
┌─────────────────────────────────────────┐
│          Build texture information        │
└─────────────────────────────────────────┘
                     │
                     ▼
┌─────────────────────────────────────────┐
│    Define rotation of viewing transformation │
└─────────────────────────────────────────┘
                     │
                     ▼
┌─────────────────────────────────────────┐
│     Apply model transformation and save it │
│                  on stack                 │
└─────────────────────────────────────────┘
                     │
                     ▼
┌─────────────────────────────────────────┐
│       Rebuild the model view matrix by first │
│           multiplying by the viewing      │
│        transformation, then by the model  │
│               transformation              │
└─────────────────────────────────────────┘
                     │
                     ▼
┌─────────────────────────────────────────┐
│           Call for draw3ds function       │
└─────────────────────────────────────────┘
                     │
                     ▼
┌─────────────────────────────────────────┐
│          Display new memory buffer        │
└─────────────────────────────────────────┘
```
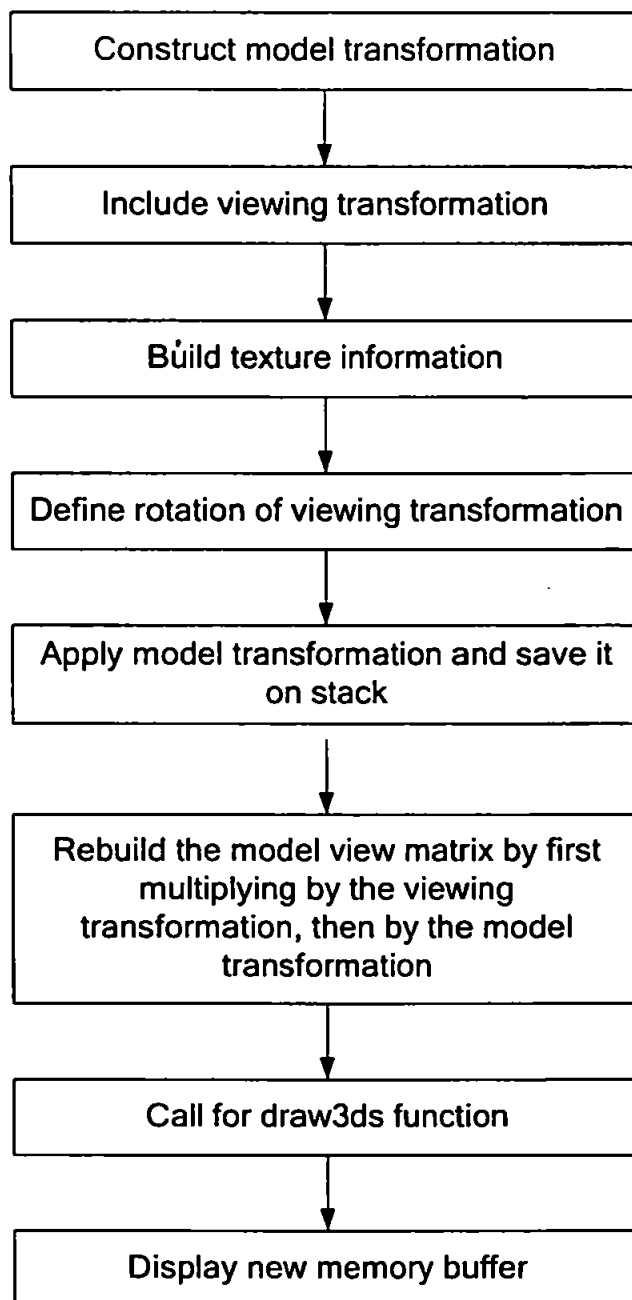
Figure 7.9: Flow diagram of the display function

First, the type name angle is defined for use in the rotation routine of this function. Then, the colour and depth buffers (which holds all the pixel depth values of the model) are cleared to the background colour (black) for the drawing of the model to be displayed. The projection-transformation matrix is generated by first setting the OpenGL projection mode (glMatrixMode (GL_PROJECTION). The glLoadIdentity command clears the current modifiable matrix and sets it equal to the identity matrix to erase the effect of any current viewing transformation. The gluPerspective command generates a perspective projection

- 98 -

matrix and the parameters are set for optimal viewing of the model. In this application, the parameters have to be adjusted manually in the programming line for each model loaded. The four parameters set the vertical field of view angle (fovy), the aspect, which is the width of the view divided by the height of the view (1.0 specifies a square), and the near and far values along the depth axis. Figure 7.10 illustrates the gluPerspective parameters.
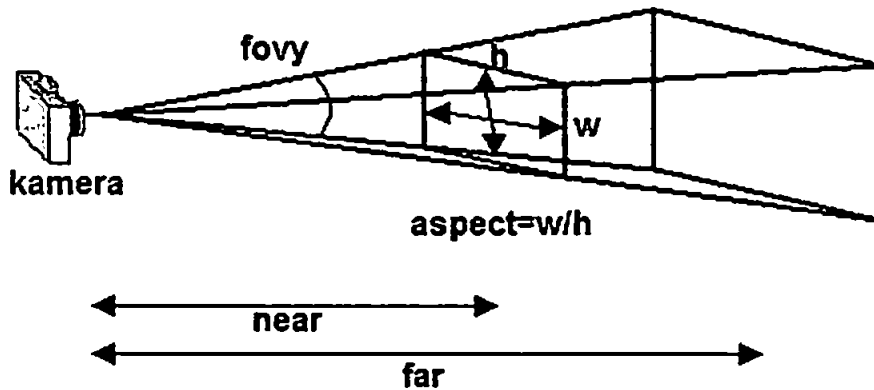
Figure 7.10: The gluPerspective parameters. (Source: Root.cz, 2005)

Next, the modelling transformation mode is set (GL_MODELVIEW). The modifiable matrix is cleared again before the texture information is built. As in the Light_tex functions, the 1D texture generation and texture coordinate (s-coordinate) generation is enabled. The glTexGeni automatically generates the texture coordinates, in this case the s-coordinate that specifies the RGB colour in the texture to be wrapped around the model. The texture generating mode is set to GL_EYE_LINEAR that specifies the function to be used when generating the texture coordinate. GL_EYE_LINEAR calculates the texture coordinate in an "eye referenced" coordinate system, which use the positions of vertices after all modelling and viewing transformations are performed (i.e. they use the positions of the vertices on the screen). The function generates a field of texture coordinates that is favorable when producing dynamic contour lines on moving objects, in this case dynamic color contours on the model. The next four lines of code define the ramp limits (Df and Db) along the z-axis with respect to the eye point (ep) and the texture generating parameters as described in chapter 7.2. The ramp function values have to be manually

adjusted for each model loaded, and may also require adjustment as the model is rotated to ensure the optimal fitting of the ramp function to the model. The texture vectors are then generated using the glTexGenfv function with the input of the textureparametres. The glBindTexture routine creates the new 1D texture object and names it texturename. The viewing parameters are specified by the gluLookAt function. First the viewpoint coordinates are specified (vp, vp, vp/4), then reference point coordinate at which the camera is pointing are defined (0.0, 0.0, 0.0) and finally the view up vector (0.0, 0.0, 1.0) that defines what way is up in the viewing volume. The glGetFloat querying routine gets the value of the model transformation matrix and stores it in the parameter viewproj as the current matrix. The glLoadIdentity command clears the current modifiable matrix and sets it equal to the identity matrix to erase the effect of any current viewing transformation. The next section defines the rotation of the model according to the assigned keys on the keyboard. The glRotate routine is used and the first parameter, angle, defines the increment of rotation around the axis. As the angle is set to 5°, the rotation will move 5 degrees for each time you press the designated key. A negative angle reverses the direction of the rotation. The next three parameters define which of the axes (x, y or z) the model will rotate around. After the desired rotation is performed the remaining modelling transformation is applied by multiplying it with the stored matrix using the glMultMatrix routine, the resulting matrix is stored again as the current matrix (savestate). glLoadIdentity then clears the current modifiable matrix again. The modelview matrix is rebuilt by first multiplying with the viewing transformation (viewproj) and then with the modelling transformation (savestate). The drawsurface function is called upon and finally the top matrix of the stack is erased promoting the second matrix on the stack list (viewing transformation matrix) to the top. Finally, the glSwapBuffers routine refreshes the display and allows the new memory buffer to be completely displayed.

Table 6: Display function

```
void display( void )
{
#define Angle 5.0

    glClear(GL_COLOR_BUFFER_BIT | GL_DEPTH_BUFFER_BIT);
    glMatrixMode(GL_PROJECTION);                                    ,
    glLoadIdentity();
    gluPerspective(75, 1.0, 1.0, 500.0);
    glMatrixMode(GL_MODELVIEW);
    glLoadIdentity();
    glEnable(GL_TEXTURE_1D);
    glEnable( GL_TEXTURE_GEN_S );
    glTexGeni( GL_S, GL_TEXTURE_GEN_MODE, GL_EYE_LINEAR );
    Df = vp - 50.0; Db = vp + 150.0;
    textureparametres[0] = textureparametres[1] = 0.0;
    textureparametres[2] = -1.0/(Db-Df);
    textureparametres[3] = -Df/(Db-Df);
    glTexGenfv( GL_S, GL_EYE_PLANE, textureparametres);
    glBindTexture(GL_TEXTURE_1D, texturename);

    gluLookAt( vp, vp, vp/4.0, 0.0, 0.0, 0.0, 0.0, 0.0, 1.0);
    glGetFloatv( GL_MODELVIEW_MATRIX, viewProj );
    glLoadIdentity();

    switch(ch)
    {
        case '1':
            glRotatef( Angle, 1.0, 0.0, 0.0); break;
        case '2':
            glRotatef(-Angle, 1.0, 0.0, 0.0); break;
        case '3':
            glRotatef( Angle, 0.0, 1.0, 0.0); break;
        case '4':
            glRotatef(-Angle, 0.0, 1.0, 0.0); break;
        case '5':
            glRotatef( Angle, 0.0, 0.0, 1.0); break;
        case '6':
            glRotatef(-Angle, 0.0, 0.0, 1.0); break;
    }
    ch = ' ';

    glMultMatrixf( saveState );
    glGetFloatv( GL_MODELVIEW_MATRIX, saveState );
    glLoadIdentity();

    glMultMatrixf( viewProj );
    glMultMatrixf( saveState );

    draw3ds();

    glPopMatrix();
    glutSwapBuffers();
}
```

7.3.6 Reshape function

The reshape function requires the input of two integer values for the width and height (w
and h) of the OpenGL window; these are specified in the main loop. The glViewport

routine defines a window where the model image is mapped. The first two parameters (0,0)

define the lower left corner of the window and the w and h parameters define the width and

height of the window in pixels.

Table 7: Reshape function

```
void reshape(int w,int h)
{
    glViewport(0,0,(GLsizei)w,(GLsizei)h);
}
```

7.3.7 Keyboard function

The keyboard function requires input from the specified keyboard keys. The integers x and

y indicate the present location (x and y coordinates) of the mouse cursor. This function is

specified by the glutKeyboardFunc in the main loop and is part of the OpenGL Utility

Toolkit. The desired keys for rotation of the model, in both directions and around three

axes, are specified and when the keys (1, 2, 3, 4, 5, and 6) are pressed and the

corresponding ASCII value is generated. Pressing the capital letter E will exit the

application.

Table 8: Keyboard function

```
void keyboard(unsigned char key, int x, int y)
{
    ch = ' ';
    switch (key)
    {
        case '1' :
        case '2' :
        case '3' :
        case '4' :
        case '5' :
        case '6' :
            ch = key; break;
        case 'E' :
            exit(0); break;
    }
}
```

7.3.8 Animation function

This function is provided for animation functionality, which was tried out on simple

models in the early part of the project. As the 3DS model loader was implemented, the

animation functionality became too demanding for computer resources and of little

- 102 -

significant value to explore the stereoscopic effect. It will, however, be interesting to pursue the animation functionality in the application development stage following this project. It is not removed from the application because it is used as an argument in the glutIdleFunction in the GLUT main loop (7.3.9). The glutPostRedisplay function prompts the glutDisplayFunc in the GLUT main loop that the current window needs to be redrawn.

Table 9: Animation function

```
void animation(void)
{
    {
        t += 0.1;
    }
    if (t > 1) t-= 1;
    glutPostRedisplay();
}
```

7.3.9 GLUT Main loop

The first part of the GLUT main loop initialisation checks if GLUT can be properly initialised, in essence if an invalid file or command line option is attempted to be executed. The argc variable contains the number of arguments passed to our program, while argv is a pointer to the arguments. If the 3DS file has an invalid format, the error message "Unable to open file, filename" will be printed in the window. If no argument is passed to the program, the error message "The program requires 1 command line argument" will be printed in the window. The rest of table 9 consists of a standard GLUT initialisation. The glutInit function initialises the glut framework library. The glutInitDisplayMode function specifies double buffering (GLUT_DOUBLE), which enables the application to finish drawing the model before sending it to the display window. The GLUT_RGB flag specifies that a RGB colour buffer is to be used and the GLUT_DEPTH flag specifies that a depth buffer is applied. The depth buffer ensures that objects in the model closer to the viewer will be displayed in front of the objects farther away. The glutInitWindowSize sets the initial window size to be 500 by 500 pixels, and the glutInitWindowPosition places the lower left corner of the window 70 pixels to the right and 70 pixels up from the lower left

corner of the display. These are initial settings; the window can be moved and resized in a traditional windows way. The next two lines will create a window title "Model read from file: Filename" where glutCreateWindow will actually create the specified window including the window title. The glutDisplayFunc is a call-back function which GLUT will call in response to a specific event (in this case it will call for the display function when GLUT decides that the window display has to be updated). The glutReshapeFunc call-back function will call for the reshape function when the window is moved or reshaped. The next function, glutIdleFunc, continuously calls the animation function when other events are not received enabling the application to perform continuous animation or background processing tasks. The keyboard function is called from glutKeyboardFunc every time a keyboard key press is generates an ASCII character. The light_tex function is called, before finally, the glutMainLoop routine enters the GLUT event processing loop that will call, as necessary, any registered GLUT call-back function.

Table 10: Main loop initialisation

```
int main(int argc, char *argv[])
{
    if (argc > 1)
        if (!scene.LoadFile(argv[1]))
        {
            fprintf(stderr, "Unable to open file %s\n", argv[1]);
            return -1;
        } else;
    else
    {
        fprintf(stderr, "The program requires 1 command line
        argument\n");
        return -2;
    }

    glutInit(&argc,argv);
    glutInitDisplayMode (GLUT_DOUBLE | GLUT_RGB | GLUT_DEPTH);
    glutInitWindowSize(500,500);
    glutInitWindowPosition(70,70);
    char windowTitle[100];
    sprintf(windowTitle, "Model read from file: %s", argv[1]);
    glutCreateWindow(windowTitle);
    glutDisplayFunc(display);
    glutReshapeFunc(reshape);
    glutIdleFunc(animation);
    glutKeyboardFunc(keyboard);

    light_tex();

    glutMainLoop();
}
```

7.3.10 Summary

This chapter has described the OpenGL pipeline and the software packages used in the application development. Further the application structure is described, followed by a detailed description of the application programming development. The chromo stereoscopic texture is applied to the imported 3ds Studio Max 6 model in a satisfactory manner, however the user interface is laborious and it makes the chromo stereoscopic process time consuming. The user interface also makes it difficult to set the optimal parameter settings for chromo stereoscopic texture. It is, however, not the scope of this study to develop an optimal user interface for the application. The important result is the chromo stereoscopic texture applied to hydrographic models. It would be an important task for further work to develop the user interface.

Chapter 8: Data analyses and Results

Chapter 8 will describe the different 3ds max models created to evaluate the CS

application. Further the chapter will assess if the chromo stereoscopic effect, which is

added to the models when processed in the CS application, will improve the perception and

understanding of the hydrographic data in the models.

Chapter 2 concluded that the visual perception will improve with an increasing number of

visual depth cues present. When a model is processed by the CS application six of the eight

monocular depth cues are included. These are:

- linear perspective

- relative size

- known size

- interposition

- light and shadow distribution

- height in picture plane

The aerial perspective and texture gradient monocular depth cues are not present, and the

motion parallax depth cue is only present when the model is examined directly in the CS

application where the model is rotated. The aerial perspective depth cue would affect the

colouring and contrast of the model and greatly decrease, or render the chromo

stereoscopic effect impossible.
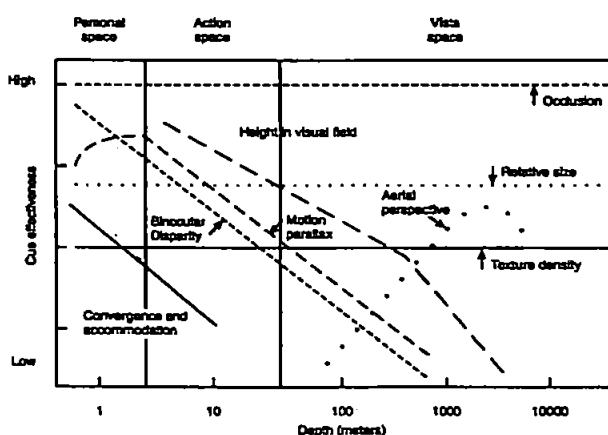
Figure 8.1: Depth Cue effectiveness as a function of distance (Source: Wickens and Hollands, 2000)

Figure 8.1 clearly shows that the binocular disparity depth cue (included within chromo stereoscopy) is far more effective on short distances than the aerial perspective depth cue. It is also obvious from figure 8.1 that the texture gradient is a powerful depth cue at any range. Therefore, it would be desirable to include this depth cue in a further development of the application. It is clear from figure 8.1 that a rotating view of the model, including the powerful motion parallax depth cue, will increase the depth perception.

It is important to emphasize that the viewer should wear the super chromatic prism glasses attached to the inside the back cover of the thesis in order to experience the desired effect when observing the chromo stereoscopic figures in chapter 8 or observing the models directly on the computer screen. Chapter 8.2 describes how to install the CS application and hydrographic models on a computer.

The assessment method for the chromo stereoscopic technique and subsequent increase of depth perception was qualitative rather than quantitative; it was proved in the earlier chapters that including stereoscopic depth cues theoretically increases the depth perception, and in general the increase of depth perception is obvious when viewing the hydrographic models with the eyewear. As a usability assessment from people external to the project, 20 staff and students at Aalesund University College have observed figures 8.3 to 8.22 with the eyewear and thereafter answered the some simple questions. Description and results from this assessment are implemented in chapter 8.3.3.

8.1 Description of the hydrographic data models used

Hydrographic data are classified into 5 different classes in the discussion of chapter 5. The models developed in the 3ds max 6 application reflect these classes with the exception of the sea surface class. If the sea surface is included as an object in the models and the viewer observes the model through the sea surface object the rest of the model would be obscured. It is not possible to make the sea surface transparent, with red as the nearest object, and show the objects behind with a proper chromo stereoscopic colour coding. A

model of only the sea surface is possible to build, but it would be similar to a bathymetric model with relatively minute variations along the vertical axis. A frame, and for some of the models a ship, is added to the models to establish the sea surface reference plane. Figure 8.2 illustrates the different models created including both the frame and the ship.
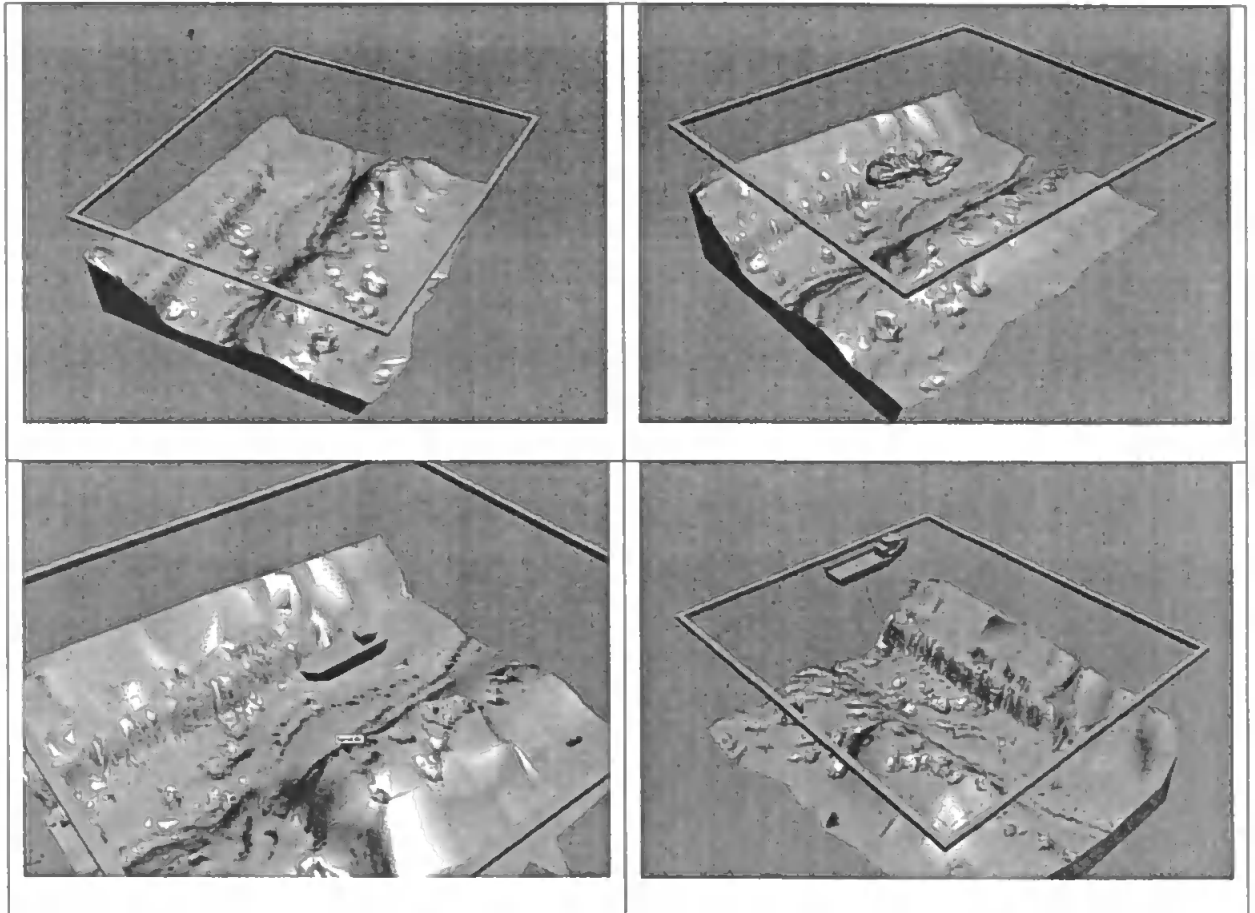
Figure 8.2: The 4 models created in 3ds max 6. The bathymetric data model (upper left), Biological/organic data in water volume (upper right), ocean – and tidal current data (lower left) and man made objects data (lower right)

The bathymetry is the same for the 4 models and it is imported into the 3ds max 6 from an AutoCAD (.dwg) drawing file in 3D format. The file is the product of an as-left survey performed by Stolt Offshore AS on the Garn West oil field in the North Sea for Norwegian Shell in 2003 (Norwegian Shell, 2003). The bathymetry shows a segment of the area extending approximately 190 metres by 170 metres horizontally and approximately 70 metres vertically. The trench, clearly visible in the model, is vertically exaggerated to expand the vertical limits of the model. This improves the variation in the depth of the scene resulting in a better model to illustrate the chromo stereoscopic effect.

The sea surface reference frame and the ship are simple objects created directly in 3ds max 6. The shoal of fish illustrating organic data in the water volume, the tidal current vector fields and the man made objects (ROV's and oil production manifold) are all objects built in 3ds max 6. In a more refined and developed version of the application the data for these objects would possibly be imported directly into the application. It is not considered necessary to include this functionality, in order to examine the chromo stereoscopic effect on the models. The ocean- and tidal currents vector field (arrows in layers with 15 metres of vertical separation) is not easy to distinguish from the rest of the model in figure 8.2. The models are built by adding the different objects to the scene, but before the models were processed by the CS application all the objects in each separate model were merged into one object. The origin of the model's coordinate system is set in the geometric centre of each model. All distances in the CS application referred to in this chapter are referenced to this point.

Table 11: Details of the model files

File name	File size	Number of polygons
Bathymetry.3ds	314 kilobytes	17693
Organic.3ds	672 kilobytes	33367
Current.3ds	683 kilobytes	26623
Rov.3ds	385 kilobytes	18892

Table 11 gives an overview of the names of the different 3ds files imported into the CS application with the respective file size and the number of polygons that each model contains. The relatively small file sizes are achieved by processing the bathymetry model through simplifying routines in 3ds max 6 and making relatively simple additional objects in the models. This is done to increase processing speed, and has little, if any, effect on the chromo stereoscopic presentation.

8.2 Evaluation of chromo stereoscopic effect on models

Each of the 4 models is evaluated in the following text. Before running the CS application in Microsoft Visual C++, the model to be imported had to be identified and the different

viewing parameters set. The observer view point (vp) (figure 7.5) is generally set to 100

metres (table 1) to keep the vp outside the model and to enable a good view of most of the

model when rotating it. The vp was reduced for some of the processing runs to zoom in on

details. The limits of the ramp function (Df and Db) in figure 7.5 were adjusted (table 6)

for each processing pass to achieve the optimal colour distribution in the model. A CD

containing the figures in chapter 8.2 in the Microsoft Word format (.doc) and executable

program files of the CS application is attached to the back cover. The 4 program files

contain compilations of the 4 models with fixed values for vp distance and colour ramp

function limits, this due to the limited user interface functionality of the application. Read

the readme.txt file on the attached CD for instructions on how to run the application.

8.2.1 Bathymetric data model

The bathymetric data model is integrated into all the other models; however it is evaluated

independently to focus only on the bathymetric features. Four different views are produced

of the bathymetric model. In figure 8.3 the direction of view is nearly horizontal looking

into the model from the corner (the values of vp = 100, Df = 70 and Db = 230). The front

ramp limit Df = 70 is apparent in the transition between the dark solid red colour and the

rest of the colour spectrum. The back ramp limit (Db) is set such that the blue end of the

colour spectrum is located in the distant corner of the model. The frame is the reference of

the sea surface. In this side view, however, the chromo stereoscopic effect will not enhance

the depth perception of the sea surface in relation to the bathymetry. The chromo

stereoscopic effect on the closest ridge in relation to the trench is clearly improving the

depth perception. The chromo stereoscopic effect on the ridge on the opposite side of the

trench is also clear and the depth perception is increased, particularly in relation to the

areas behind the ridge. This is because you get a more distinct transition between colours

widely separated in the colour spectrum. This gives a greater chromo stereoscopic effect

than a gradual transition between the colours.
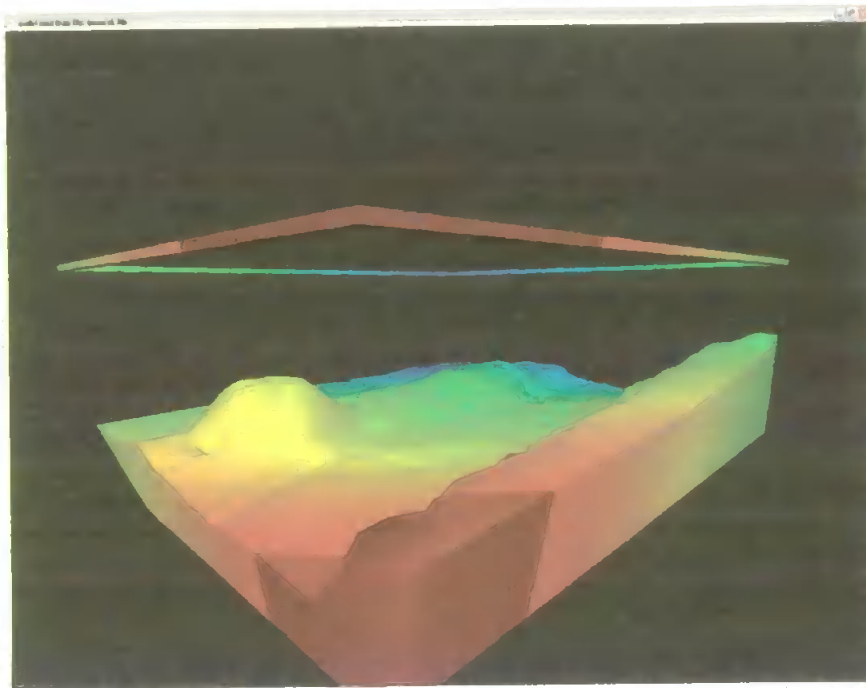
Figure 8.3: Bathymetric data model, corner side view

In figure 8.4 the model is viewed from the opposite side with the model slightly tilted. The vp, Df and Db values are unchanged. From this viewpoint the colour separation between the major features, the elevated area in front (yellow) to the even more elevated area (green) and to the ridge wall in the back of the scene (blue), is greater than in figure 8.3. Consequently, the chromo stereoscopic effect is increased and the depth perception and understanding of the spatial relations in the model is enhanced.
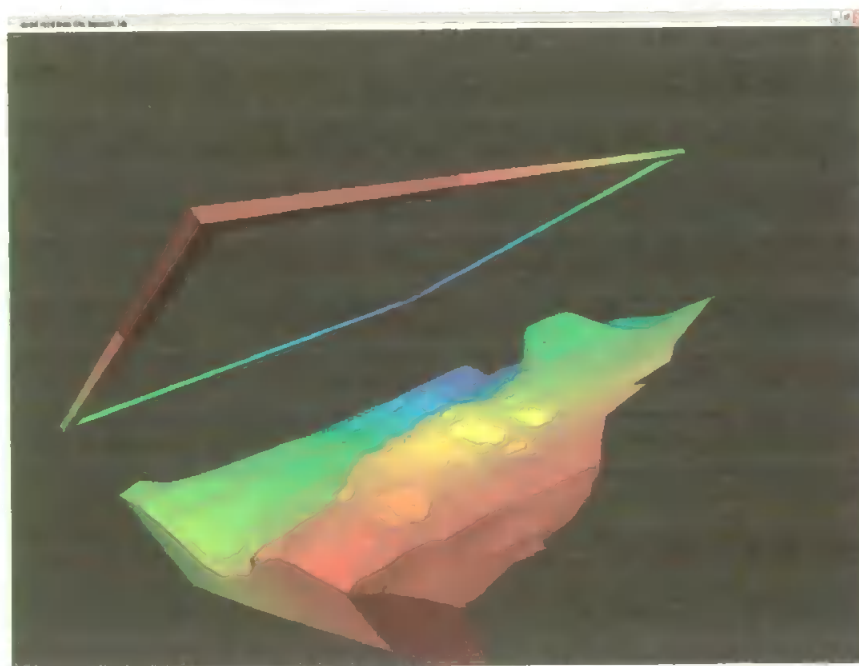
Figure 8.4: Bathymetric data model, side view opposite corner

In figure 8.5 the model is viewed vertically down along the z axis. The values of vp = 100, Df = 115 and Db = 165. By setting these values for the ramp function Df is set closer to the viewer than the model, resulting in a dark red frame representing sea level. The area with dark blue colour at the bottom of the trench is just outside the Db limit.
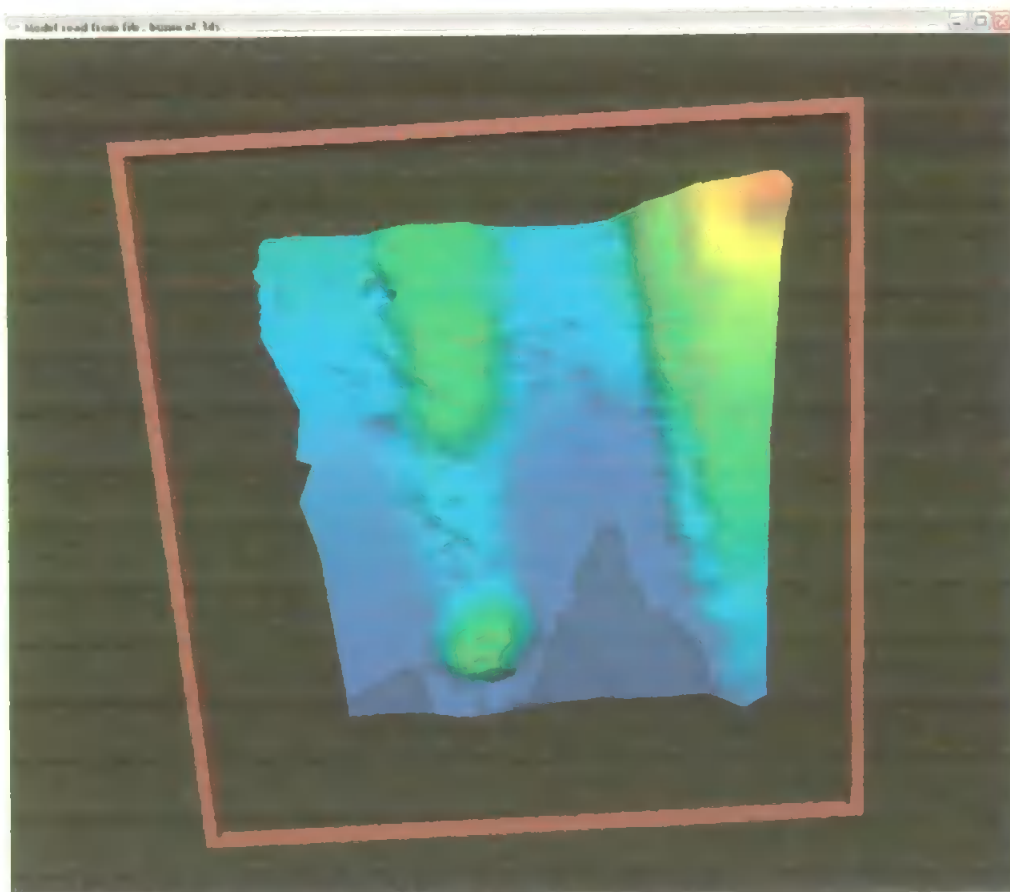
Figure 8.5: Bathymetric data model vertical view

The ramp function is thus made somewhat narrower than the model; this is done to make more of the colour spectrum covering the actual bathymetry of the model. If the ramp function is set to exactly enclose the model, the bathymetry would be covered by only the blue band of the colour spectrum and the bathymetric features would not be effectively represented by chromo stereoscopy. The chromo stereoscopic effect clearly places the sea surface frame closer to the viewer giving a good perception of the height of the water column. In figure 8.6 the view point is elevated and the model is observed from above at approximately 30° downward angle.
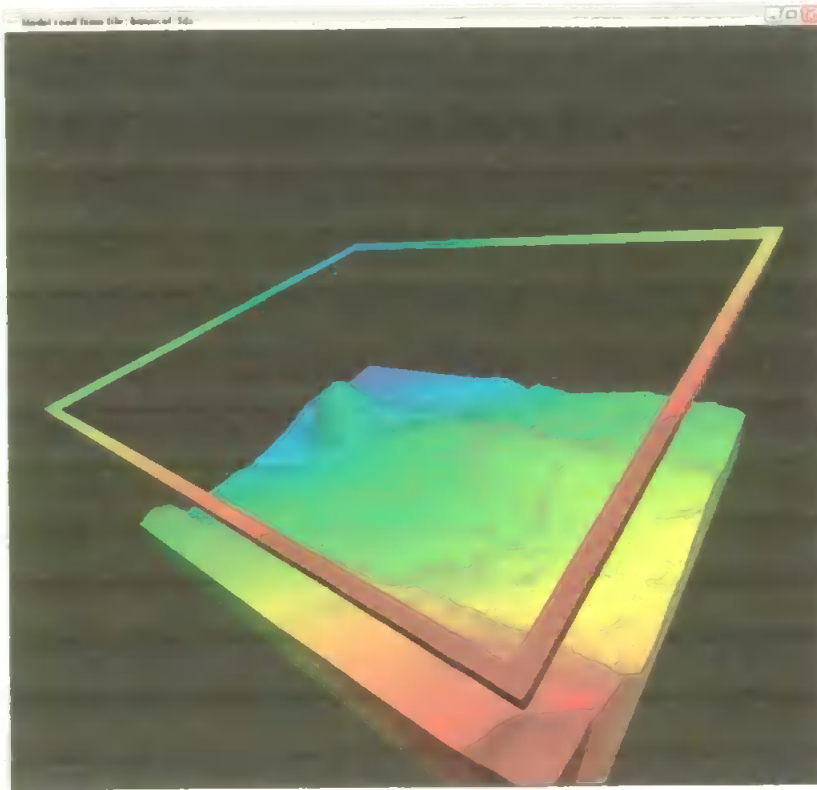
Figure 8.6: Bathymetric data model elevated corner view.

The sea surface frame does not lie at the same distance from the viewer; the chromo stereoscopic effect will in this case only give a true representation of the distance between the sea surface and the bathymetry along the line of sight. At the nearest corner in figure 8.6 the effect is good, but in the far side corner both the frame and the bathymetry is the same colour (blue) which is expected since they are located at the same distance from vp. It is obvious that it is important to select the right viewing direction in order to get the desired chromo stereoscopic effect between objects.

8.2.2 Biological / organic data in the water volume model

Five different views and colour ramp settings are selected to elevate the biological / organic data in the water volume. In figure 8.7 the shoal of fish is located approximately in the middle of the model between the bathymetric model and sea surface reference frame. This object constitutes the outer limits of the shoal, similar to the presentation on the state of the art fishery sonars. The values of vp = 100, Df = 70 and Db = 230 are set for both figures 8.7 and 8.8. The chromo stereoscopic effect gives a good perception of depth in the

figure and the green shoal is clearly perceived at a closer distance that the blue bathymetry behind it. In figures 8.7 and 8.8 the ramp function limits are set wide and therefore the entire shoal is located in the green section of the colour spectrum. The whole object is then at the same distance from the view point with respect to chromo stereoscopy.
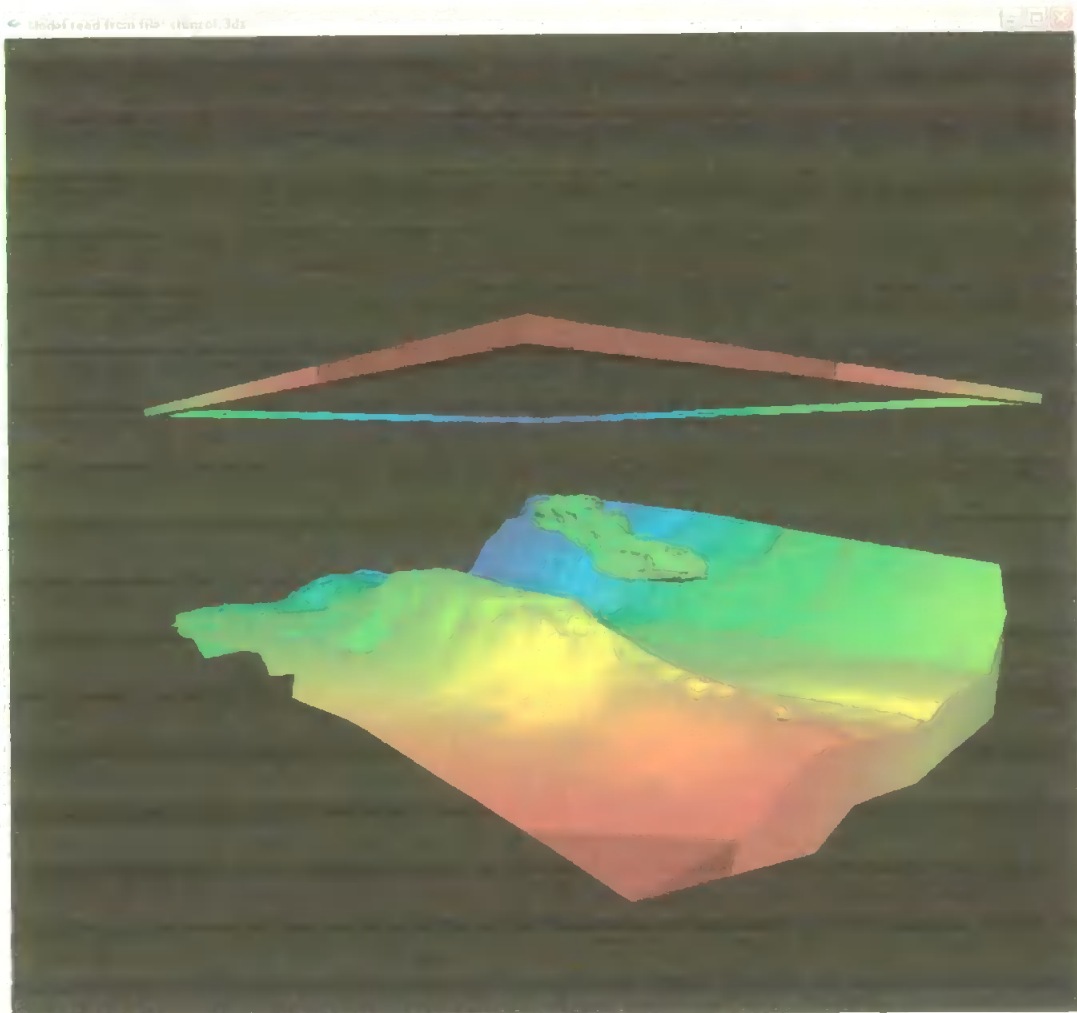
Figure 8.7: Biological / organic data model, corner side view

When rotating the model in the CS application the chromo stereoscopic effect and motion parallax gives an excellent sensation of the shoal floating above the bathymetry.
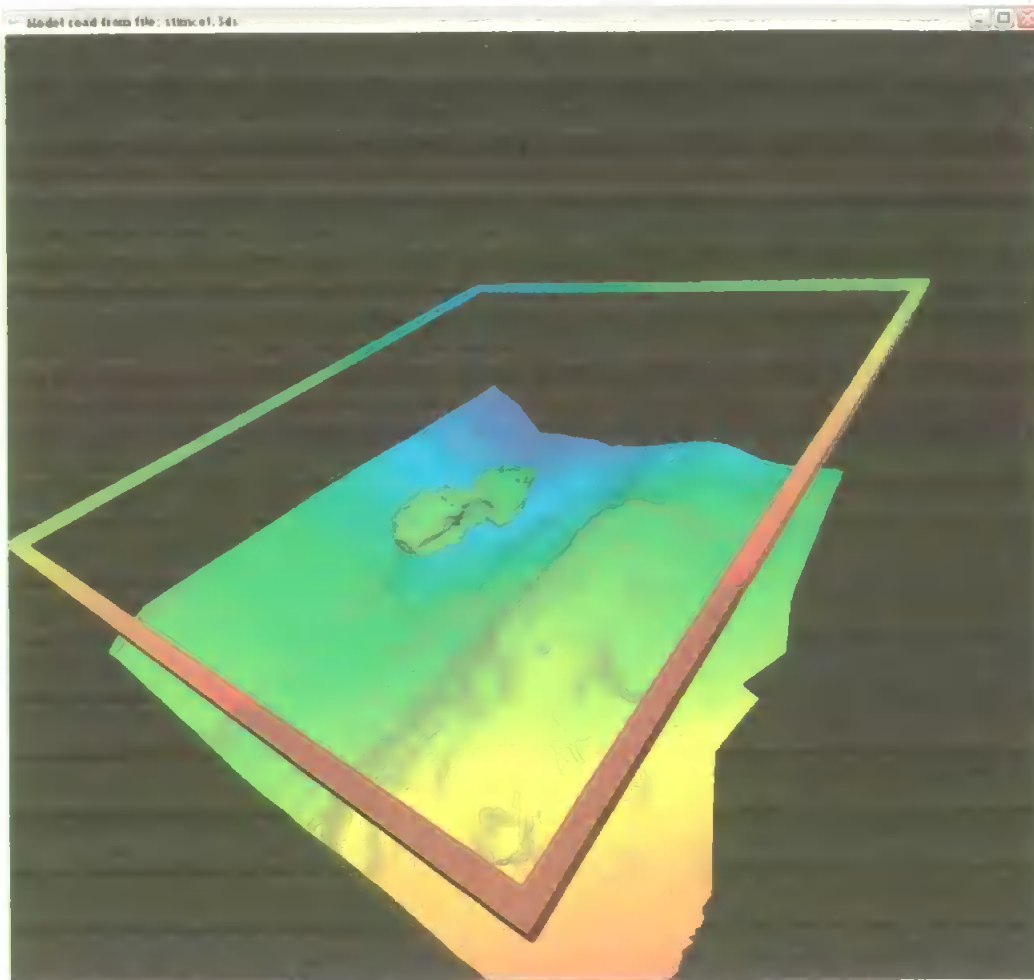
Figure 8.8: Biological / organic data model, elevated corner view

Figure 8.8 gives similar results in the improvement of the depth perception. This is because the distance from the shoal to the background bathymetry is similar, resulting in the same colour contrast between the shoal and the bathymetry.

Figure 8.9 shows a vertical view looking down on the shoal. The view point vp = 100 and the ramp function limits are set to Df = 115 to Db = 165. This view gives excellent perception of the relative depth of the shoal in relation to sea surface and the bathymetry. As in the vertical view of the bathymetric data model, the ramp function is compressed such that the entire colour spectrum is shown over a distance of 50 metres. This is done in order to make the contrast between the colours of the shoal, bathymetry and the sea surface reference frame optimal.
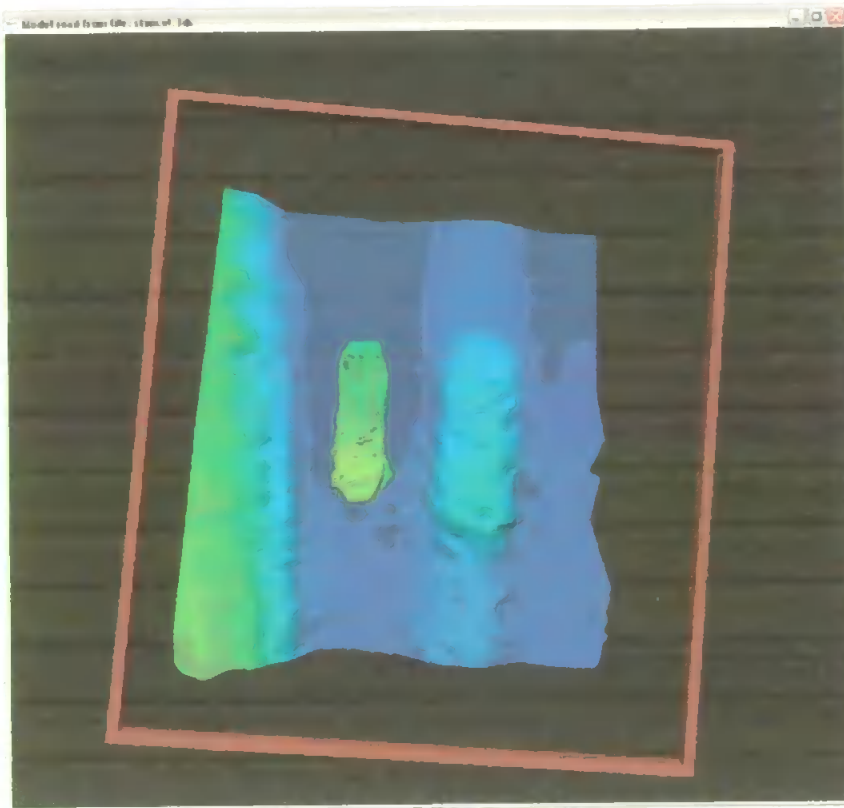
Figure 8.9: Biological / organic data model, vertical view

Figure 8.10 shows a horizontal side view in the direction down along the trench with the

ramp function approximately enclosing the outer boundaries of the model with vp = 100,
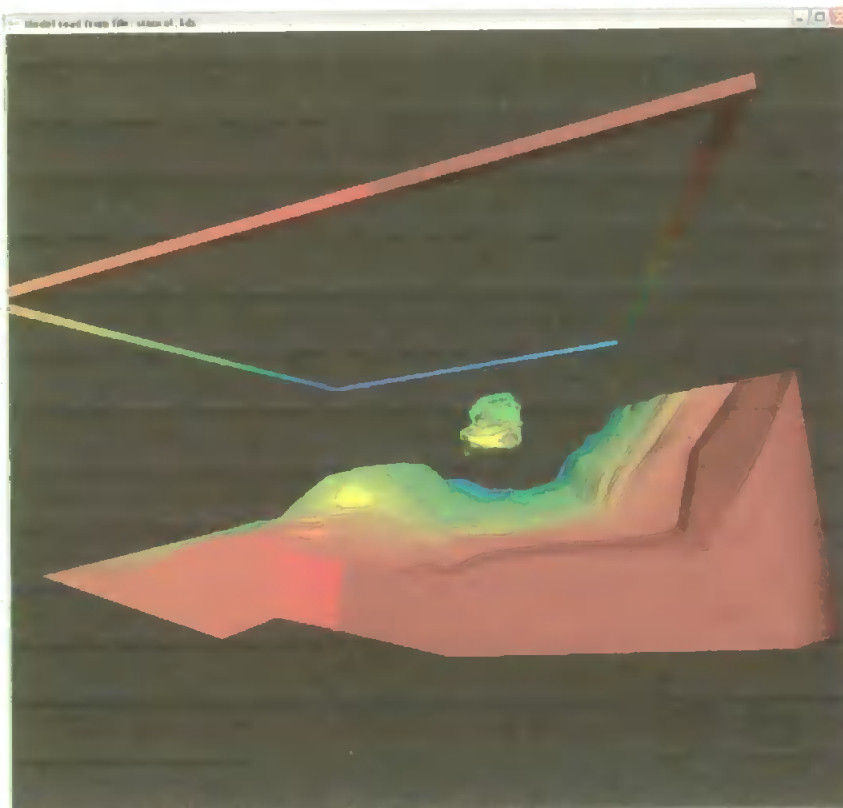
Figure 8.10: Biological / organic data model, side view along trench

Df = 70 and Db = 230. The depth perception in this view is also excellent, and the location of the shoal in the trench is obvious. From this point of view the shoal is extending into the yellow part of the colour spectrum, resulting in a two coloured shoal, this helps in perceiving the horizontal extent of the shoal (or depth of view).

Figure 8.11 shows a corner side view of the biological / organic data model. The particular difference on this model, compared to the previous ones, is that the ramp function limits are considerably narrower than the entire model. The ramp limits are enclosing a desired object within the model in order to distribute the colour spectrum over that particular object. The viewer will then get a more detailed perception of the depth of that particular object.
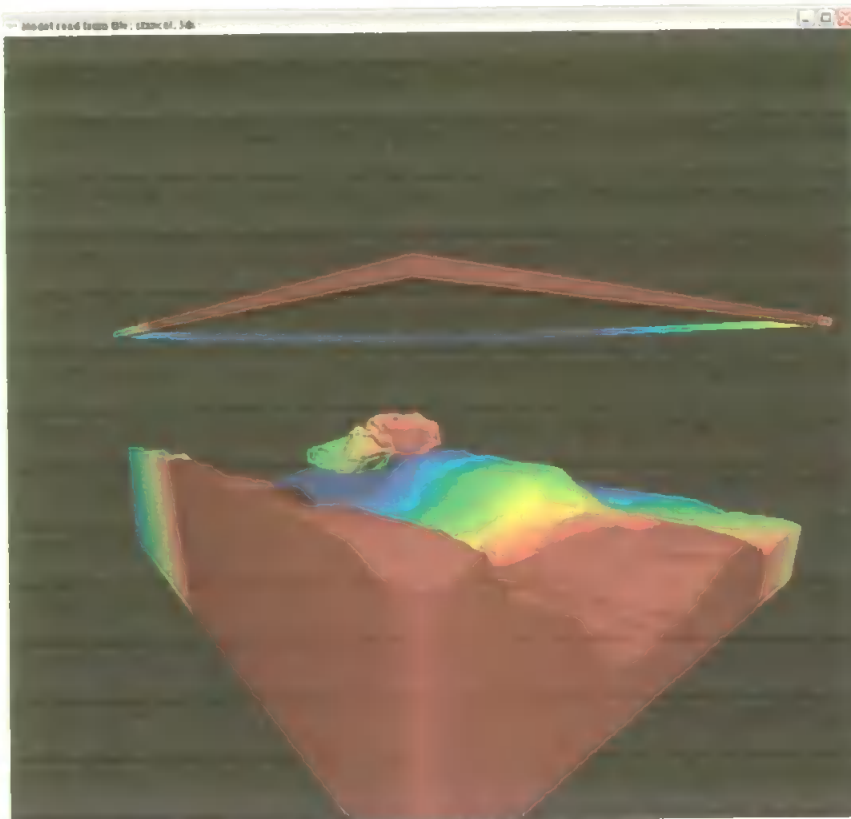
Figure 8.11:   Biological / organic data model, corner side view with narrow colour distribution

In figure 8.11 the vp = 100, the Df = 85 and Db = 160. By setting the ramp with these values most of the colour spectrum is represented on the desired object, the shoal. In addition the depth perception of the shoal with respect to the dark blue bathymetry behind

- 117 -

is increased. However, in the dark red band in front of Df and in the dark blue band in the back of Db there are no difference in the chromo stereoscopic effect and the image depth for the entire model is not correctly illustrated. The viewer must be aware of this effect when examining the model. The narrow ramp function limit view is further illustrated in figure 8.12 where the viewpoint is elevated, vp and the ramp function limits are the same as for figure 8.11. In figures 8.7 and 8.8 the shoal of fish object is almost mono colour (green), and the shape along the sight axis of the shoal itself is not that easy to determine. In figure 8.11 and figure 8.12 the front end of the shoal, orange in colour, are clearly closer to the viewer than the back part of the shoal, green in colour. The viewer will get a better understanding of the shape of the shoal in figure 8.12 where the chromo stereoscopic effect increases the depth perception of shoal. In figures 8.7 and 8.8 a better understanding of the relations of depth between the different features in the complete model is achieved.
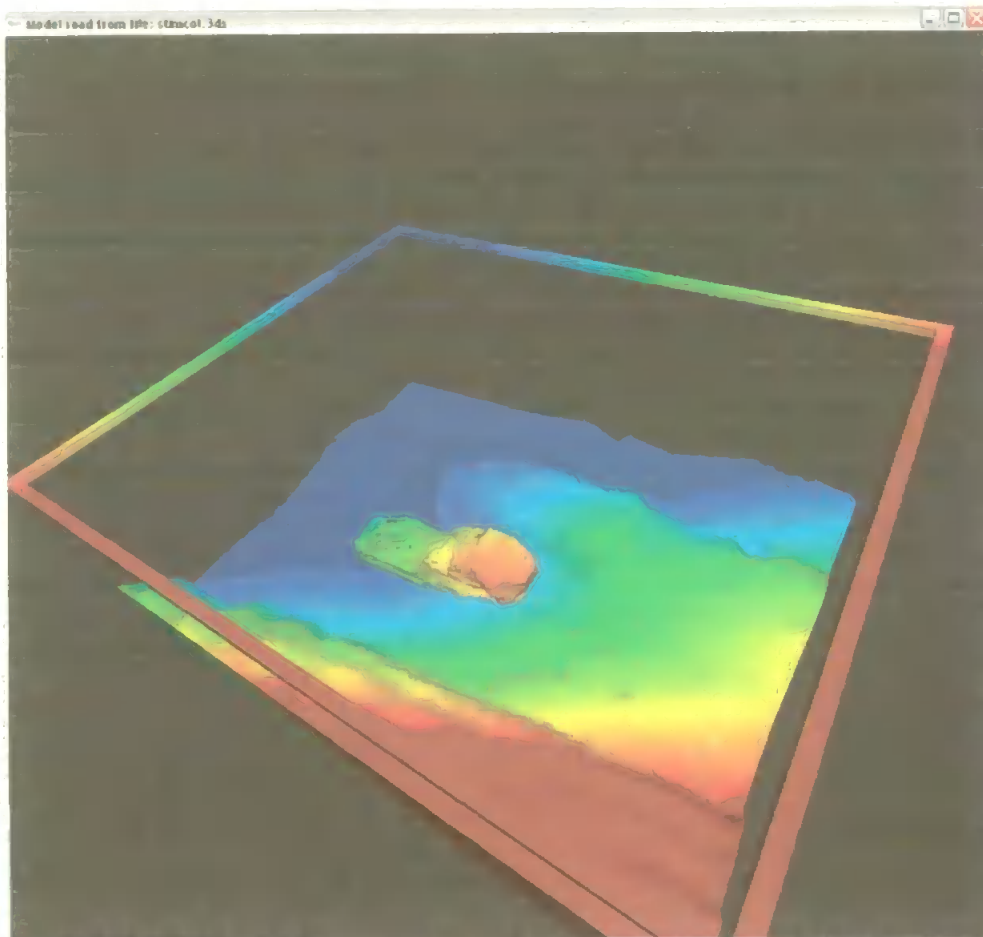
Figure 8.12: Biological / organic data model, elevated corner view with narrow colour distribution

8.2.3 Ocean – and tidal current data model

Four different views of the ocean – and tidal current data are used to examine the chromo stereoscopic effect on this model. An extra reference object, a vessel, is added to the sea surface reference frame to increase the perception of the sea surface layer. Vector fields illustrate the currents at different layers of depth. In this model the spacing between layers is approximately 15 metres; three layers are presented at approximately 15, 30 and 45 metres. The great advantage of presenting the current data in this way is that the viewer will be able to view the complete dataset in one image, where the chromo stereoscopic effect will increase the viewer's ability to separate the layers at different depths.
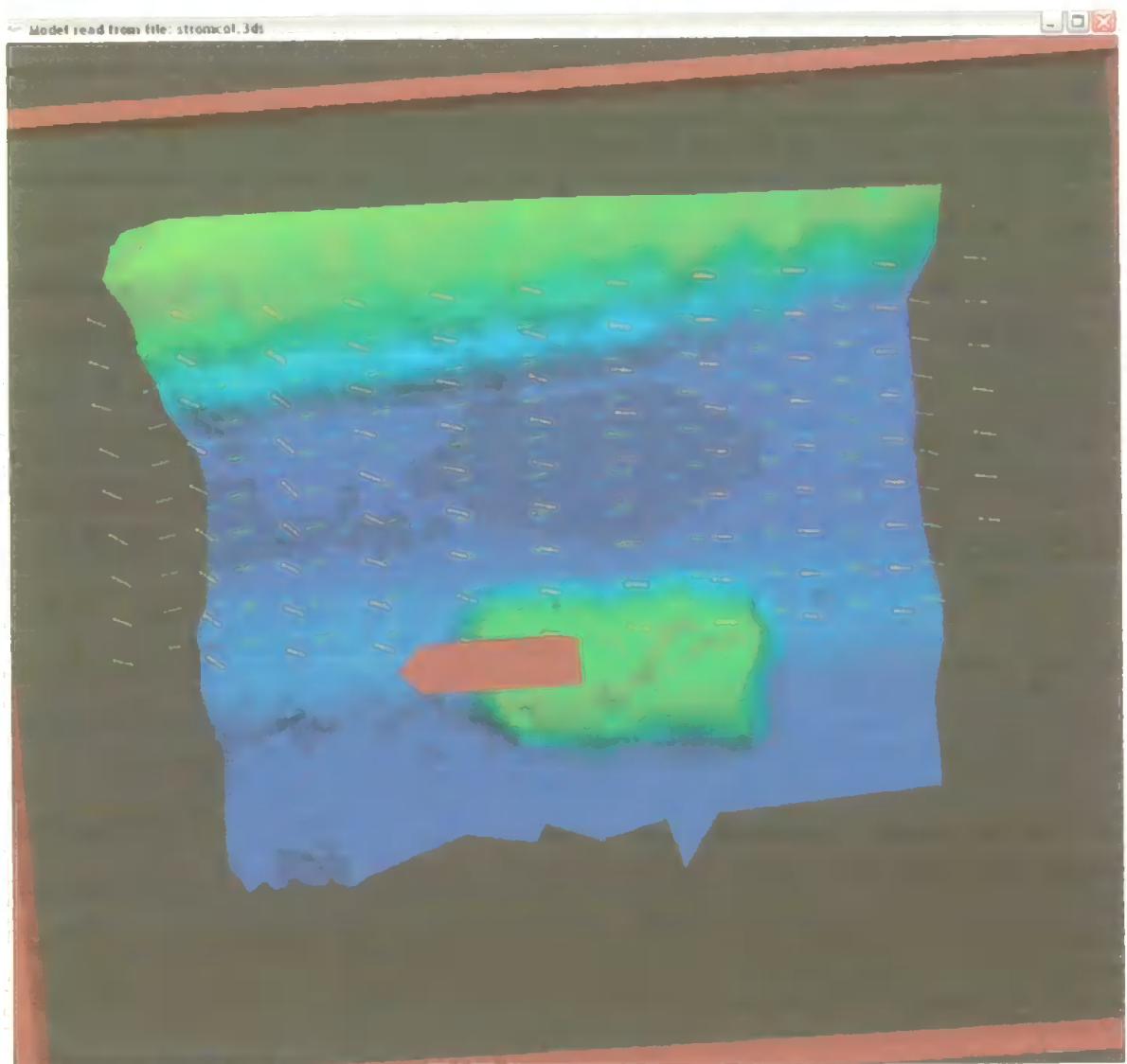
Figure 8.13: Ocean – and tidal current data model, vertical view

Figure 8.13, the vertical view looking down on the model, has an unchanged vp = 100 and the ramp function limits are Df = 115 and Db = 175. The sea surface reference frame and vessel is dark red because it is just outside the nearest ramp limit. The first current layer is orange, the second layer is light green and the third layer is light blue. The layers are homogenous in colour, i.e. all the colours in a layer have approximately the same colour. It is easy to separate the different layers, and the chromo stereoscopic effect effectively places the layers at the appropriate depths. The arrows in the vector field are selected to be fairly small; this prevents the arrows in the upper layers obscuring the arrows in the lower layers. To enhance the presentation further different ways to present the vector information should be investigated. This is however not covered by the scope of this thesis.
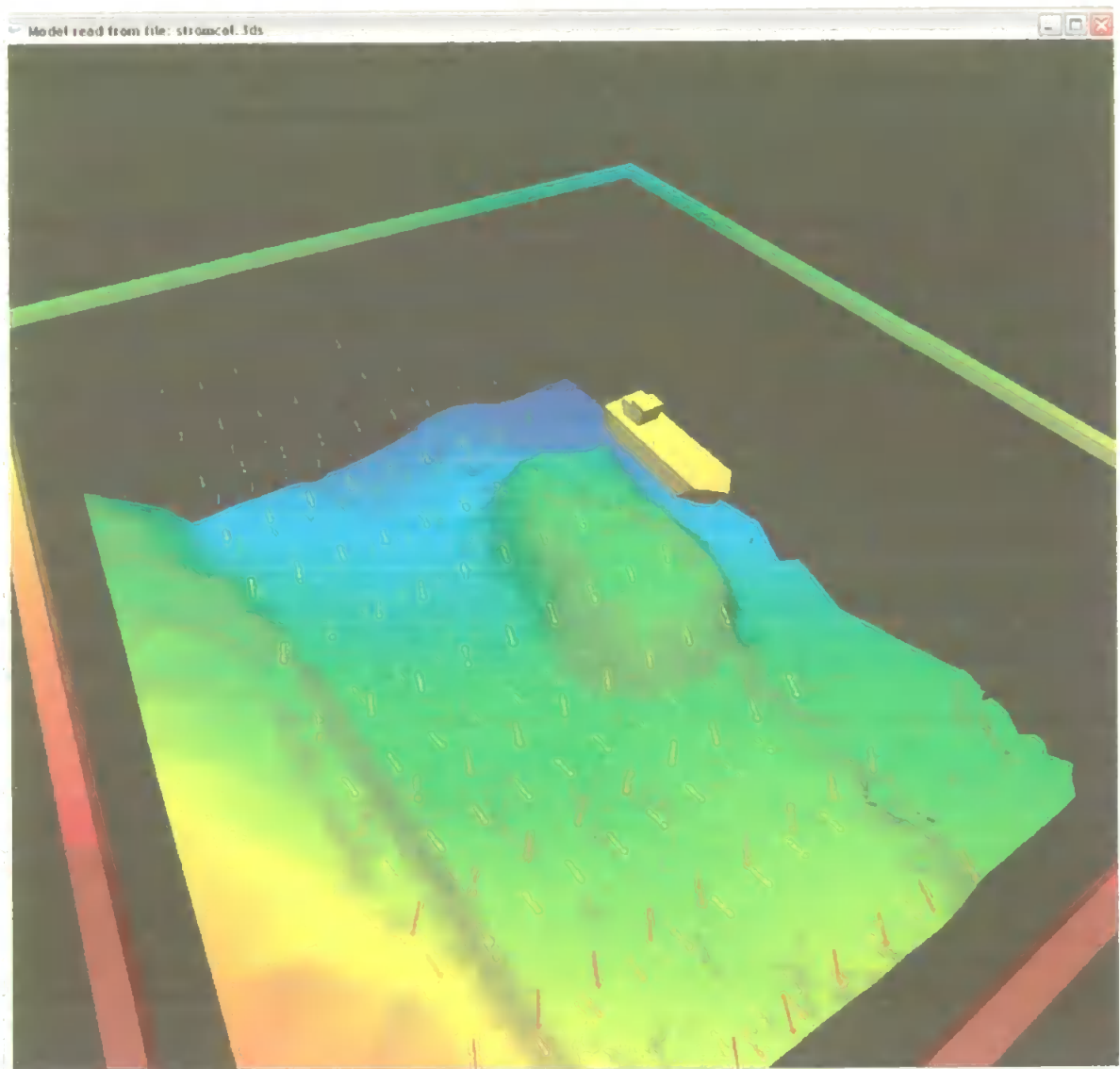
Figure 8.14: Ocean – and tidal current data model, elevated corner view

The elevated corner view of the data model uses the viewing parameters vp = 100, Df = 70 and Db = 230. It is clear that the vectors in each current layer are not homogenous in colour; this is because the vectors in each layer are not equally distant to the view point. The effect is confusing and it is not easy to differentiate the data at each layer. The chromo stereoscopic effect will separate the layers to some extent at the nearest parts of the model, because the view is relatively vertical. However, as the view is moved further away in the model vectors in different layers will have the same colour, because they are at the same distance from the view point. The chromo stereoscopic effect on the rest of the model, bathymetry and reference frame is effective and the vessel increases the sea surface reference plane.
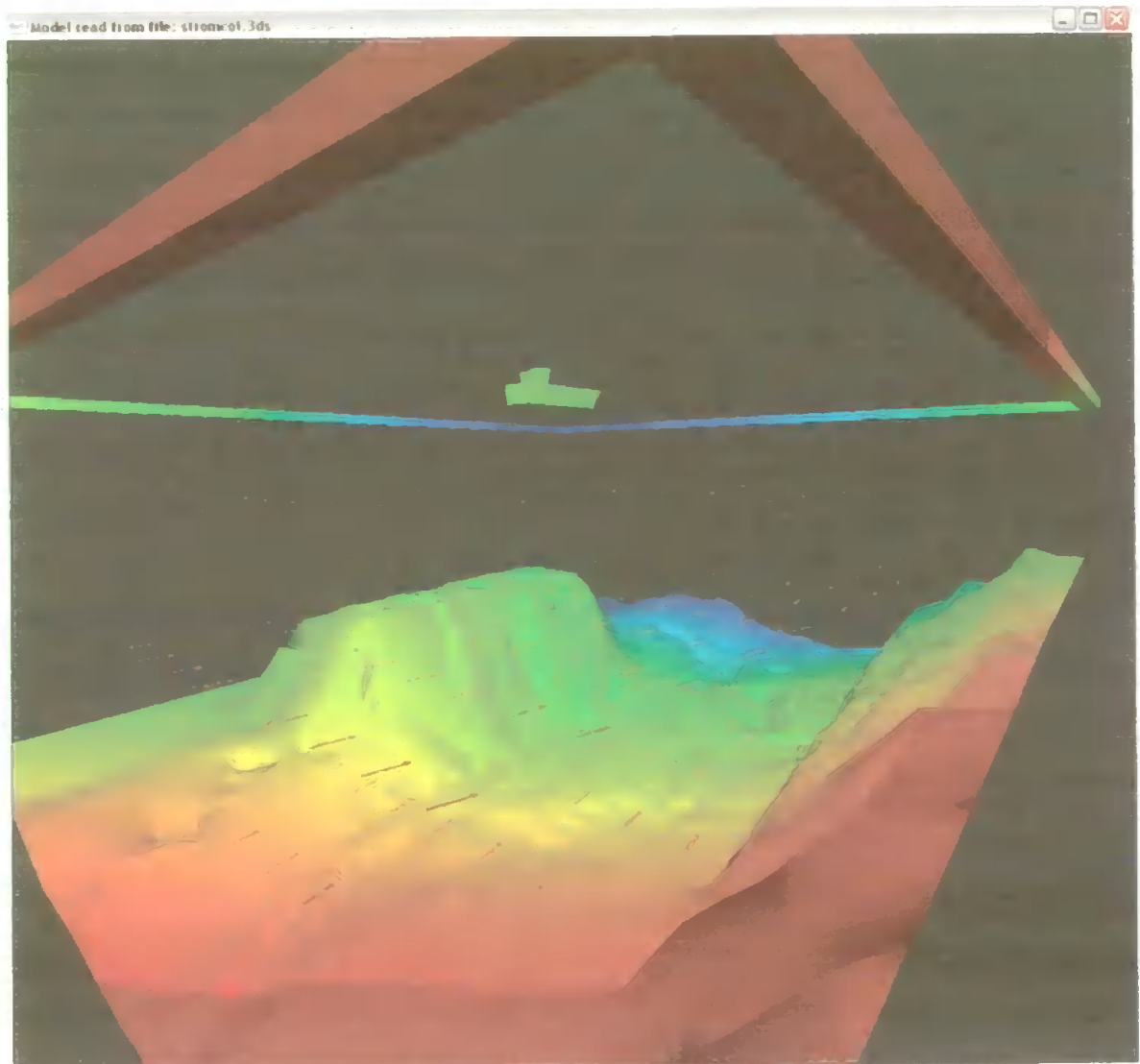
Figure 8.15: Ocean – and tidal current data model, corner side view

Figure 8.15 shows a corner side view of the data model looking nearly horizontal through the model. The line of sight is approximately in line with the layer at 15 metres depth. The vp = 100, Df = 70 and Db = 230. The vector fields are poorly presented from this angle, which is not unexpected since the data is distributed in horizontal layers. The 15 metres layer is barely visible represented by small scattered dots along the line of sight. The layers at 30 and 45 metres are more visible but the size and orientation are not recognizable for the majority of the vectors. The nearest vectors can be placed relative to the bathymetry and surrounding vectors water volume with the presentation somewhat increased by chromo stereoscopy. The non homogenous colours in the different layers will however make the presentation confusing.
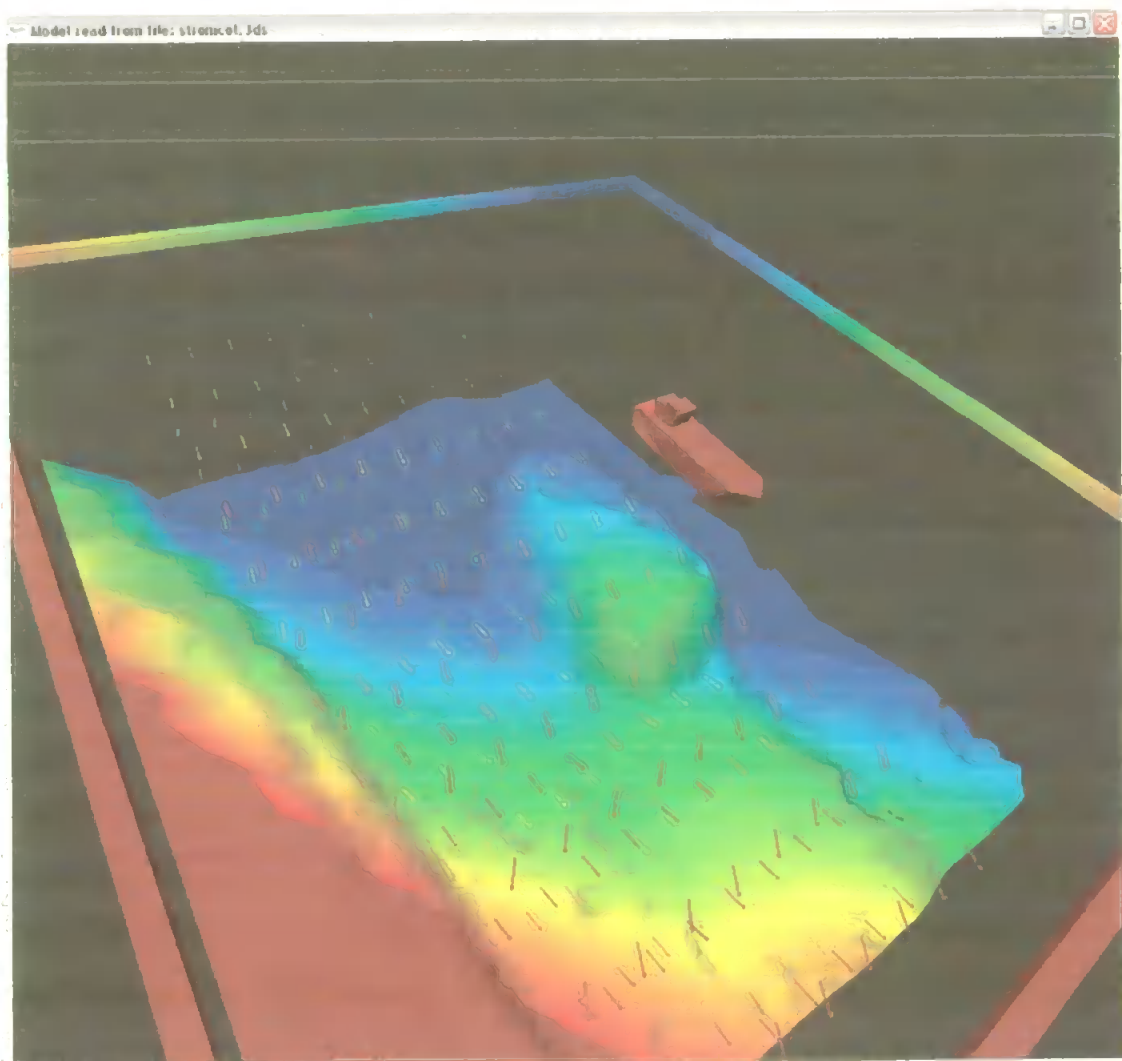
Figure 8.16: Ocean – and tidal current data model, elevated side view, narrow colour distribution

The view in figure 8.16 is as figure 8.14 an elevated side view. However, the colour distribution band is narrower (Df = 85 and Db = 165, vp =100). The front ramp function limit (dark red) is intersecting the vessel, making all the vectors closer to the view point dark red, and from a chromo stereoscopic point of view, at the same distance from the view point. This iş obviously not correct, and makes the presentation of the red vectors in front of the view confusing. When looking at the current vectors in the middle of the figure, a good chromo stereoscopic effect is present when looking along the line of sight at different depths. Separating the currents at the different layers, as in figure 8.14 and figure 8.16, is difficult because of the non homogenous colours in the respective layers.

8.2.4 Man made objects data model

To illustrate a typical man made object data model an offshore construction vessel is presented in the following figures. Attached to the vessel through "umbilical cords" are two ROVs operating in the water column, and placed on the seabed, in the trench is an oil production manifold. The manifold can be seen on the seabed between the ROVs. The objects are built in the 3ds Max 6 application.
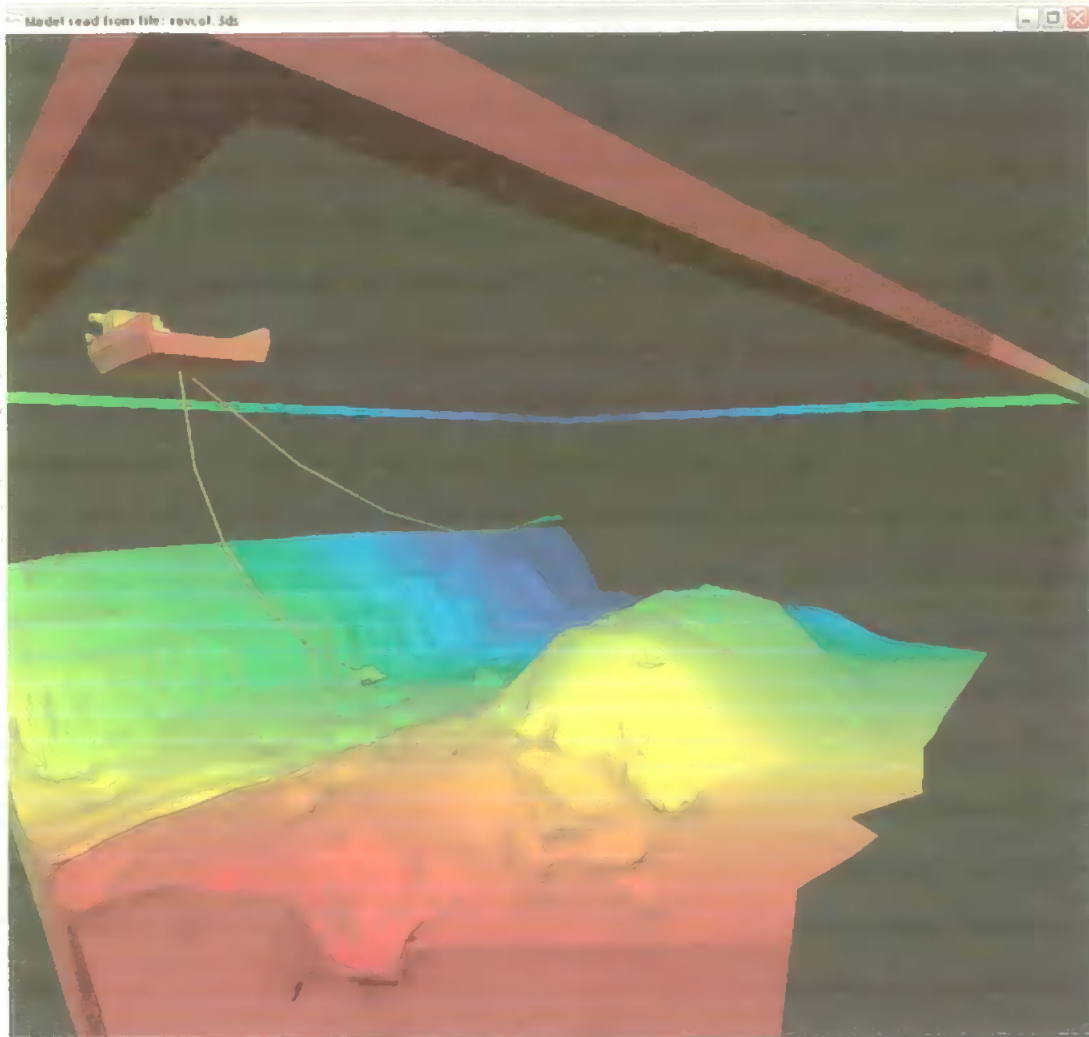
Figure 8.17: Man made objects data model, corner side view

In figure 8.17 the colour ramp function approximately encloses the entire model, the Df = 70, Db = 230 and vp = 100. The chromo stereoscopic effect clearly places the surface vessel closer to the viewpoint than the two ROVs, making it easier for the viewer to judge the relative position between the vessel and the ROVs. Because the ROVs, the manifold and the surrounding seabed are all in the green band of the colour spectrum, chromo stereoscopy cannot increase the understanding of depth between these objects. The chromo stereoscopic effect is very apparent with the umbilical cords and the highest ROV in relation to the seabed wall in the background.

Figure 8.18 is similar to figure 8.17, the ramp function settings and vp is the same and the wide colour ramp is also here nearly eliminating the chromo stereoscopic effect between the nearest ROV, the manifold and the adjacent seabed. The chromo stereoscopic effect

between the vessel, the more distant ROV and the bathymetry increases the depth perception between these objects.
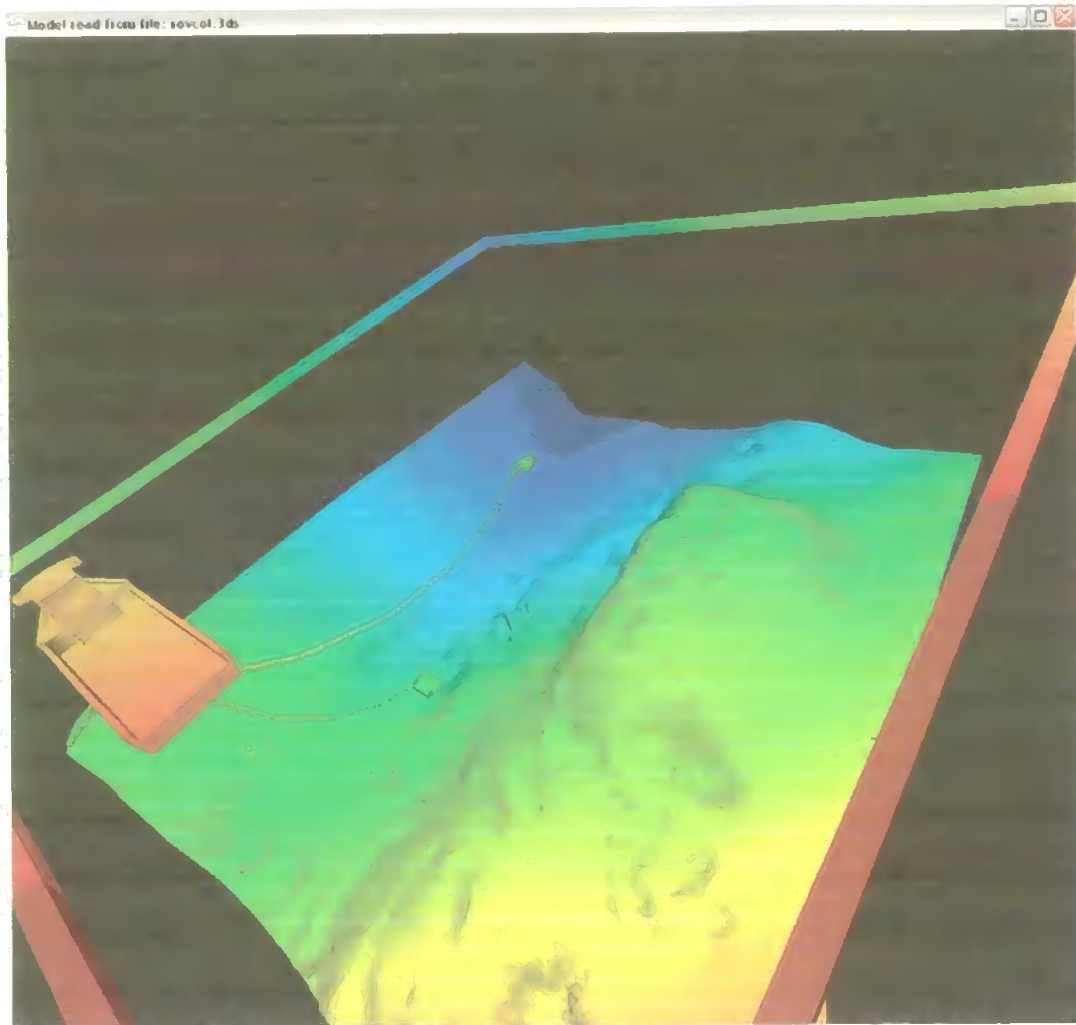
Figure 8.18: Man made objects data model, elevated corner view

The colour ramp function limits in figure 8.19 are adjusted to make the colour spectrum cover a shorter distance in the model. The colour separation between the different objects thereby increases and the chromo stereoscopic effect is enhanced. Df = 90, Db = 200 and vp = 100. The increased depth perception along the trench is obvious and the ROVs , the umbilical cords, the vessel, the manifold and the bathymetry can easily be placed at the correct depth in the figure.
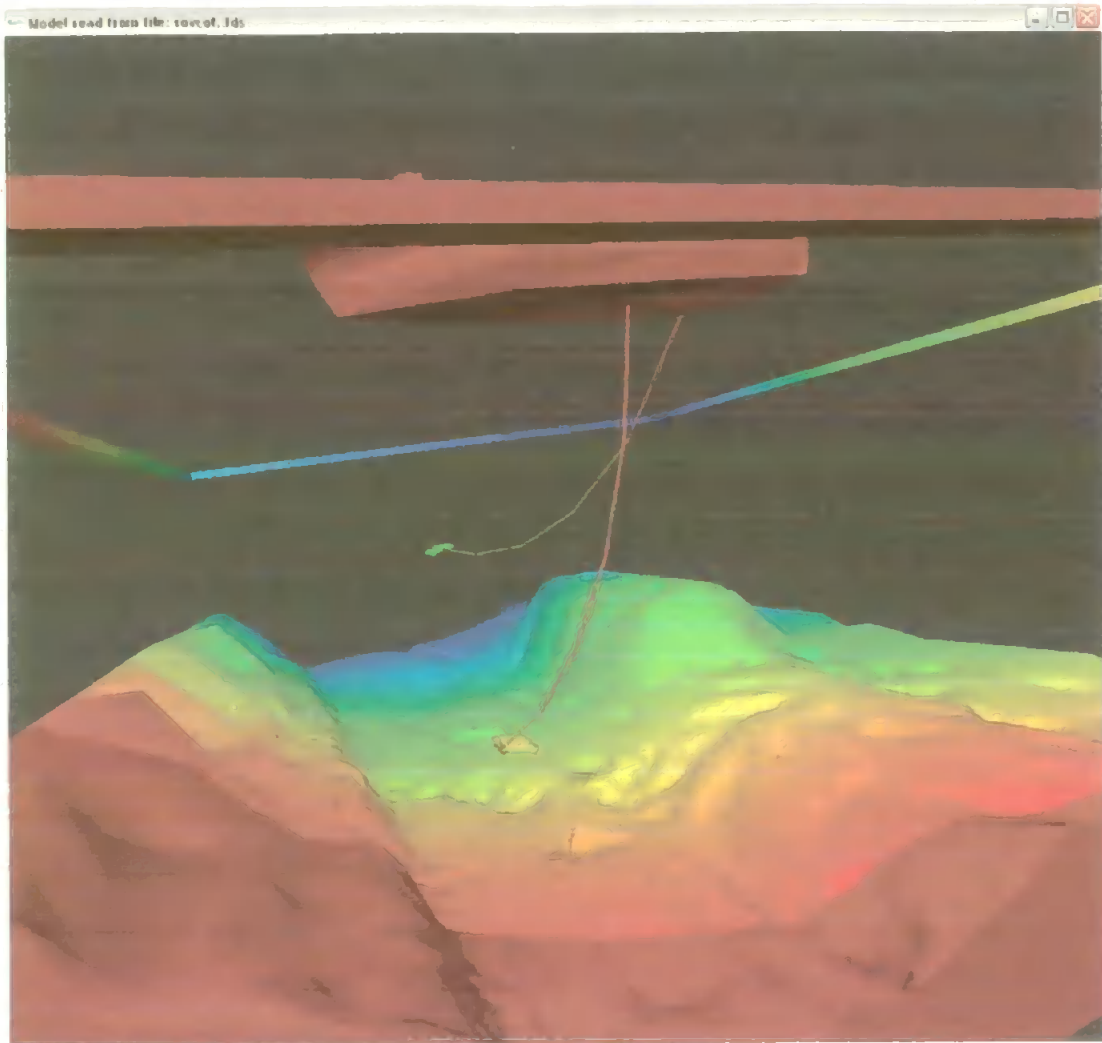
Figure 8.19: Man made objects data model, side view

As in the previous vertical views of the models, the ramp function limits in figure 8.20 are closer (Df = 115 and Db =180), in order to distribute most of the colour spectrum over the desired objects in the model (here the two ROVs in relation to the manifold, bathymetry and the vessel). Again the chromo stereoscopic effect is clear and it is easy to establish the relative altitude between the two ROVs in the water column and the manifold on the seabed.
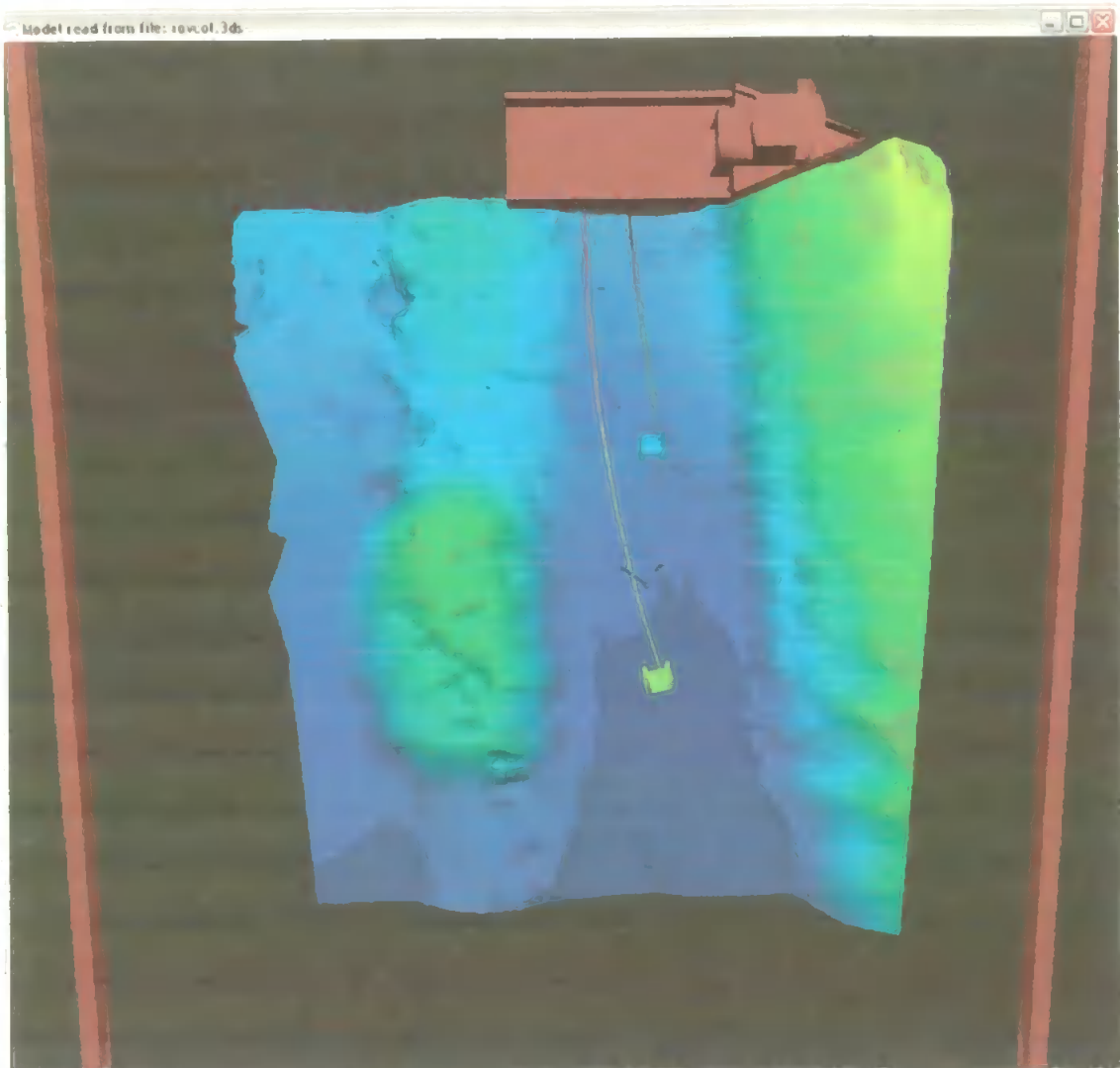
Figure 8.20: Man made objects data model, vertical view

In figure 8.21 the colour ramp function is set narrower (80 metres wide), $Df = 85$ and $Db =$ 165, for the colour spectrum to cover the desired objects in the model. The objects of interest in the model then get a greater separation in the colour spectrum, resulting in an increased chromo stereoscopic effect; the relative depth between the features in the bathymetry outside the ramp function limits are not subject to chromo stereoscopic enhancement. Compared to figure 8.17 and figure 8.18 where the ramp function is 160 metres wide, the chromo stereoscopic effect and the understanding of the spatial relations between the objects of interest is increased.
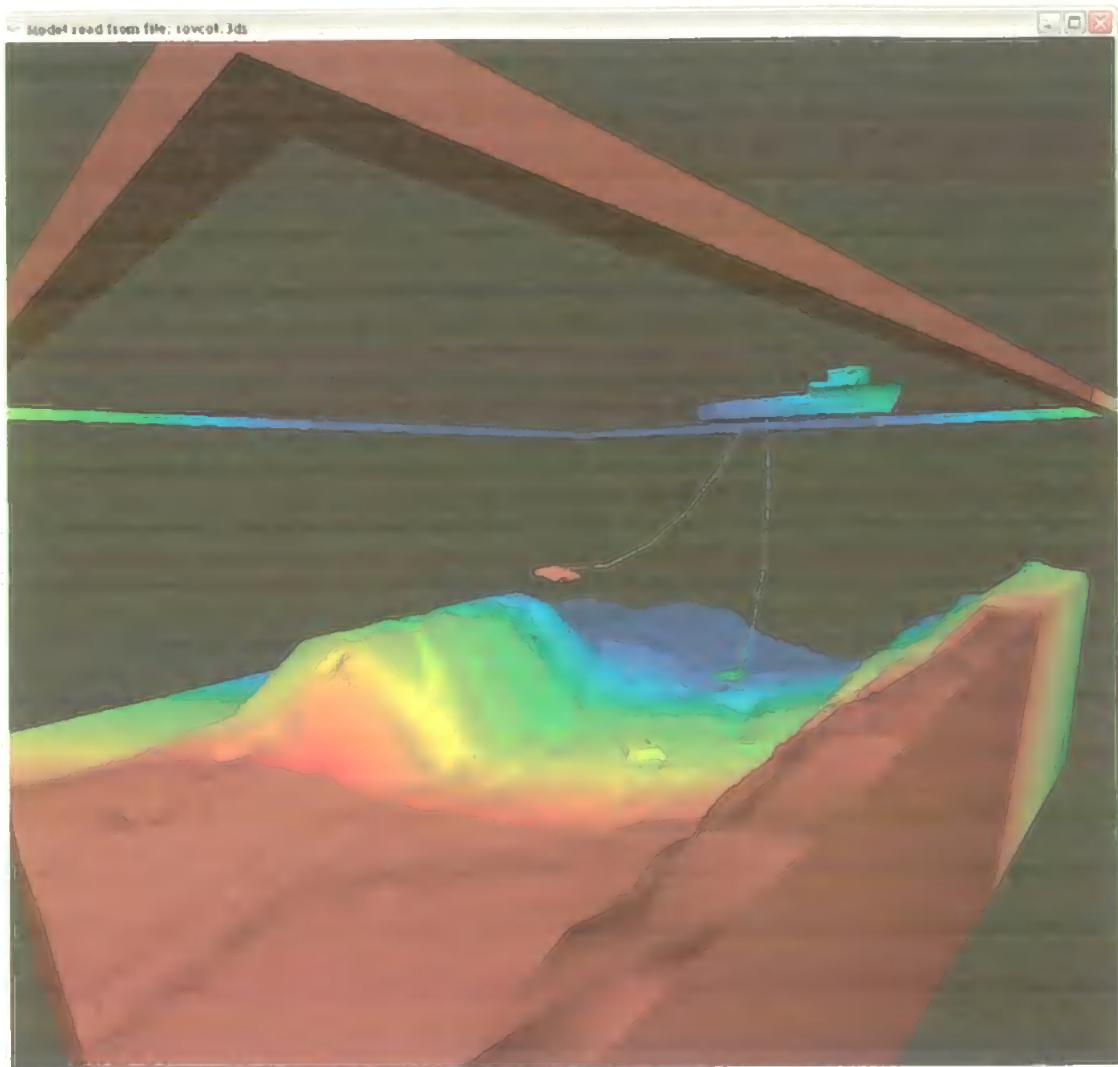
Figure 8.21: Man made objects data model, corner side view, narrow colour distribution

In the side view of figure 8.22 the view point distance is reduced (vp = 40), the view point is now within the model, 60 metres closer to the objects of interest. The ramp function limits are adjusted to enclose the scene of interest (Df = 0 and Db = 80). The relation between the objects with regards to the image depth is clear and the chromo stereoscopic effect apparently increases the depth perception. By zooming in on the objects of interest the relative distances between the objects becomes greater compared to the distance to the view point. This increases the image depth of the scene making it more suitable for the chromo stereoscopic technique.
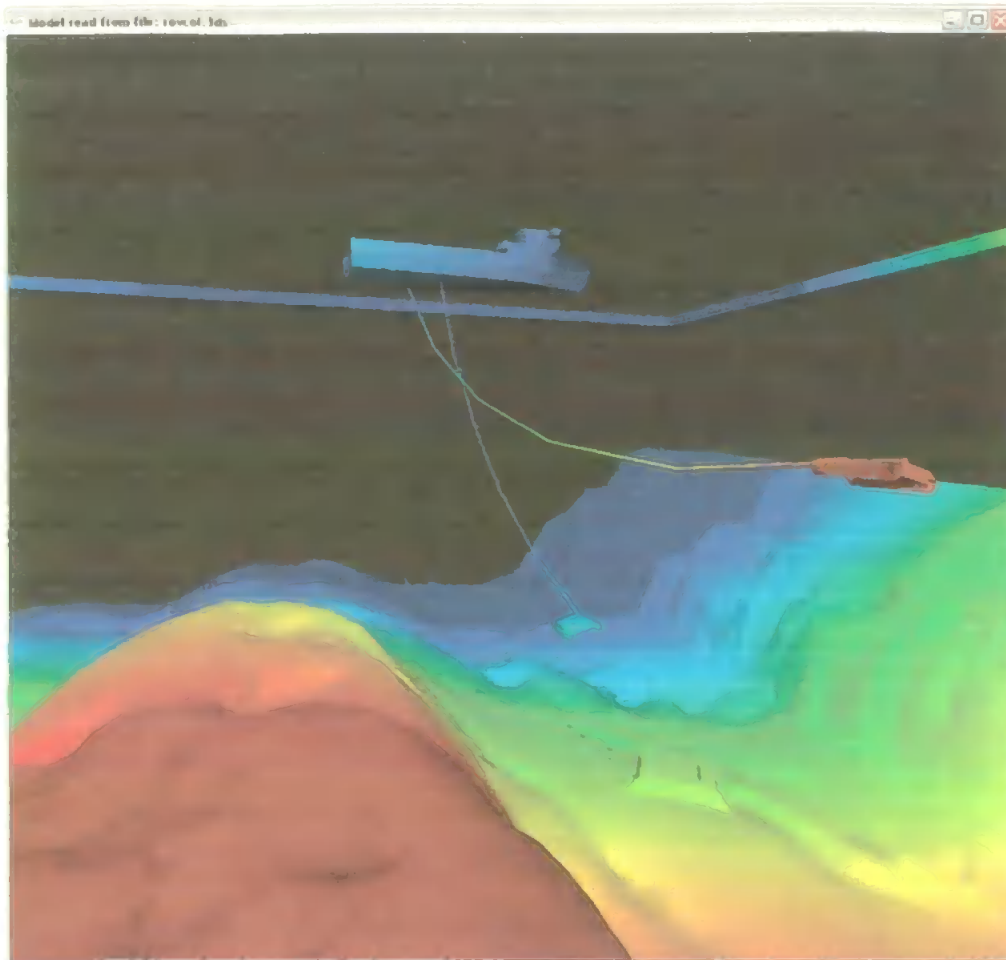
Figure 8.22: Man made objects data model, side view and zoomed in

8.3 Results of evaluation

The results from the evaluation of the chromo stereoscopic effect on the models can be divided into two groups, the general results which are common for all the models, and the model specific results which are particular to each of the four model groups.

8.3.1 General results

The sea surface reference frame is used in all the models and it defines the upper and outer limits of the model. The chromo stereoscopic effect by using the frame is obviously best in the vertical, or near vertical views of the model, where the frame defines the closest parts of the model. When looking at the model in the horizontal or the elevated views the chromo stereoscopic effect on the frame has little value in increasing the depth perception of the model. An elevated view can give a confusing effect on the sea surface reference

frame. The reference frame constitutes a 2D layer in the model, and as in figure 8.6 the CS application distributes the colour spectrum along the frame. The yellow parts of the frame in the upper right hand corner of the model are computed to be at the same distance from the view point as the yellow parts of the bathymetry, but when observing the model from this view it seems to be further away from the viewpoint.

The chromo stereoscopic effect depends on the viewing direction, it is important to use effort in selecting the optimum viewing direction to get the best possible depth perception of the model. Figure 8.3 and the opposite view (figure 8.4) illustrate this. In figure 8.4 there is greater distance in the colour band between the features in the model and thus the depth perception is increased. A more gradual change in the colour spectrum does not induce the same chromo stereoscopic effect. The effect of the motion parallax depth cue also increases the depth perception when changing the viewing direction by rotating the model.

The colour ramp is decreased in some of the views in order to isolate the distribution of the colour spectrum to objects of particular interest. This enhances the chromo stereoscopic effect on that object, giving a better perception of depth in that particular area of the model. Figure 8.11 is an example of a narrow colour ramp on a model. The viewer must be aware of the effect on the entire model, in the areas of dark red in front of, and dark blue behind the object of interest the chromo stereoscopic effect is absent. The narrow colour ramp is also used to increase the colour spectrum separation, and thereby the chromo stereoscopic effect, between objects that with a ramp function enclosing the whole model would lie in the same colour band.

More complex datasets or models with several objects of interest are better suited for chromo stereoscopic enhancement to increase the depth perception. The relative depth between objects of interest are easily determined if the ramp limits are properly set. In figure 8.20 it is easy to establish the relative distance between the vessel and the two

ROVs.

A better representation of the colours in the model will increase the chromo stereoscopic effect. A high quality colour print paper will translate the colours better than a low quality paper, and thereby provides a better chromo stereoscopic effect. A high resolution computer display with good and bright colour representation will probably give the best chromo stereoscopic effect.

The current application has a poor user interface. The user first has to enter the name and directory path of the model file, then the values for the view point distance, and the ramp limits have to be entered into the source code before the source code is debugged and run from Microsoft Visual C++. The whole process has to be repeated for just a slight change in the parameters. It would greatly improve the application to be able to change the ramp function limits and view point distance instantly when having the model in view, without running through the whole process. It would then be much easier to apply the correct cut and colour distribution on the model, ensuring optimal chromo stereoscopic effect.

8.3.2 Model specific results

The depth perception in the views of the bathymetric model is clearly improved by the chromo stereoscopic effect, especially in areas where the bathymetric model has distinct variation and a distinct separation between the colours exists. In the vertical view the sea surface reference frame gives a good indication of the depth of the water column (figure 8.5). If the distance from the highest point of the seabed to the surface is large compared to the vertical extent of the bathymetry, the ramp limit should be adjusted to only enclose the bathymetry. If not, the colour distribution over the bathymetry will not be sufficient to reveal its features. For this reason the optimal colour distribution for vertical views through the entire water column are generally not evenly distributed across the model due to the nature of the dataset.

The chromo stereoscopic technique is very well suited to enhance the depth perception of

models with objects of interest such as biological or organic features in the water column. The relative placement of the shoal in the model in relation to the bathymetry and the sea surface is easy to establish. With the narrow colour distribution in figure 8.11 and figure 8.12 the horizontal extent of the shoal itself is clearly perceived.

The ocean – and tidal current data model is a complex multiple layered data model. It is clear that the vertical view is excellent when viewing all layers of data at the same time (figure 8.13). The chromo stereoscopic technique separates the layers in depth, giving the viewer a very good comprehension of the entire dataset. The vessel also provides increased reference to the surface layer. It is also clear that layered datasets can be confusing to observe using chromo stereoscopy when the viewing direction is not normal to the layers (figure 8.14). A viewing direction parallel to the feature of interest's extent will of course not give an increased understanding of the dataset (figure 8.15).

The man made objects data model is a more complex model with more objects of interest. Generally the chromo stereoscopic effect increases the depth perception of this model very well. The objects of interest's relative positions and relative distance from the view point are easily determined by the viewer. The ramp function limits must however be adjusted to get the desired colour separation between the objects of interest in the data model.

8.3.3 Usability assessment

Nielsen and Landauer (1993) proved that with only a number of 5 test users it is possible to find approximately 85% of all usability problems in a user interface design. The number of usability problems found is established by the Poisson model and is given by equation 8.1.

$$\text{Found(i)} = N(1 - (1 - \lambda)^i) \qquad (8.1)$$

Where i is the number of evaluators, N is the total number of problems in the interface and λ is the probability of finding the average usability problem by using a single evaluator. Nielsen and Landauer (1993) found that in average $\lambda = 31\%$. The 20 students and staff

used as evaluators in this usability assessment found 99.9% of the usability problems (eq. 8.1). The number of evaluators was set that high because it did not present any noticeable extra workload to get the results.

After evaluating figures 8.3 to 8.22 the evaluators answered the following simple questions: ,

- Did you experience the chromo stereoscopic effect?

- Does the chromo stereoscopic effect enhance the depth perception of the model?

- Which of the figures gives best chromo stereoscopic effect?

- Is the chromo stereoscopic effect influenced by the viewing direction?

All 20 staff and student evaluators experienced the chromo stereoscopic effect and stated that the depth perception of the models in general was increased, giving a better understanding of the spatial relations in the hydrographic models. All 20 evaluators said that the effect of the chromo stereoscopic technique is dependent of the viewing direction, which supports the results in chapter 8.2. 13 were of the opinion that the vertical view of the ocean – and tidal current data model (figure 8.13) gave the best chromo stereoscopic effect and 7 believed that the man made objects data model (figure 8.22) gave the best chromo stereoscopic effect. This supports that more complex data models with several spatial objects are better suited for chromo stereoscopic presentation.

Chapter 9: Conclusion and discussion

This chapter draws together the earlier chapters, discusses the chromo stereoscopic technique and the results from the evaluation of the CS application. Then issues for further work are discussed.

9.1 Review of study

The aim of this thesis has been to investigate opportunities and benefits of improved visualisation, through increased depth perception of hydrographic data and to develop a novel technique to improve the visualisation of hydrographic data.

It is clear from this study that an increasing number of depth cues present in the display image will increase the depth perception and understanding of a 3D dataset. The binocular depth cue is one of the most powerful depth cues at close ranges and hence including this depth cue in the presentation on a computer display is of significant value for increased depth perception as the display is part of the personal space.

Current 3D stereoscopic display techniques were reviewed and the chromo stereoscopic technique was identified as a technique that has several advantages when visualising hydrographic data, especially in a semi operational environment. Except for presentation of vertical view remote sensing data (chapter 4.1.7), it has not been possible to find cases where chromo stereoscopy is applied to visualise scientific data.

After reviewing how digital hydrographic data is currently presented, it was clear that stereoscopic presentation of hydrographic data is almost non existent, but 3D perspective presentations are increasingly popular in the hydrographic community. Four classes were identified as especially suited for stereoscopic presentation due to the general 3D nature of the data. The four classes are; bathymetric data, biological/organic data in water volume, ocean- and tidal current data, and man made objects data. It was decided to investigate the chromo stereoscopic technique further and apply it to the presentation of appropriate

hydrographic datasets. An application that applies a chromo stereoscopic texture on

datasets was developed and the application performs well in distributing the chromo

stereoscopic texture over the model. However, the user interface is very simple, making the

processing and parameter determination complicated and time consuming.

Four hydrographic data models were built, each representing one of the previously

identified digital hydrographic data classes. These data models were used to evaluate the

chromo stereoscopic effect on relevant hydrographic data models.

Generally, the chromo stereoscopic technique enhances the depth perception and

understanding of the spatial relations in the models examined. However the stereoscopic

effect is dependent on the viewing direction and amount of 3 dimensionality in the model.

The depth perception is increased if the viewing angle is selected such that the main

features in the model are separated in the colour band. It can be confusing to interpret

layered datasets if the viewing direction is not normal to the layers. As established in the

earlier stages of the study, more complex datasets (i.e. datasets with an increasing number

of objects or features of interest) will profit even more from a chromo stereoscopic

presentation, enhancing the understanding of the relative spatial location between the

features or objects.

The quality of the colour representation in the chromo stereoscopically textured model also

affects the chromo stereoscopic effect. When transferred to paper copies it seems like the

chromo stereoscopic effect is somewhat reduced, according to the quality of paper used. A

high definition colour display with bright colour representation and backlight gives the best

chromo stereoscopic effect.

9.2 Issues for further work

It would be very useful to develop the application user interface. The ability to set the ramp

function limits and view point distance directly when viewing the model would greatly

improve the user interface. Slide bars to adjust Df, Db and vp would make it much easier

to set optimal values for these parameters, an optimal solution for the viewing angle and zooming functionality would be a "fly-through" capability where the viewer could more easily move relative to the model. A functionality where the viewer could toggle between a natural texture and a chromo stereoscopic texture would compensate for the negative aspect of the unnatural colouring of chromo stereoscopic models. These extended functionalities were not necessary to include for the investigation on the chromo stereoscopic effect, however for a further investigation into optimal parameter settings and viewing direction it would be necessary.

Further usability testing during the application development will provide quality assurance and deeper insight of the development process (Nielsen and Landauer, 1993).

References

1. Actuality Systems Inc. World Wide Web page latest accessed August 2002. http://www.actuality-systems.com

2. Baird Software. World Wide Web page latest accessed August 2004. http://www.bairdsoftware.com

3. Barfield, W., Rosenberg, C. (1995). **Judgements of Azimuth and Elevation as a Function of Monoscopic and Binocular Depth Cues Using a Perspective Display.** Human Factors 37(1), (pp.173-181).

4. Berbaum, K., Tharp, D., Mroczek, K. (1983). **Depth Perception of Surfaces in Pictures: Looking for conventions of depiction in Pandora's box.** Perception, 12, (pp. 5-20)

5. Bemis, S. V., Leeds, J. L., Winer, E. A. (1988). **Operator Performance as a Function of Type of Display: Conventional versus Perspective.** Human Factors, 30(2), (pp. 163-169).

6. Benton, S.A. (1985). **Display Holography: an SPIE Critical Review of Technology.** Proceedings SPIE, Holography, A86-32351 14-35 (pp.8-13).

7. Brassard, L. (1998). **The Perception of the Image World.** PhD Thesis at Simon Fraser University, BC, Canada. World Wide Web page latest accessed 23 July 2002: http://www.ensc.sfu.ca/people/grad/brassard/personal/THESIS

8. Brouns, G., De Wulf A., Constales, D. (2001). **Multibeam dataprocessing: Adding and deleting vertices in a Delauney triangulation.** The Hydrographic Journal No 101 July 2001, (pp. 3-9)

9. Brown, J. L. (1965). **The Structure of the Visual System.** In C. H. Graham (Ed.), Vision and Visual Perception. (pp. 39-59). John Wiley & Sons (New York).

10. Börner, R. (1999). **Four Autostereoscopic monitors on the level of industrial prototypes.** Displays 20 (pp. 57-64)

11. Carr, H. A. (1935). **An Introduction to Space Perception.** Longmans, Green. (New York).

12. CAVE Automatic Virtual Environment. National Centre for Supercomputing Applications (NCSA) World Wide Web Page latest accessed in January 2004. http://cave.ncsa.uiuc.edu/

13. Chartwork Ltd. World Wide Web Page latest accessed February 2003.http://www.chartwork.com/

14. Clark, M., Jackson, P.L., Cohen, H.H. (1996). **Understanding the Role of Depth Perception in Slip, Trip and Fall Incidents.** Ergonomics in Design, July, (pp.16-21).

15. Cormack, R. H., Fox, R. (1985). **Stereoscopic Depth Perception at Far Viewing Distances.** Perception & Psychophysics, 35, (pp. 423-428).

16. Coren, S., Ward, L.M., Enns, J.T. (1993). **Sensation and Perception. 4th Ed.** Harcourt Brace & Company (Orlando, Fl.).

17. de Jong, C.D., Lachapelle, G., Skone, S., Elema, I. A. (2002). **Hydrography**. Delft University Press (The Netherlands).

18. Diner, D. B., Fender, D. H. (1993). **Human Engineering in Stereoscopic Viewing Devices**. Plenum Press (New York).

19. Discreet, a Subdivision of Autodesk, Inc. World Wide Web page latest accessed August 2004. http://www.discreet.com

20. Eindhofen, W. (1885). **Stereoscopie durch Farbendifferenz**. Albrecht von Gaefes Archiv fur Ophtomologie, No. 31. (pp.211-238)

21. Ellis, S. R., McGreevy, M. W., Hitchcock, R. J. (1987). **Perspective Traffic Display Format and Airline Pilot Traffic Avoidance**. Human Factors 29(4), (pp. 371-382).

22. Ellis, S. R., (1993). **Pictorial Communication: Pictures and the Syntetic Universe**. In R. Ellis, M. Kaiser, J. Grunwald (Eds.), Pictorial Communication in Virtual and Real Environments. (2nd ed.). (pp. 22-40). Taylor & Francis (London).

23. Ellis, S. R. (2000). **On the design of Perspective Displays**. Proceedings, IEA 2000/HFES2000 44th Ann. Meeting Human Factors & Ergonomics Society.

24. Endsley, M. R. (1995). **Measurement of Situational Awareness in Dynamic Systems**. Human Factors, 37(1), (pp.65-84).

25. Erdas Stereo Analyst product Information page on the World Wide Web latest accessed August 2004. http://www.gis.leica-geosystems.com/products/documents/ Stereo_Analyst_Product_Description.pdf

26. European Space Agency (ESA) Earthnet Online World Wide Web page latest accessed March 2003. http://earth.esa.int/

27. European Space Agency / Tromsø Satellite Station (ESA/TSS) World Wide Web page latest accessed March 2003. http://www.tss.no/tssweb/gallery/images/Oil/Slide1.gif

28. Fakespace Labs. Inc. World Wide Web Pages latest accessed August 2002. http://www.fakespacelabs.com

29. Favalora, G. E., Napoli, J., Hall, D. M., Dorval, R. K., Giovinco, M. G., Richmond, M. J., Chun, W. S. (2002). **100 Million-voxel Volumetric Display**. SPIE Cockpit Displays IX: Displays for Defence Applications (SPIE's 16th Annual International Symposium on Aerospace/Defence Sensing, Simulation and Controls).

30. Foley, J. D., van Dam, A., Feiner, S. K., Huges, J. F. (1990). **Computer Graphics Principles and Practice 2nd Ed.** Addison Wesley (Massachusetts).

31. Furuno Norge AS (2003). **CH-37 Fish Finding Sonar brochure** available at World Wide Web page http://www.furuno.no/files/documents/ch37.pdf

32. Gonzalez, R. C., Woods, R. E. (2002). **Digital Image Processing 2nd Ed.** Prentice Hall Inc. (New Jersey).

33. Graham, C. H. (1965). Visual Space Perception. In C.H Graham (Ed.), **Vision and Visual Perception** (pp. 504-547). John Wiley & Sons (New York).

34. Grunwald, A. J., Ellis S. R. (1993). **Design and Evaluation of a Visual Display Aid for Orbital Manoeuvring.** In R. Ellis, M. Kaiser, J. Grunwald (Eds.), Pictorial Communication in Virtual and Real Environments. (2nd ed.). (pp. 207-231). Taylor & Francis (London).

35. Haber, R.B., McNabb, D.A. (1990). **Visualization Idonoms: A Conseptual Model for Scientific Visualization systems.** IEEE – Visualization in Scientific Computing. (pp. 74 – 93).

36. Hearn, d., Baker, P. (2004). **Computer Graphics with OpenGL. 3rd ed.** Prentice Hall (New Jersey).

37. Hershenson, M. (1999). **Visual Space Perception.** MIT Press (Cambridge, MA).

38. Hochberg, J. E. (1978). **Perception (2nd ed.).** Prentice Hall (New Jersey).

39. Howard, I.P. (1993). **Spatial Vision within Egocentric and Exocentric Frames of Reference.** In R. Ellis, M. Kaiser, J. Grunwald (Eds.), Pictorial Communication in Virtual and Real Environments. (2nd ed.). (pp. 338-358). Taylor & Francis (London).

40. Hydro International. (2002). **Product Survey: Hydrographic Navigation Software.** Hydro International, November 2002. Vol. 6 (9) (pp. 39-43).

41. Interactive Visualization Systems (2004). World Wide Web Page accessed June 2004. http://www.ivs.unb.ca/products/fledermaus/index.html

42. International Communications and Navigation Ltd. (ICAN) World Wide Web page latest accessed in March 2003. http://www.ican.nf.net/FINS.htm

43. IHO (1994). International Hydrographic Office. **Hydrographic Dictionary Part I Volume I, English.** Special Publication No. 32 (5th ed.). IHO (Monaco).

44. IHO (2000). International Hydrographic Office. **IHO transfer standard for digital hydrographic data S-57 ed 3.1.** IHO (Monaco).

45. Ingham, A. E., Abbott, V.J. (1992). **Hydrography for the Surveyor and Engineer (3rd ed.).** Blackwell Scientific Publications (Oxford).

46. Javidi, B., Okano, F. (2002). Three-Dimensional television, Video, and Display Technologies. Springer Verlag (Berlin).

47. Kantowitz, B.H. & Sorkin R.D. (1983). **Human Factors: Understanding People-Systems Relationships.** John Wiley & Sons (New York).

48. Kim, W. S., Ellis, S. R., Tyler, M.E., Hannaford, B., Stark, L.W. (1987). **Quantitative Evaluation of Perspective and Stereoscopic Displays in Three-Axis Tracking Tasks.** IEEE Transaction on System. Man and Cybernetics, 17(1), (pp. 61-71).

49. Kim, W. S., Tendick, F., Stark, L. (1993). **Visual Enhancements in Pick-and-Place Tasks: Human operators controlling a simulated cylindrical manipulator.** In R. Ellis, M. Kaiser, J. Grunwald (Eds.), Pictorial Communication in Virtual and Real Environments. (2nd ed.). (pp. 265-282). Taylor & Francis (London).

50. Kishto, B. N. (1965). **The colour Stereoscopic Effect.** Vision Research. Volume 5 (pp. 313-329) Pergamon Press, UK.

51. Kjerstad, N. (2002). **Elektroniske og Akustiske Navigasjonssystemer for Maritime Studier.** Tapir Akademiske Forlag. (Trondheim, Norway)

52. Klein Assosiates Inc. World Wide Web page latest accessed February 2003. http://www.kleinsonar.com/image/3000/glwreck2.html

53. Kohler, I (1962). **Experiments with Goggles.** Scientific American 206 (pp. 69-72)

54. Kongsberg Norcontrol AS (2002). **Sea Map 10 ECDIS Operations Manual.** KMSS CN-0276-G/09-Jan/02.

55. Lavender, S. (2001). **The application of Remote Sensing to Hydrography.** The Hydrographic Journal No 99 January 2001, (pp. 9-13)

56. Leica Geosystems World Wide Web page latest accessed August 2004. http://gis.leica-geosystems.com/products/Imagine/add_ons/stereo_analyst.asp

57. LH Systems World Wide Web page latest accessed March 2004. http://www.lh-systems.com/products/am2000.htm

58. Lillesand, T.M., Kiefer, R.W. (2000). **Remote Sensing and Image Interpretation.** 4th **Ed.** John Wiley & Sons (New York).

59. Lipson, S.G. (1995). **Optical Physics.** Cambridge University Press.

60. Lipton, L. (1997). **Stereo-Vision Formats for Video and Computer Graphics.** Proceedings of SPIE Volume 3012, Stereoscopic Displays and Virtual Reality Systems IV.

61. Lockhart, D., Saade, E., Wilson, J. (2001). **New Developments in Multi-beam Backscatter Data Collection and Processing.** Thales Geosolutions (Pacific), Inc. World Wide Web page latest accessed November 2002. http://www.fisherieshabitat.net/whitepapers/NewDevelopmentsinMultbeam.doc

62. MacDonald, L.W., Lowe, A.C. (1997). **Display Systems. Design and Applications.** John Wiley & Sons (New York)

63. Makai Ocean Engineering Inc. World Wide Web page latest accessed August 2003.

http://www.makai.com/cab-sw.htm

64. McLean, G. F., Prescott, B., Podhorodeski, R. (1994). **Teleoperated System Performance Evaluation.** IEEE Transactionon System, Man and Cybernetics, 24(5), (pp. 796-803).

65. Moe, H., Ommundsen, A., Gjevik, B. (2002). **A high-resolution tidal model for the area around The Lofoten Islands, northern Norway.** Continental Shelf Research 22 (2002) (pp.485-504).

66. Murdock, K.L. (2003). **3ds max® 5 Bible.** Wiley Publishing Inc. (New York)

67. Nansen Environmental and Remote Sensing Center (NERSC) World Wide Web page latest accessed in March 2003. http://www.nersc.no/index2.php

68. National Aeronautics and Space Administration (NASA) World Wide Web page latest accessed in August 2002. http://mars.jpl.nasa.gov/MPF/ops/TwinPeaks_glyph_md.gif

69. Nemire, K., Jacoby, R.H., Ellis S. R. (1994). **Simulation Fidelity of a Virtual Environment Display.** Human Factors, 36(1), (pp. 79-93).

70. Nielsen, J., Landauer, T. K. (1993). **A Mathematical Model of the Finding of Usability Problems.** ACM Interchi '93 Conference Proceedings (Amsterdam, The Netherlands, 24-29 April 1993), (pp.206-213).

71. Norwegian Shell (2003). Bathymetric data file in the AutoCAD dwg format made available by the topographic department of Norwegian Shell in Stavanger, Norway.

72. Okoshi, T. (1976). **Three-Dimensional Imaging Techniques.** Academic Press Inc. (New York).

73. OpenGL World Wide Web page latest accessed in October 2004. http://www.opengl.org

74. Pastoor, S., Wöpking, M. (1997). **3D displays: A review of current technologies.** Displays, 17 (1997), (pp. 100-110).

75. Patterson, R., Martin, L. (1992). **Human Stereopsis.** Human Factors, 34 (6). (pp. 669.692).

76. Patterson, R., Moe, L., Hewitt, T. (1992). **Factors that Affect Depth Perception in Stereoscopic Displays.** Human Factors 34(6), (pp. 655-668).

77. Pender, K. (1998). **Digital Colour in Graphic Design.** Focal Press (Oxford, UK).

78. Petrie, G. (2001). **3D Stereo-Viewing of Digital Imagery. Is Auto-Stereoscopy the Future for 3D?** Dossier in Geoinformatics December 2001, (pp.24-29).

79. Prevett, T. T., Wickens, C. D. (1994). **Perspective Displays and Frame of Reference: Their independence to realize performance advantages over planar displays in terminal area navigation task.** (ARL-94-8/NASA-94-3). University of Illinois, Aviation Research Laboratory.

80. Quality Positioning Services BV (QPS) (2003). **QINSy 6 hydrographic Software Package** brochure. Available at the World Wide Web page: http://www.qps.nl/Eng/Pages/QINSy.htm

81. Ramachandran, V.S. (1988). **Perceiving Shape from Shading.** Scientific American, 259, (pp76-83).

82. Root.cz World Wide Web page latest accessed January 2005. http://www.root.cz/clanek/2349

83. Sato, K. (2001). **Recent research development and subject for electro-holography.** Society for Information Display Conference Record of the International Display Research Conference. (pp. 1357-1360)

84. Shibata, T. (2002). **Head Mounted Display.** Displays 23 (pp. 57-64).

85. Sinclair, M. (1999). **Laser Hydrography – Commersial Survey Operations.** Paper presented at the U.S. Hydro 1999 conference in Mobile, Alabama April 27-29.

86. Steenblik, R.A. (1987). **The Chromostereoscopic process: A Novel Single Image Stereoscopic Process.** SPIE Vol. 761. True 3D Imaging Techniques and Display Technologies.

87. Stereographics Corporation World Wide Web page accessed in August 2002. http://www.stereographics.com/index.htm

88. Stoper, A. E., Cohen, M. M. (1993). **Optical, Gravitational and kinaesthetic determinants of judged eye level.** In R. Ellis, M. Kaiser, J. Grunwald (Eds.), Pictorial Communication in Virtual and Real Environments. (2nd ed.). (pp. 390-403). Taylor & Francis (London).

89. Sundet, J. M. (1972). **The Effect of Pupil Size Variations on the Colour Stereoscopic Phenomenon.** Vision Research. Volume 12 (pp. 1027-1032).

90. Suthau, T., Vetter, M., Hassenpflug, P., Meinzer, H.P., Hellwich, O. (2002) **A concept work for Augmented Reality visualisation based on a medical application in liver surgery.** ISPRS, the International Archives of the Photogrammetry, Remote Sensing and Spatial Information Sciences;Volume XXXIV, Part5, Commission V, Proceedings of the ISPRS Commission V Symposium, close-range imaging, long-range vision. (pp. 274-280) (Corfu, Greece).

91. Taylor University, Computing and System Sciences Department World Wide Web pages latest accessed November 2004. http://www.css.tayloru.edu/~btoll/resources/graphics/opengl/xp/visualc.html

92. Toutin, T. (1997). **Qualitative Aspects of Chromo Stereoscopy for Depth Perception.** Photogrammetric Engineering & Remote Sensing (PE&RS) Vol. 63, No. 2 (pp.193-203)

93. Trayner, D., Orr, E. (1996). **Autostereoscopic Display using Holographic Optical Elements.** Proceedings SPIE, 1996.

94. Tromsø Satellite Station World Wide Web page viewed February 2003. http://www.tss.no/tssweb/index.html

95. University of Illinois, Department of Atmospheric Sciences World Wide Web page latest accessed August 2004. http://www.atmos.uiuc.edu/pdf/BWATMOS.PDF

96. University of Oslo, Department of Mathematics World Wide Web page latest accessed March 2003. http://math-www.uio.no/~bjorng/tidevannsmodeller/tidemod.html

97. University of Toronto, Department of Physics World Wide Web page latest accessed January 2005. http://www.upscale.utoronto.ca/GeneralInterest/Harrison/Spectra/prism.gif

98. Wahl, T. (1998). **Integrated use of radar satellites for fisheries enforcement operations.** Proceedings from the 27th International Symposium of Remote sensing. (pp. 123-126) Tromsø, Norway.

99. Watt, a. (2000). **3D Computer Graphics. 3rd ed.** Addison-Wesley Publishing Company Inc. New York.

100. Wearcam, University of Toronto, Department of Electrical Engineering World Wide Web page latest accessed August 2002. **http://wearcam.org/head-mounted-displays.html**

101. Wei, S. K., Huang, Y. F., Klette, R. (1998). **Colour Anaglyphs for Panorama Visualizations.** Technical report, CITR – TR – 19, Computer Science Department of The University of Auckland (New Zealand).

102. Wickens C.D. (1992). **Engineering Psychology and Human Performance (2nd ed.).** Harper Collins Publisher (New York).

103. Wickens, C. D., Hollands, J. G. (2000). **Engineering Psychology and Human Performance. 3rd ed.** (Prentice Hall, New Jersey).

104. Wickens, C. D., Merwin, D. H., Lin, E. L. (1994, a). **Implication of Graphics Enhancements for the Visualization of Scientific Data: Dimensional Integrity, Stereopsis, Motion and Mesh.** Human Factors, 36(1), (pp. 44-61).

105. Wickens, C. D., Liang, C., Prevett, T., Olmos, O. (1996). Electronic **Maps for Terminal Area Navigation: Effects of Frame of Reference and Dimentionality.** The International Journal of Aviation Psychology, 6(3), (pp. 241-271).

106. Wickens, C. D., Liang, C. C, Prevett, T. T., & Olmos, O. (1994). **Egocentric and Exocentric Displays for Terminal Area Navigation.** Proceedings of the Human Factors and Ergonomics Society 38th Annual Meeting.

107. Woo, M., Neide., J., Davis, T., Shreiner, D. (1999). **OpenGL Programming**

Guide 3rd ed. The Official Guide to Learning OpenGL, Version 1.2. Addison
Wesley Longman Inc. (Massachusetts)

108. Yeh, Y. (1992). **Spatial Judgement with Monoscopic and Stereoscopic
Presentation of Perspective Displays.** Human Factors, 34(5), (pp. 583-600).

Bibliography

1. Boardman, T. (2002). **3DS Max 5 Fundamentals.** New Riders Publishing

2. Chapman, D. (2001). **Teach Yourself Visual C++. NET in 21 Days.** SAMS Publishing Inc.

3. Chaomei, C. (2003). Mapping Scientific Frontiers. The Quest for Knowledge Visualization. Springer Verlag (London).

4. Dietel, H.M., Dietel, P.J. (2001). **How to program C++ 3ed. Prentice Hall Inc.** (New Jersey)

5. Edelman, S. (1999). **Representation and Recognition in Vision.** The MIT Press (Massachusetts)

6. Fisher, P., Unwin, D., (2002). **Virtual Reality in Geography.** Taylor &Francis (London)

7. Griffiths, I., Flanders, J., Sells, C. (2003). **Mastering Visual Studio .NET.** O'Reilly & Assosiates Inc.

8. Gulick, W.L., Lawson, R.B. (1976). **Human Stereopsis - A Psychophysical Analysis.** Oxford University Press (New York)

9. Howard, I.P., Rogers, B.J. (1995). **Binocular Vision and Stereopsis.** Oxford University Press (New York)

10. Jackson, R., MacDonald, L., Freeman, K. (1994). **Computer Generated Colour: a practical guide to presentation and display.** John Wiley & Sons (New York).

11. Javadi, B. et. al., (2002). **Three-Dimentional Television, Video and Display Technologies.** Springer Verlag (Berlin, Heidelberg)

12. Johnsen, B., Skibo, C., Young, M. (2003). **Inside Microsoft Visual Studio .NET version 2003.** Microsoft Press

13. Kennish, M. J. (2001). **Practical Handbook of Marine Science 3ed.** CRC Press. Marine Science Series.

14. Nielson, G. M. et. al., (1997). **Scientific Visualisation.** IEEE Computer Society Press (Los Alamitos, CA).

15. Palmer, S. E. (1999). **Vision Science – Photons to Phenomenology.** The MIT Press (Cambridge, MA).

16. Pashler, H., Yantis, S. (2002). **Stevens' Handbook of Experimental Psychology 3ed. Sensation and Perception Volume 1.** John Wiley & Sons Inc. (New York).

17. Pickover, C. A., Tewksbury, S. K. (1994). **Frontiers of Scientific Visualisation.** John Wiley & Sons (New York).

18. Templeman, J., Olsen, A. (2002). **Microsoft Visual C++.NET Step by Step.**

Microsoft Press.

19. Thurman H. V. (1997). **Introductory Oceanography 8th ed.** Prentice Hall.

20. Ware, C. (2000). **Information Visualization. Perception for Design.** Morgan Kaufmann Publishers.

21. Yantis, S., (2001). **Visual Perception.** Taylor & Francis (Philadelphia).

Appendixes

Appendix 1

Peer reviewed publications resulting from this project:

1. Ostnęs, R., Abbott, V.J., Lavender, S.J. (2004). **Visualisation Techniques: An Overview.** The Hydrographic Journal No. 113 July.

2. Ostnes, R., Abbott, V.J., Lavender, S.J. (2004). **Visualisation Techniques and Applications to Hydrographic Data.** The Hydrographic Journal No. 114 October.

VISUALISATION TECHNIQUES: AN OVERVIEW – PART 1

Runar Osmes*, Victor Abbott and Samantha Lavender

School of Earth, Ocean and Environmental Sciences, University of Plymouth, UK

* *Lecturer at Aalesund University College, Norway, and PhD student at UoP*

Abstract

Practically unchanged for several hundreds of years, hydrographic and nautical information has been presented on a 2 dimensional (2D) paper chart. With the advances in computer and information technology, new techniques of presenting spatial data have emerged. Electronic charts have revolutionised navigation and the collection of digital hydrographic data is increasingly efficient.

Computerised 3D visualisation techniques are now developed in several fields, from computer gaming to advanced scientific visualisation. The visualisation of hydrographic data might employ such techniques to the increasingly detailed and complex hydrographic datasets in order to improve the perception and comprehension of the data.

This paper, the first of two, presents the range of visual depth cues available plus an evaluation of 2D, 3D perspective and 3D stereoscopic displays. Part two will present the 3D stereoscopic display techniques presently available and discuss the suitability, opportunities and benefits of implementing these techniques when presenting hydrographic data.

Introduction

A basic limitation of a conventional visual display is that the surface of the display screen is 2D whereas the natural world is 3D. In order to improve the visualisation of hydrographic data, it is necessary to represent depth or distance perception as a third dimension along the line of sight. When presenting hydrographic data, perspective models frequently include several visual cues to increase the depth perception. However one of the most powerful visual cues, stereopsis (i.e. the effect generated through binocular vision), is rarely used.

This paper reviews the characteristics of human visual perception of depth and distance, including the different visual cues to increase depth perception. It will compare 2D, 3D perspective and 3D stereoscopic displays and review the 3D stereoscopic display techniques available. As this paper focuses on the basic characteristics of depth perception and different displays the reader might miss a greater hydrographic setting, however the authors find it pertinent to establish these relationships before advancing further. The second paper will discuss how to improve the perception of relevant hydrographic datasets and through relevant examples expand the overall hydrographic relevance to the reader.

Depth Perception and Visual Cues

Depth and distance perception is achieved through the combination of several depth cues. The term, cues, has been utilised to formalise the specification of stimulus conditions for space perception (Carr, 1935). To distinguish between perceived and physical space the relation between distal stimuli and proximal stimuli is important. Any physical objects and scenes are distal stimuli, where distal stimuli rouse our nervous system by patterns of energy (e.g. light energy, sound waves). Patterns of energy that reach and affect our sense organs are termed proximal stimuli and by projecting the energy patterns from distal stimuli onto a surface (e.g. a screen or retinal surface) the proximal stimulus patterns can be observed.

Hochberg (1978) defined a depth cue as a pattern of proximal stimulation that contains information about the spatial location of distal objects. Depth cues can be classified into two types: monocular and binocular. Monocular depth cues require the activity of a single eye; binocular depth cues require the use of both eyes. Pictorial depth cues are a subset of monocular depth cues and include linear perspective, relative size, known size, interposition, shadow distribution, aerial perspective, height in picture plane
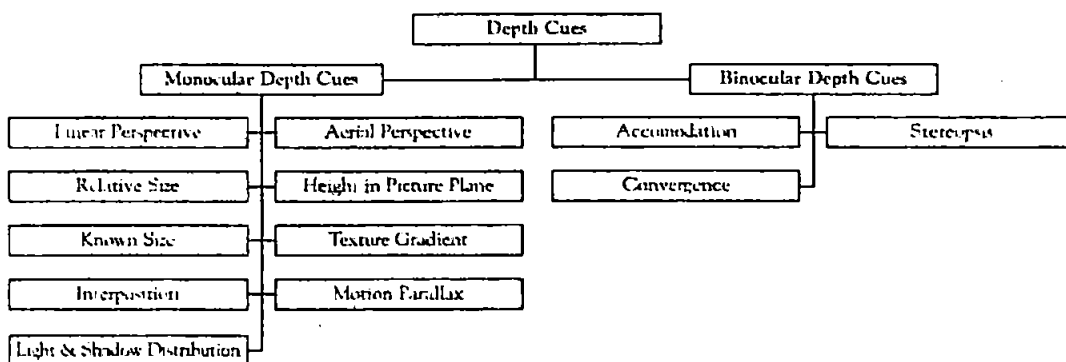

Figure 1: Block diagram portraying the different Depth Cues in two classes, Monocular and Binocular Depth Cues

and gradient of texture-density (Hochberg, 1978; Hershenson, 1999). Motion parallax is also described as a monocular depth cue and is also relevant in this review. Binocular depth cues include accommodation, convergence and stereopsis (Hershenson, 1999). Figure 1 illustrates the different depth cues available.

Monocular Depth Cues

This section describes each of the different monocular depth cues.

Linear Perspective

If the size of a distal object is fixed, the visual angle will be inversely proportional to the distance from the object; this is called linear perspective or outline shape (Kantowitz and Sorkin, 1983). A constant distance between points subtends a smaller and smaller angle at the eye as the points withdraw from the eye. For example, railway tracks appear to approach each other (the retinal images of the lines converge) as the distance from the eye increases although they are parallel. Therefore, converging lines are a cue that they are parallel and receding in depth (Wickens, 1992). Figure 2 shows the linear perspective of a cube in relation to the horizon.
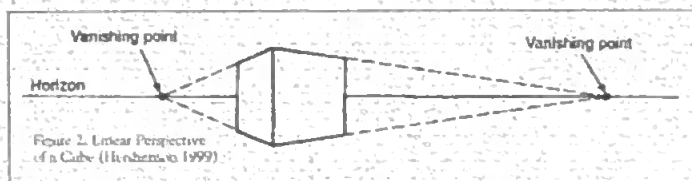

Figure 2. Linear Perspective of a Cube (Hershenson 1999)

Relative size

Two similar shaped objects with different size will affect the relative perceived distance to the objects. The larger object will appear closer than the smaller. By comparing the apparent size of a distant object with that of a similar, much closer object, the relative distance of the distant object can be approximated (Hershenson, 1999). Relative size is also tied directly to linear perspective. In figure 2, the more distant side of the cube can be observed as relatively shorter than the nearest side.

Known size

We can use an object's known size to deduce relative depth. If the object has known size (S) the distance (d) can be determined as (Coren et al, 1993):

$$d = \frac{S}{\tan\alpha}$$

For example, a man is taller than a boy. However, if they produce the same size of retinal image, then the brain deduces the man is located farther away than the boy. This is often a weak or ineffective cue because cognitive factors influence the perceived distance.

Interposition

When a closer object (B in figure 3) interrupts the outline of a further (overlapped) object (A in figure 3) it appears to be closer to the viewer. This is an effective depth cue, but can only indicate which object is in front, not the distance separating them (Hershenson, 1999).
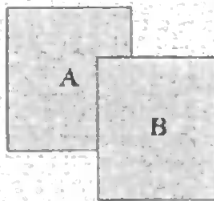

Figure 3: Interposition of Objects

Light and shadow distribution

Shadows provide some information about the orientation of objects and their 3D shapes (Ramachandran, 1988). Objects may appear to lie at different distances and have different dimensions as combinations of shadow and highlight change (Graham, 1965). If objects have a light source from one direction, they will have shadows unique to their shape and orientation.

Aerial Perspective

Atmospheric scattering of light by molecules (also termed Rayleigh scattering) causes de-saturation of an object's colour, resulting in a more bluish colour and less contrast. This affects the perceived depth of an object (Hershenson, 1999). Hence a more distant object will appear in a more bluish in colour and have less contrast. Underwater, this would be termed veiling light and is caused by the light scattering from water molecules.

Height in picture plane

An object's vertical position in the display can act as a depth cue. Distant objects appear higher on the display, where it is assumed that the ground plane is extended horizontally to the horizon. Two objects at the same vertical height on the display are perceived to be at the same distance from the observer (Perbaum et al 1983).

Gradient of texture-density

A gradient is the rate of some measured property changing over a continuous, extended stimulus. The surface of most objects is likely to be covered with a reasonably uniform texture or pattern. When looking straight ahead at a textured surface, the gradient of texture-density is zero; as the slant increases, the gradient increases. The gradient of texture-density can provide precise and relatively unambiguous information about the distances and sizes of surfaces and objects in the world (Hochberg, 1978). The crossed squares in the front of figure 4 have the same dimensions as the ones placed in the back in the figure, but as they are located further away from the observer they appear smaller, hence giving a finer texture.
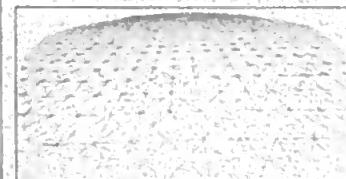
Figure 4: Texture density variation as function of distance (Brunard, 1998)

Motion parallax

When a subject's eye moves with respect to the environment, or vice versa, there exists a differential angular velocity between the line of sight to an object (fixated) and the line of sight to any other objects. This relative lateral movement of objects at varying distances from the viewer is called motion parallax (Hershenson, 1999). By observing the amount and relative direction that a given image moves on the retina, its distance can be approximated (Clark et al, 1996).

Binocular Depth Cues

The binocular depth cues listed in figure 1 are:

Accommodation

When adjusting the focal length of the eyes' lenses to bring objects at different distances into focus, a muscular strain is present in the ciliary body. This strain is called accommodation, and is effective up to a range of a few metres (Coren et al 1993).

Convergence

The eyes are capable of convergence, in which both eyes turn inward toward the medial plane (Brown, 1965). The convergence is proportional to the convergence angle (γ in figure 5) with a large convergence corresponding to near objects and a slight convergence to distant objects. The brain receives messages from the ocular muscles about the degree of convergence, and by analysing the information can approximate the effect of the change (Hershenson, 1999). In this way, convergence may serve as a depth cue. A large convergence may lead to the response 'nearer', while a slight convergence may lead to the response 'far-off'.

- 149 -
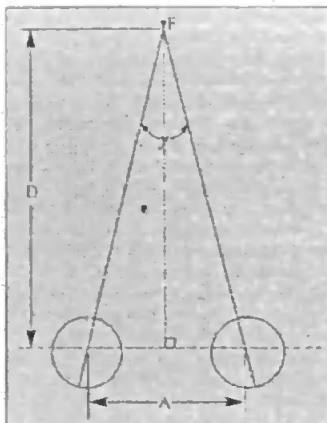
Figure 5: Convergence angle, y = convergence angle, A = inter pupillary distance and D = distance to fixation point (Henderson 1999)

Stereopsis

The factors important for the design of stereoscopic display systems include the geometry of stereoscopic depth perception, visual persistence, perceptual interaction among stereoscopic stimuli, and the neurophysiology of stereopsis. This section reviews the geometry of stereoscopic depth perception presented by Patterson and Martin (1992). Stereopsis with regard to visual displays will be discussed further.

Retinal disparity and horopter

Stereopsis is produced by horizontal retinal disparity, which results from an interocular difference in the relative position of corresponding monocular images. Figure 6 shows the concept of retinal disparity where F is the fixation point and object A on the horopter produces corresponding retinal points; point a in the left eye and point a' in the right eye. These two points are equally distant from f and f' on the retina, respectively. Therefore, A' has zero disparity with respect to F. Object B in front of the horopter, however, produces non-corresponding retinal points; point b in the left eye and point b' in the right eye. These two points are not equally distant from f and f', respectively. Therefore, B has a certain amount of disparity with respect to F (Patterson and Martin, 1992).

The horopter in figure 6, represented by the line through F (fixating point) can be formed by connecting points, which give zero disparity. Any images from objects on the horopter stimulate corresponding retinal points in the two eyes (Patterson and Martin, 1992). In other words, for every point on the retina of the left eye, there is a corresponding point on the right eye. Therefore, the horopter can be defined as the locus of all points, which have zero disparity (Henchenson, 1999).
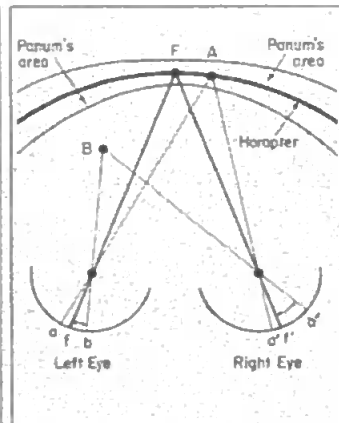

Figure 6. Longitudinal Horopter and Panum's Fusion Area (Patterson and Martin, 1992)

In many applications, the horopter is considered to be placed on the surface of the display screen; the disparity is then defined with respect to the screen. This definition may create problems in designing accurate stereoscopic displays, because, if the viewer converges to a depth plane other than the defined horopter (i.e., the surface of the screen), the intended relevant disparities become inaccurate.

Panum's Fusional Area

Fusion is the perceptual process of blending two corresponding images into a single image. The range at which the resulting disparity can be fusible (i.e. the area surrounded by the boundary of the limit of the disparity fusion) is called Panum's fusional area (see Figure 6). This describes an area where the viewer can force fusion despite an offset in the objects' locations (Diner and Fender, 1993).

Thus objects within Panum's area result in small disparities, which are fusible. Objects outside Panum's area result in large disparities, which are not fusible, producing double images. Factors affecting the extent of the area include stimulus size, spatial frequency, eccentricity, and temporal modulation of disparity information (Patterson and Martin, 1992). The disparity limit for fusion increases as the stimulus size increases (e.g. large disparity can be fused with large stimuli), and decreases as the spatial frequency increases. The disparity limit increases with eccentricity (i.e. degrees away from the fovea). The fovea is the most light-sensitive area of the retina near its centre. This is the focal point of the retina, and vision is optimal in this part of the retina. The disparity limit also increases as the temporal frequencies of modulation decrease. These factors must be carefully manipulated in order to improve the binocular fusion in designing stereoscopic displays.

Discussion

It is interesting to note that, except for interposition and stereopsis, most of the depth cues discussed cannot be applied to an orthogonal (i.e. parallel projection) 2D display format (e.g., a chart) that conveys information in two dimensions at once. A perspective display format can utilise most of the depth cues except for binocular disparity, which can only be provided by using a stereoscopic display. Pictorial depth cues are patterns that can occur not only in the picture plane, but also in the proximal stimulation at the eye when objects are scattered around in a three-dimensional landscape. Consequently, such indications of 3D space are necessarily ambiguous. Therefore, any theory that bases our perception of space on pictorial depth cues must consider space perception to be ambiguous. Any pattern in the optic array is much more ambiguous than that. A number of different three-dimensional arrangements can produce the same proximal stimulus pattern at the eye (Hochberg, 1978). Binocular disparity in itself is a powerful depth cue. However, it cannot be the basis of all space perception. One-eyed individuals may show good depth perception, even at a very early age (Hochberg, 1978).

Visual Displays and Techniques

A visual display system with appropriate format can provide an efficient Man-Machine-Interface. Many applications of visual displays and their evaluations are reported in the literature e.g. advanced teleoperation, aircraft cockpit display, and air traffic control displays. Various types of information displays include traditional 2D plan-view, 3D perspective, and stereoscopic displays with or without visual enhancements.

This section reviews the basic literature, the basic geometry and factors that are considered to be important for the design of these displays. A comparison of 2D, 3D perspective and stereoscopic displays is presented with reference to experimental studies.

Geometry of 2D and 3D perspective displays

The mechanism of visual spatial judgments uses one of a variety of coordinate systems. Howard (1993) discussed the reference frames:

'An egocentric frame of reference is defined with respect to some part of the observer. Four major egocentric frames of reference include: a station-point frame associate with the nodal point of the eye, a retinocentric frame associate with the retina, a head centric frame associated with head, and a bodycentric frame associate with the torso. An exocentric frame of reference is external to the observer'.

Visualisation Techniques: An Overview – Part 1

The evaluation of an egocentric display and three different exocentric displays in pilot navigational performance has been discussed by Prevett and Wickens (1994). The results showed that the egocentric perspective display was better in a tracking task than the others including the planar display, while a middle distance exocentric display resulted in better performance in the global awareness tasks than the others. This advantage of the perspective displays was varied with the viewpoint location distances. However, these results support the advantage of perspective displays over planar displays.

Dimensionality

In addition to the choice of reference frame, the choice of dimensionality (2D vs. 3D) is important when presenting data on visual displays. A 3D perspective display can be achieved by projecting an object onto the view (projection) plane and then mapping the view plane onto the display screen. There are two methods to generate the perspective projection: the viewpoint-transformation and the object-transformation (Kim et al 1993). In a central projection, projection lines emanate from the centre of the projection (viewpoint). The intersection of the projection line with the view plane forms a projected image of an object. If the viewpoint is set at an infinite distance, a parallel projection is obtained.

A perspective projection can be obtained by setting the viewpoint at a finite distance. In general, two processes are performed to generate a perspective display.

- Perspective projection onto the view planes and

- Mapping of the view plane window onto the display screen.

Wickens et al (1994, a) examined the effectiveness of 2D versus 3D perspective displays, which were designed to present a series of 3D data sets. Results showed that 3D perspective displays were superior to 2D displays for the task that required integrative attention (i.e. focusing on several objects across more than one dimension). Wickens et al (1994, b) also presented a study that contrasted a 2D display, a 3D egocentric display (i.e. the display is presented from the perspective of the pilot sitting in the cockpit) and a 3D exocentric display (i.e. presented from the perspective of the pilot viewing the aircraft from a certain distance from the aircraft) for terminal area navigation. Based on this discussion, the use of 3D perspective displays requires less visual scanning effort than that of two (or three) orthogonal plan-view displays. Furthermore, a 3D ego-referenced display is capable of providing visual information that is congruent both with the pilot's view and control axes.

Stereoscopic Displays

Utilising the human stereoscopic vision capability of fusing two retinal images into one image, the stereoscopic display generates the powerful additional depth cue called stereopsis. However, it should be noted that stereopsis has its limitation as discussed by Clark et al (1996):

- Stereopsis is effective only within short distances, about 200 metres or less;

- Stereopsis provides information about distance between objects but cannot provide information about the distance between any objects and the observer;

- Using stereopsis, people tend to underestimate depth at close distance, and overestimate at far distance.

The stereoscopic display presents two slightly different views of an object on the display. In the 3D world, the view each eye receives is somewhat different because the two eyes see the object from slightly different positions. Differences in these views give two possible depth cues: double image (each eye contributes a different image of the far object when viewing near and vice versa) and binocular disparity (Hochberg, 1978). The disparity is the difference between where a target falls on the right eye and the left eye as discussed earlier.

The disparity can generate a powerful depth cue (Hochberg, 1978). This depth cue can be obtained by taking two photographs of a scene (a stereoscopic picture pair, a 'stereogram'), one from the position of each eye (65mm apart on average), and presenting each picture to its appropriate eye, and then viewing such photographs with special devices called stereoscopes. The stereoscope is composed of two converging lenses and a supporting frame that simply separates right and left views. Different stereoscopic techniques will be reviewed in Part 2.

2D versus 3D perspective displays

Ellis et al (1987) conducted an experiment to compare a conventional 2D plan view with a 3D perspective air traffic information display for an identical traffic situation. No significant difference in manoeuvre decision time between the conventional and the perspective display was found, except in a head on traffic situation where decision time with the perspective display was much shorter. The mean number of selecting avoidance manoeuvres between the two display situations was not significantly different; however, more manoeuvres with a vertical component were found using the perspective display.

Bemis et al (1988) performed a similar experiment to evaluate operator performance on a perspective and a conventional naval tactical display. Results showed that operators had fewer errors and shorter response times when using the perspective display.

Prevett and Wickens (1994) compared pilot navigational performance using a 2D planar display (consisting of a 2D map and profile view) with four 3D perspective displays. The results showed that the egocentric perspective display was better in a tracking task than the others including the planar display, while the middle distance exocentric display resulted in better performance in the global awareness tasks than the others. This advantage of the perspective displays was varied with the viewpoint location distances. However, the results support the advantage of perspective displays over planar displays.

In these studies, the use of 3D perspective displays resulted in relatively better performance than for 2D displays. However, the superiority of perspective displays can be degraded by the following factors as discussed by Wickens et al (1994, b):

- *Position distortion* - The perspective display presents the world from a non-orthogonal angle (e.g. views other than looking straight forward or down). Therefore, certain portions of the world will be covered in a greater detail than others. The potential remedy of this problem is to widen the field of view. However, such a technique produces the distortion of the real position;

- *Display resolution inconsistency* - Distances not orthogonal to the line of sight will be presented with less resolution than those orthogonal to the line of sight;

- *Ambiguity along line of sight* - The representation of a 3D world (or objects) on a 2D display surface is inherently ambiguous.

3D perspective versus 3D stereoscopic displays

A comparison of 3D perspective and 3D stereoscopic displays in a simulated tracking task has been presented by Kim et al (1987). The stereoscopic display resulted in lower tracking error over all visual conditions. However, the perspective display with appropriate perspective parameters (i.e. optimal viewing angles in both the vertical and horizontal plane) and visual enhancement depth cues (such as vertical reference lines) resulted in equivalent performance as compared with the stereoscopic display.

Yeh (1992) investigated spatial judgments (relative depth and altitude) with monoscopic and stereoscopic

presentation of perspective displays. The results showed that the presence of binocular disparity in the stereoscopic view improved the spatial judgment. In another study, McLean et al, (1994) compared a 3D perspective video display (one camera view without visual enhancement) with a stereoscopic video display for a peg in a hollow task. The results showed that the stereoscopic video was superior to the 3D perspective video. Yeh (1992) discussed the problem associated with perceptual distortions in perspective projection resulting from the enhancement cues. The benefit associated with using stereoscopic displays was further reported by Barfield and Rosenberg (1995). Their experiment showed that the stereoscopic display was superior to the perspective display (monoscopic) in judging the relative elevation. However, the judgments of relative azimuth angle were not improved by the use of the stereoscopic display.

Intermediate Conclusion

In this paper the different monocular and binocular depth cues have been investigated. Visual displays and techniques have been discussed with special emphasis on stereoscopic displays. The discussion has established that stereopsis is a powerful depth cue, and by employing 3D stereoscopic display techniques the perception of the displayed data will be enhanced in many instances. Part 2 will review 3D stereoscopic display techniques in the context of how hydrographic data is presented currently. Part 2 will also investigate hydrographic datasets available with a discussion on the suitability, opportunities and benefits of including stereoscopic depth cues when presenting hydrographic data.

The concluding part will be published in The Hydrographic Journal No. 114, October 2004.

REFERENCES

Barfield, W., Rosenberg, C. (1995). Judgements of Azimuth and Elevation as a Function of Monoscopic and Binocular Depth Cues Using a Perspective Display. Human Factors 37(1), (pp.173-181).

Berbaum, K., Tharp, D., Mroczek, K. (1983). Depth Perception of Surfaces in Pictures: Looking for conventions of depiction in Pandora's box. Perception, 12, (pp. 5-20)

Bemis, S. V., Leeds, J. L., Winer, E. A. (1988). Operator Performance as a Function of Type of Display: Conventional versus Perspective. Human Factors, 30(2), (pp. 163-169).

Brassard, L. (1998). The Perception of the Image World. PhD Thesis at Simon Fraser University, BC, Canada. World Wide Web page accessed 23 July 2002. http://www.ense.sfu.ca/people/grad/brassard/personal/THESIS

Brown, J. L. (1965). The Structure of the Visual System. In C. H. Graham (Ed.), Vision and Visual Perception. (pp. 39-59). John Wiley & Sons (New York).

Carr, H. A. (1935). An Introduction to Space Perception. Longmans, Green, (New York).

Clark, M., Jackson, P.L., Cohen, H.H. (1996). Understanding the Role of Depth Perception in Slip, Trip and Fall Incidents. Ergonomics in Design, July, (pp.16-21).

Coren, S., Ward, L.M., Enns, J.T. (1993). Sensation and Perception. 4th Ed. Harcourt Brace & Company (Orlando, Fl.).

Diner, D. B., Fender, D. H. (1993). Human Engineering in Stereoscopic Viewing Devices. Plenum Press (New York).

Ellis, S. R., McGreevy, M. W., Hitchcock, R.J. (1987). Perspective Traffic Display Format and Airline Pilot Traffic Avoidance. Human Factors 29(4), (pp. 371-382).

Ellis, S. R. (2000). On the design of Perspective Displays. Proceedings, IEA 2000/HFES2000 44th Ann. Meeting Human Factors & Ergonomics Society.

Graham, C.H. (1965). Visual Space Perception. In C.H Graham (Ed.), Vision and Visual Perception (pp. 504-547). John Wiley & Sons (New York).

Hershenson, M. (1999). Visual Space Perception. MIT Press (Cambridge, MA).

Hochberg, J. E. (1978). Perception (2nd ed.). Prentice Hall (New Jersey).

Howard, I.P. (1993). Spatial Vision within Egocentric and Exocentric Frames of Reference. In R. Ellis, M. Kaiser, J. Grunwald (Eds.), Pictorial Communication in Virtual and Real Environments. (2nd ed.). (pp. 338-358), Taylor & Francis (London).

Kantowitz, B.H. & Sorkin R.D. (1983). Human Factors: Understanding People-Systems Relationships. John Wiley & Sons (New York).

Kim, W. S., Ellis, S. R., Tyler, M.E., Hannaford, B., Stark, L.W. (1987). Quantitative Evaluation of Perspective and Stereoscopic Displays in Three-Axis Tracking Tasks. IEEE Transaction on System, Man and Cybernetics, 17(1), (pp. 61-71).

Kim, W. S., Tendick, F., Stark, L. (1993). Visual Enhancements in Pick-and-Place Tasks: Human operators controlling a simulated cylindrical manipulator. In R. Ellis, M. Kaiser, J. Grunwald (Eds.), Pictorial Communication in Virtual and Real Environments. (2nd ed.). (pp. 265-282). Taylor & Francis (London).

McLean, G. F., Prescott, B., Podhorodeski, R. (1994). Teleoperated System Performance Evaluation. IEEE Transaction on System, Man and Cybernetics, 24(5), (pp. 796-803).

Nemire, K., Jacoby, R.H., Ellis S. R. (1994). Simulation Fidelity of a Virtual Environment Display. Human Factors, 36(1), (pp. 79-93).

Patterson, R., Martin, L. (1992). Human Stereopsis. Human Factors, 34 (6), (pp. 669.692).

Patterson, R., Moe, L., Hewitt, T. (1992). Factors that Affect Depth Perception in Stereoscopic Displays. Human Factors 34(6), (pp. 655-668).

Prevett, T. T., Wickens, C. D. (1994). Perspective Displays and Frame of Reference: Their independence to realize performance advantages over planar displays in terminal area navigation task. (ARL-94-5/NASA-94-3). University of Illinois, Aviation Research Laboratory.

Ramachandran, V.S. (1988). Perceiving Shape from Shading. Scientific American, 259, (pp76-83).

Stoper, A. E., Cohen, M. M (1993). Optical, Gravitational and kinaesthetic determinants of judged eye level. In R. Ellis, M. Kaiser, J. Grunwald (Eds.), Pictorial Communication in Virtual and Real Environments. (2nd ed.). (pp. 390-403). Taylor & Francis (London).

Wickens C.D. (1992). Engineering Psychology and Human Performance (2nd ed.). Harper Collins Publisher (New York).

Wickens, C. D., Merwin, D. H., Lin, E. L. (1994, a). Implication of Graphics Enhancements for the Visualization of Scientific Data: Dimensional Integrity, Stereopsis, Motion and Mesh. Human Factors, 36(1), (pp. 44-61).

Wickens, C. D., Liang, C., Prevett, T., Olmos, O. (1994, b). Egocentric and Exocentric Displays for Terminal Area Navigation. Proceedings of the Human Factors and Ergonomics Society 38th Annual Meeting.

Yeh, Y. (1992). Spatial Judgement with Monoscopic and Stereoscopic Presentation of Perspective Displays. Human Factors, 34(5), (pp. 583-600).

VISUALISATION TECHNIQUES: AN OVERVIEW – PART 2

Runar Ostnes*, Victor Abbott and Samantha Lavender

School of Earth, Ocean and Environmental Sciences, University of Plymouth, UK

* Lecturer at Aalesund University College, Norway, and PhD student at UoP

Abstract

Three dimensional (3D) effects and depth perception in a display system can be achieved in a number of different ways, which were discussed in Part 1 of this paper. The simplest method is to apply one or more monocular depth cues, but to establish stereoscopic effects, and further enhance depth perception; a binocular depth cue has to be applied. The left and right eye images of a stereo pair have to be channelled to the respective eyes with the exception of the chromo stereoscopic technique (only needs one colour-coded image to establish the stereoscopic effect).

This paper describes the most accepted 3D stereoscopic display techniques presently available and summarises how hydrographic data is currently presented. It then discusses the suitability, opportunities and benefits of implementing stereoscopic techniques when presenting hydrographic data. Concluding that with relatively simple means, stereoscopic techniques can be implemented in the software tools presently available and used to improve hydrographic data visualisations.

Introduction to 3D Stereoscopic Display Techniques

A large number of techniques have been developed over the years; they can generally be classified as stereoscopic and auto-stereoscopic techniques. The major distinction between stereoscopic and auto-stereoscopic display techniques is that the former requires the observer to use some form of viewing aid whereas the latter provides free viewing.

The advancement in stereoscopic display technology continues as a result of increased computer power and display technology that have evolved by orders of magnitude over the last decades. The latest stereoscopic display techniques include virtual retinal displays that project the stereo pair directly onto the eyes' retinas and the latest auto stereoscopic techniques include electro holography and complete virtual environments with immersive large format environments like the CAVE Automatic Virtual Environment (National Center for Supercomputing Applications, 2004).

Stereoscopic Display Techniques (Aided Viewing)

While viewing stereoscopic displays the observer normally wears glasses that may have near complimentary colour filtered lenses, polarised lenses or lenses that occlude one eye sequentially in order to channel each of the images in the stereo pair to their respective eyes. Figure 7 gives an overview of the aided viewing stereoscopic techniques described in this section.

Colour multiplexed (Anaglyph)

Colour multiplexing or anaglyph is perhaps the most familiar stereoscopic technique. The technique is widely used to display stereoscopic images in books, movies and on the Internet. The anaglyph consists of a stereo pair with near complimentary colours, red and green or red and blue are the most commonly used. The two images in the stereo pair are transparent and the observer views the stereoscopic image through a pair of near complimentary filters corresponding to the colours used in the stereo image. Each filter will exclude the corresponding image in the stereo pair and in that way give the required separation of the left and right image for stereoscopic viewing (Diner and Fender, 1993).

The advantages of this method are that it is inexpensive to implement, can accommodate multiple observers and the stereo image will be of the same resolution as the display. Translation of the anaglyph onto hard copy (e.g. paper) is also an uncomplicated process. Generally the method has been limited to monochrome (black and white) images; however recent developments have shown that a limited colour rendition in the stereo image is possible (Wei et al, 1998).

Colour rivalry occurs under some instances when an illuminated area of one colour presented to one eye appears to rival a similar area of another colour presented to the other eye. Colour rivalry limits the application of the anaglyph method as the viewer
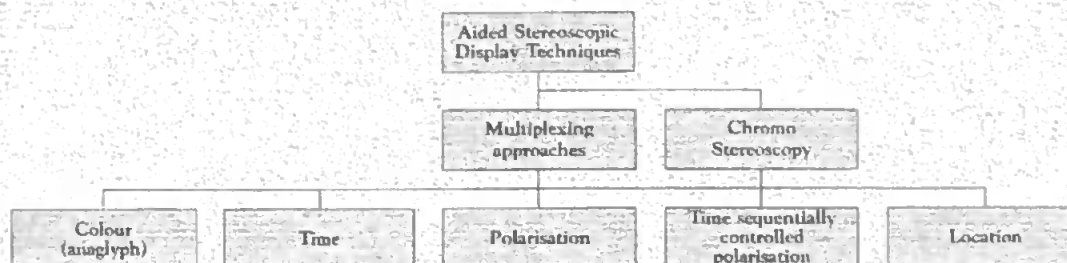

Figure 7: Block diagram describing stereoscopic display techniques.

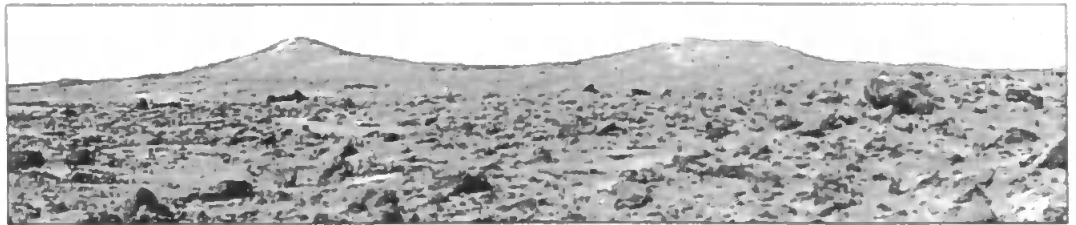Visualisation Techniques: An Overview – Part 2

Figure 8: A typical anaglyph of the Terrain on Mars, where the near complementary images are merged (Source: National Aeronautics and Space Administration, NASA)

will experience unpleasant after effects such as headaches and nausea from wearing the anaglyph filters. Stereo crosstalk is a significant problem; this occurs when the image meant for one eye is faintly visible to the other eye. The image becomes blurred as a phenomenon called ghosting is created. Crosstalk can create difficulty in fusing the two images together. Viewed without the colour coated glasses, the image will appear blurred and interpretation is impeded.

Polarisation multiplexed
In order to separate the left and right image this method applies linear or circular polarisation techniques. Polarisation glasses are used in combination with orthogonally polarised images presented on two displays. In the two-display set-up, the displays are covered with orthogonal polarisation filters and arranged at a 90 degrees angle (Figure 9). A beam splitter (semi reflector) is used to channel the left and right images to the observer. The observer wears appropriately polarisation glasses to separate the images. This stereoscopic technique is still widely in use, however the hardware requirement makes the technique more expensive compared to comparable techniques (Lipton, 1997). An alternative method of combining the stereo images is to interlace the images on the display by row or column; only requires a single display. Cross polarisation of alternating areas of the display will separate the images. For the multiplexing techniques, the observer can view the stereo image at full colour and full resolution, the technology is becoming fairly inexpensive and the technique can have multiple viewers (each with their own headset). The multiplexing methods are also compatible with non-stereoscopic presentations. Polarisation multiplexing has the disadvantages that the efficiency or transmission is poor; the intensity of the light emitted from the display is low (with a light intensity loss of up to 70% the image will appear dark); the interlacing techniques will reduce the resolution by 50%. To maintain an acceptable, flicker free presentation, the frame rate should not decrease below 120Hz (Macdonald and Lowe, 1997).
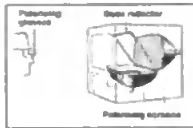

Figure 9: A two-display polarisation multiplexed arrangement (Petrie, 2001)

Time multiplexed
By displaying the left and right eye images alternately at high speed (50-60Hz/image) on a single display it is possible to obtain a stereoscopic effect. The observer must wear electro-optical shutters (Figure 10), one for each eye, which are synchronised with the alternating images on the display. When the left eye image is displayed, the left eye shutter is open allowing the left eye to observe the image; the right eye shutter is closed.

It is the human visual system's ability to store and merge stereo pairs with a time lag of up to 50ms that makes this technique possible (Hershenson, 1999). To avoid display flicker, the technique requires that the display refresh rate is close to 120Hz for reasonable quality, similar to the requirements of the interlacing polarisation multiplexed method.
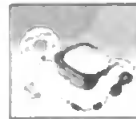

Figure 10: A typical time multiplex stereo kit with shutter glasses, synchronisation cable and software (Source: Stereographics Corporation)

The temporal resolution will be halved, as each eye only perceives the image half the time which can result in a reduction of the display brightness. The relatively heavy glasses may be cumbersome to wear, but more advanced workbench systems such as the Fakespace Immersadesk R2 (Fakespace Labs Inc, 2004) are also available. These systems are portable but the costs of obtaining such systems are high.

Time sequentially controlled polarisation
This method combines both the polarisation and time multiplexing techniques by displaying alternating polarised images to the viewer. The display screen is covered with a Liquid Crystal (LC) layer, which functions as a polariser. The alternating left-eye and right-eye images on the display have

different polarisation patterns (clockwise/anti-clockwise). The observer wearing glasses with appropriate polarisation for each eye is able to separate the left and right image. The key advantage to this method is that the observer only needs simple, inexpensive and lightweight polarising glasses that require no extra synchronisation devices (Pastoor and Wöpking, 1997). The main disadvantage is display flicker and a reduction of display brightness due to halved temporal resolution.

Location multiplexed
In photogrammetry, analytical stereo plotters have been widely used. These instruments are very complex, expensive and require special skills to operate. A more familiar and simple location multiplexed technique is used by the view-master® stereoscope that many children have used as a toy for decades.

Head Mounted Displays (HMD) which are a further development of the location multiplexed technique are increasingly used in Virtual Reality (VR) and stereoscopic visualisation (Figure 11). An HMD consists of a miniature display system (two displays, one in front of each eye) and optics to focus the display at a comfortable distance in front of the eyes.

Figure 11: A typical head mounted display (Source: Wearman)

The HMD can simply be a pair of goggles or a full helmet. The viewer's immediate surroundings are usually occluded by the HMD, giving a feeling of total immersion in the displayed scene. A head-tracking device is included in the system, which

allows the system to respond to head movements, that is particularly important when the observer is immersed in a VR environment where changes in viewing direction will alter the picture displayed (Shibata, 2002). One of the major constraints of HMDs is their limited volume of activity due to cabling and overall weight. The considerable amount of computing power required for the displayed image to be updated in accordance with the head movement may introduce a delay which has a tendency to cause motion sickness in HMDs. 'See-through' HMDs have also been developed, to free the observer from immersion, and are particularly suited for augmented reality applications where the stereoscopic image is merged with the real world. The disadvantage of see-through HMDs is that the background of the displayed image will be diffuse.

Chromo stereoscopy

Eindhoten (1885) found that it is possible to place objects with different colours at different depths when the objects are placed at the same distance (chromo stereopsis). In the early 1990s, researchers found renewed interest in this method for creating a stereoscopic effect from colour-coding images, but the interest then diminished. The principle of chromo stereoscopy is relatively simple. As white light is refracted through a glass prism, it is separated into the colours of the visible spectrum; the different colours have different refraction angles (Figure 12).
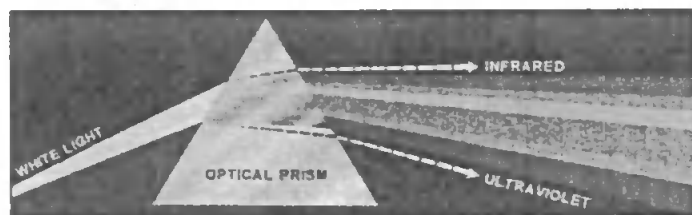

Figure 12, above: White light refracted through a glass prism (Source: Gonzalo and Woods, 2002)

Figure 13 below right: Chromo stereoscopic effect using Chromadepth™ spectacles and an example of a colour-coded image (Source: Toutin, 1997)

A red object has positive chromo stereopsis and will appear closer than a blue object at the same distance. By viewing a colour-coded image with double prism eyeglasses to enhance the chromo stereopsis effect, the required depth perception is achieved (Figure 13). When the observer is wearing single prism glasses the object appears closer to the observer than desired, so double prism glasses has been developed (Toutin, 1997). The main disadvantage is that it is not possible to view the image in its true colours; however, the image is easily translated into different mediums. Chromo Stereoscopy is the only stereoscopic technique where only one image is required for stereoscopic effect; this will increase the readability of the image in non-stereoscopic presentations, increase resolution and decrease the need for extra computer power and advanced display technology.
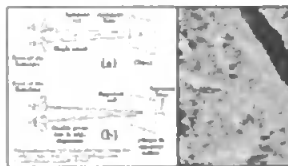
Autostereoscopic Display Techniques (Free Viewing)

As stated earlier, the research and development of different auto stereoscopic techniques are continuing. Figure 14 summarises the more common current techniques in autostereoscopy. Pastoor and Wöpking (1997), Börner (1999) and Okoshi (1976) give more detailed descriptions.

This paper will focus on Lenticular Imaging technique only. The electro holography and volumetric display techniques still represent a major challenge to the research establishments due to the enormous amount of computing power and data transfer rates required. As these techniques are still not widely available outside the research establishments they will not be covered in this text.

Direction multiplexed displays

Direction multiplexed displays are the most common auto stereoscopic displays and are most compatible with computer graphics. The observer directly views the same display area with both eyes. The left eye image is presented only to the left eye and the right eye image is presented only to the right eye. The difference in viewing angle is caused by the separation of the eyes, and vertical bars or lenses are built into the display, permitting or blocking certain parts of the underlying display from view.

Several techniques based on the physical principles of diffraction, refraction, reflection and occlusion have been developed (Pastoor and Wöpking, 1997). The most established refraction based method is lenticular imaging. An array of long narrow lenses (lenticules) is built into the display screen (Figure 15), where each lens focuses on the image information located behind it and directs the light in different directions (Börner, 1999). In order to view the stereo image, the observer must be placed in particular locations relative to the display (stereo zones), if not the stereo image may be blurred or the stereoscopic effect may be lost. However, certain lens arrays will allow more than one observer to view the stereo image. The main disadvantages of this technique are that the display resolution is effectively halved and interpretation of the image without the lenticular plate is inhibited.
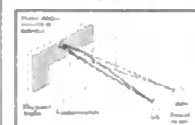

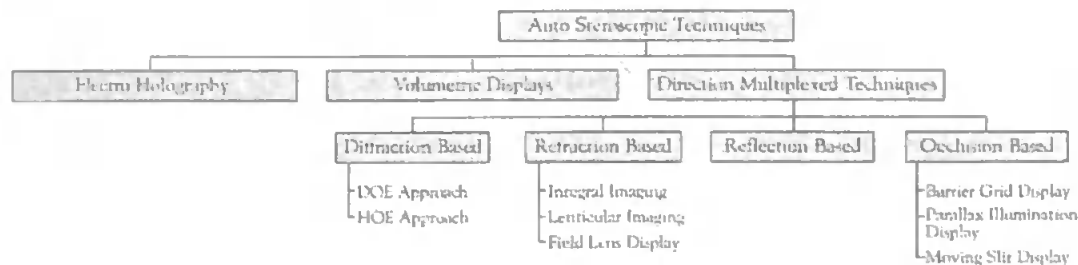*Figure 15: Principle of the lenticular imaging technique (Source: Börner, 1999)*

Figure 14. Block diagram summarising current autostereoscopic techniques

Visualisation Techniques: An Overview – Part 2

Discussion on 3D Stereoscopic Display Techniques

The majority of auto stereoscopic techniques are still at a developmental stage; they are expensive and require a vast amount of computer power to produce a 3D image (Javidi and Okano, 2002). The lenticular imaging technique is currently the most accessible, but does have limitations. However the great advantage of free viewing (especially in operational applications) will probably make these techniques particularly interesting when further developed.

The aided viewing techniques are more established, and to some extent, employed in the fields of scientific visualisation such as medical imaging, photogrammetry and geological imaging in the petroleum exploration industry. It is mainly the polarisation and time multiplexing techniques that are presently employed (Macdonald and Lowe, 1997). The major disadvantages will improve as display technology and computing power develops, making these techniques suitable for scientific visualisation. The further development of HMDs will also gain from increased computer power and display technology, eliminating most of the present disadvantages. Over time the techniques will also become less expensive and thereby more available. Despite its simplicity and economical advantage, the disadvantages of the anaglyph technique, make it less probable as a future contender (Javidi and Okano, 2002).

The chromo stereoscopic technique has several advantages, but except for Toutin's application to remote sensing data, it has not been possible to find examples where this technique has been applied. The easy translation into different mediums, requirement for only one image, inexpensive glasses, no loss in resolution and no need for extra computer power are all desirable qualities, especially in a semi-operational environment such as hydrography. The major disadvantage of a non-realistic colour scheme can be overcome by present display technology, simply by switching between 3D model textures with natural colours and with a chromo stereoscopic colour scheme.

Presentation of Digital Hydrographic Data

As described in the first part of this paper, depth perception increases with an increasing number of visual depth cues. The effect of the binocular depth cues is powerful and beneficial to include in the presentation of spatial data to increase the comprehension of the dataset. This is especially true when displaying complex datasets with a number of spatially interrelated objects. Despite the large number of stereoscopic techniques available, surprisingly few are employed in scientific visualisation today. However

some scientific applications (such as the petroleum exploration industry and complex mechanical engineering) are starting to include these techniques (Hearn and Baker, 1997). Multiplexing techniques, and to an increasing degree, advanced virtual reality techniques dominate the presentations. The following sections review how digital hydrographic data is currently presented and investigate how application stereoscopic techniques are to this data. The focus is on digital hydrographic data that are 3D in nature, in essence data that is volumetric in nature, or where position is determined in a volumetric model.

In general, hydrographic data is presented as 2D images with few or no visual depth cues, or as 3D perspective models including several of the monocular visual cues to increase depth perception. One software developer with a base in an academic establishment specialising in hydrography has developed 3D presentations where stereoscopic display techniques are available (Interactive Visualization Systems, 2004). However the stereoscopic display techniques are limited to anaglyphs and time polarising multiplexing.

The International Hydrographic Organisation (IHO) defines hydrography as (IHO, 1994):

The branch of applied science which deals with the measurement and description of the physical features of the navigable portion of the Earth's surface and the adjoining coastal areas, with special reference to their use for the purpose of navigation.'

In compliance with this definition, the data investigated will be limited to the volume between the water surface and the seabed with special reference to navigation.

Sonar sensor data

Sonar (SOund Navigation And Ranging) was used for the first time in 1912, and technological development has brought enormous improvement in transducer and signal processing technology (Kjerstad, 2002). In active sonar systems the returned acoustic signal determines the range from the transducer to the detected object, and the object location in the sonar beam can be determined together with the objects relative location, shape and size. The main objective of a bathymetric survey is to produce a terrain model or relief of the seabed, which can be accomplished by correlating a position (x, y) and depth (z) measurement in a regular grid, or a Triangulated Irregular Network (TIN) giving x, y, z coordinate sets (Brouns et al, 2001). Until the early 1980s hydrographic originals (Figure 16) were edited and hand drawn by hydrographers from echograms, and the depth contours were extrapolated from the dataset.
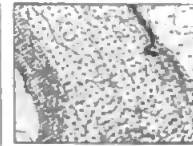

Figure 16: Hand drawn hydrographic original in scale 1:20000 (Source: Kjerstad, 2002)

Today this process is automated and positional data is merged with depth soundings to create a Digital Terrain Model (DTM) of the seabed. More recently multibeam sounders have improved the hydrographic survey of an area by producing a relatively high resolution DTM in a corridor extending each side of the survey ship's track (Kjerstad, 2002).

The traditional way of presenting the seabed and its features in an operational nautical context is in 2D on a paper chart, or electronic chart (digitised or scanned from paper charts). The bathymetric details are presented as spot depth numbers and contour lines. Figure 17 shows a computer display presenting an electronic vector chart. Contour lines and spot depths deeper than the set safety depth are excluded from the presentation to improve the readability of the chart, however areas with depths less than the safety depth are colour-coded (shades of blue in Figure 17). With the underlying DTM, a perspective view of the seabed is easily computed and several commercial software packages are capable of presenting this view of the seabed that gives a better perception of the bathymetric data (Figure 18). By including a perspective model and shading most of the monocular depth cues are included. In order to increase the depth perception further, stereoscopic depth cues can be integrated.

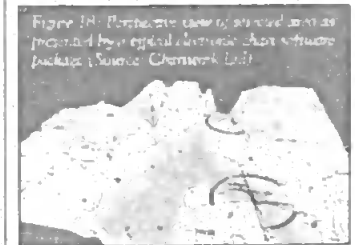Figure 17: Computer display presenting an electronic vector chart (Source: Kongsberg Norcontrol AS)

Figure 18: Perspective view of seabed area as presented by a typical electronic chart software package (Source: Chartwork Ltd)

In the offshore industry and other areas requiring a high-resolution presentation of a smaller area of the seabed with its features, high-resolution multibeam sounders and side scan sonar (SSS) are common acquisition systems. By bringing the SSS close to the seabed, with the sonar beams radiating more horizontally across the seabed, it is also possible to get a side view of the seabed features. This increases the detection of features rising from the seabed and will provide a better classification of the roughness of the seabed as shown in Figure 19. Note that Figure 19 also includes the light and shadow distribution to increase perception.

Figure 19: Typical SSS image (500kHz) of a shipwreck on a 75-metre range collected with a Klein Side Scan Sonar System 3000 (Source: Klein Associates Inc)

Several specialised hydrographic software packages are available and a product survey was presented in *Hydro International* (2002). These software packages are often comprehensive, in that they are used in the planning, collecting, processing and presentation of hydrographic data from multiple sensors.

The most sophisticated software manufacturers provide specialised 3D visualisation tools to improve presentation of data even further. The visualisation tools are capable of generating 3D surface models or 3D contour models presented in perspective view, including depth colour-coding along the z-axis. Virtual desktop environments are available with a perspective model of a DTM and objects such as ROVs, divers, SSS fish and structures are presented in real time. Several of the monocular depth cues listed in the previous part of this paper are included in the presentations; however none of the software packages presently available provide stereoscopic display techniques to further enhance the depth perception. Figure 21 gives an example of a presentation from one of the more sophisticated commercial software packages currently available on the market.

Remote sensing
Stereoscopic display techniques described earlier have been used by other sciences and technologies to enhance the display of digital geo referenced models such as

Figure 20: The QINSy6 hydrographic software package contains a virtual environment manager. This figure displays an extract from a ROV flying over a colour-coded seabed DTM in real time (Source: Quality Positioning Services BV, QPS)

DTMs. Software packages used in remote sensing (Lillesand and Kiefer, 2000) and in photogrammetry (Wolf and Dewitt, 2000) easily generate stereoscopic models from DTMs or stereo images. The main stereoscopic display techniques are anaglyphs or time-polarisation multiplexing.

The remote sensing contribution to hydrography is summarised in Lavender (2001), and this section reviews the different remote sensing systems and techniques available to collect hydrographic data where remote sensing includes systems mounted on airborne or satellite platforms. The systems can be categorised in two main groups, active and passive.

The active systems include radar systems, altimetry and LIDAR (Light Detection And Ranging). Along the platform footprint the radar altimeters are able to measure the sea surface height to a maximum accuracy of approximately 2cm provided an ideal reference ellipsoid is available. Radar altimeter systems collect point measurements; these are interpolated to produce a global map as shown in Figure 21. The small vertical variation over a relatively large area makes the data less suitable for 3D presentations.
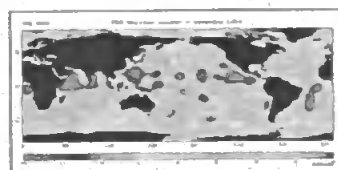

Figure 21: Radar altimeter data from the ERS satellite showing sea surface height anomalies from an average anomaly map on a global scale. The anomalies are colour-coded using the visual spectrum (Source: European Space Agency (ESA) Earthnet Online)

LIDAR systems (mounted on airborne platforms) are able to produce a high resolution bathymetric DTM, but the systems are limited to depths of 50 metres in clear water (de Jong et al, 2002).

Several national hydrographic offices are using this method to collect bathymetric data in shallow and less accessible coastal areas. Sinclair (1999) provides an overview of the capabilities and performance of the Australian LIDAR system, Laser Airborne Depth Sounder (LADS). Figure 22 shows a LIDAR data generated digital bathymetric model, which includes surface rendering with colour-coding along the z-axis.

Figure 22: High accuracy and high-resolution bathymetric model from LIDAR data collected by LADS in Norwegian waters. The model is colour-coded across the visible spectrum (Source: Sinclair, 1999)

The passive remote sensing systems used to collect hydrographic data are optical sensors mainly on airborne platforms; however optical imagery from space borne platforms such as Landsat is also used (Lavender, 2001). To include stereoscopic visual clues to the optical images traditional photogrammetric techniques are used to create 3D stereo models. Digital photogrammetry software packages make it possible to produce DTMs from scanned optical imagery (Wolf and Dewitt, 2000), and to drape orthophotos over DTMs to develop a terrain model that includes the surface details.

Tidal model data
High-resolution tidal models based on mathematical tidal dynamics computations and tidal gauge
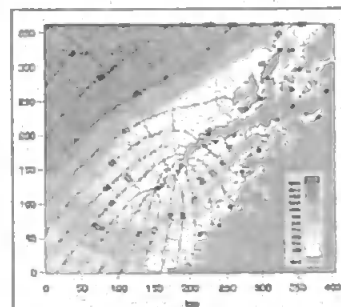

Figure 23: Isolines for amplitude (2cm separation) and phase (2 degrees separation). Tidal stations marked with red dots. Colour shading depicts water depth (Source: Moe et al, 2002)

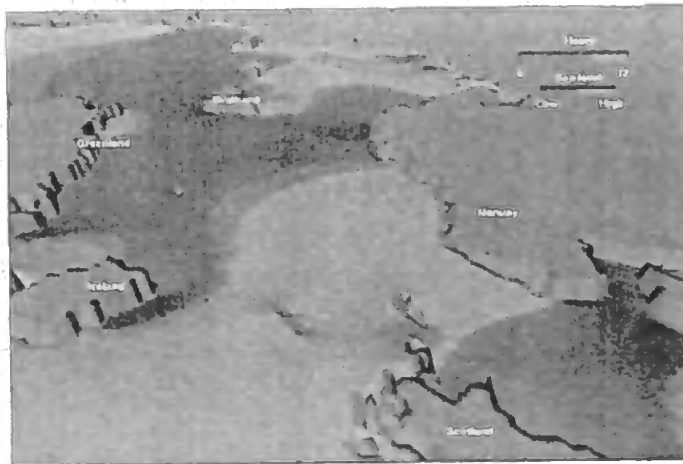Visualisation Techniques: An Overview – Part 2

Figure 14: Animation of the sea level change in the Nordic seas. Light blue colour depicts area of higher elevation (Source: University of Oslo, Department of Mathematics)

observations are available (Moe et al, 2002). Tidal data are traditionally presented in a tabular format and on charts containing bathymetric features overlaid with a grid of isolines connecting spots with equal sea surface elevation (Figure 23).

Today computerised modelling techniques provide for animations of the propagation of tides. Figure 24 shows a snapshot from an animation of sea level changes associated with the M2-tide in the Nordic Seas. The light blue area depicts the areas of high sea level, and during the animation the area changes according to the mathematical model. The tidal height will, in many circumstances, constitute the limiting surface of the hydrographic model, and particularly for local models it can be of value to present it in 3D.

Ocean and tidal current data

Ocean and tidal current data is traditionally presented as 2D vector charts, where each vector represents the local current direction and velocity depicted by the orientation and length of a vector. These presentations are often based on a combination of current measurements from current meters or Acoustic Doppler Current Profiles (ADCP) and mathematical models; with the models being frequently layered (each layer containing a vector chart representing the currents at different depths). Figure 25 shows a presentation of the tidal current in the Drøbak Sound, in the Oslo fjord in southern Norway, which shows the temporal variations of the tidal currents in the Sound. By presenting the current layers at different depths in a model volume in 3D an increased perception of the water movement can be achieved. It is possible to visualise hydro dynamical models of temperature and

salinity variations in a similar fashion. Such a representation could have improved depth perception.
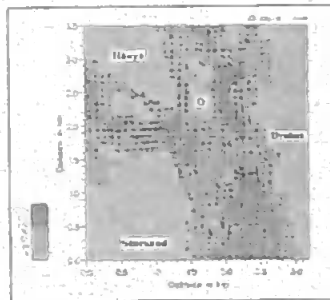

Figure 25: Computer model presentation of tidal currents in the Oslo Fjord. The picture is based on animation that shows the temporal changes of the currents (Source: University of Oslo, Department of Mathematics)

Man-made object data

Sub-surface man-made objects are mainly positioned using hydro acoustic systems, with the object's attitude and movement determined by sensors mounted on the object (e.g. inertial systems, gyro and Doppler log on an ROV) that allows for a dynamic presentation. The size and shape of the object can be known, as is the case of an ROV, or unknown, in the case for an unidentified sonar target.

Visual presentation of man made objects have generally been presented in a 2D Computer Aided Design (CAD) fashion, as a situational display with the altitude of the dynamically positioned object above the seabed terrain numerically displayed. Today, the visual presentation is evolving towards 3D perspective models, and the most advanced software packages include this

form of presentation (Figure 20). An ROV positioned by a Super Short Base Line (SSBL) Hydro-acoustic Positioning Reference (HPR) system, will allow for the objects shape, size attitude and 3D position in the water volume to be included in the visual presentation.

Discussion on Digital Hydrographic Data

This review of hydrographic datasets reveals that the sonar sensor data is suitable for stereoscopic viewing; it is 3D in nature and general availability as computer models (i.e. DTMs). However it is important to have some variations and features in the bathymetry to get the full effect of the stereoscopic techniques. An improved perception can be achieved when this is combined with man made objects in a more complex visualisation. In general the more spatially complex the model is, the greater the benefit of a stereoscopic presentation. Operating vessels in confined waters or an ROV manoeuvring around subsea structures are operational examples where stereoscopic presentation would be valuable. Remote sensing data is in generally less suitable for stereoscopic presentations due to its predominantly 2D nature with exceptions being LIDAR and to some extent radar altimetry of sea surface height. Local tidal model data would, in many cases, constitute one of the limiting surfaces of the model. Displaying ocean and tidal current data at different depths simultaneously would also give better perception of the variations in the dataset.

Conclusion

In the first part of this paper it was established that stereoscopic depth cues can increase the perception of 3D datasets, in particular more complex datasets. In this part the most widely used stereoscopic techniques have been reviewed, and the multiplexing techniques is probably best suited for current hydrographic implementations of stereoscopic depth cues, however the advancement techniques is rapid and will surely introduce alternative methods in the future. The chromo stereoscopic technique is an interesting alternative as colour-coding along the vertical axis is widely used on hydrographic datasets (e.g. bathymetry in Figure 22). By employing the colour-coding scheme along the line of sight axis and enhances by using appropriate eyewear a stereoscopic effect is produced.

When presenting increasingly detailed and complex digital hydrographic datasets, the stereoscopic techniques can supply the viewer with the desired enhanced perception. With relatively simple means stereoscopic techniques can be implemented in the software tools currently available and used to improve hydrographic data visualisations.

papers

Visualisation Techniques: An Overview – Part 2

REFERENCES

Broens, G., de Wulf A. and Constales, D. (2001). Multiscan interprocessing. Adding and deleting vertices in a Delaunay triangulation. *The Hydrographic Journal* No. 101, July 2001. (pp. 3–9).

Borner, R. (1990). Four Autostereoscopic monitors on the level of industrial prototypes. *Displays* 20. (pp. 57–64).

Chunwerk Ltd. World Wide Web Page accessed February 2003; http://www.chunwerk.com/.

de Jong, C.D., Lachapelle, G., Skone, S. and Elema, I. A. (2002). Hydrography. Delft University Press (The Netherlands).

Diner, D. B. and Fender, D. H. (1993). Human Engineering in Stereoscopic Viewing Devices. Plenum Press (New York).

Emsthoven, W. (1885). Stereoscopie durch Farbengrenze. Albrecht von Gaefes Archiv für Ophthalmologie, No. 31. (pp 211–236).

European Space Agency (ESA). Earthnet Online. World Wide Web page accessed March 2003; http://earth.esa.int/.

Fakespace Labs Inc. World Wide Web Pages accessed August 2002; http://www.fakespacelabs.com.

Gonzalez, R. C. and Woods, R. E. (2002). Digital Image Processing. 2nd Ed. Prentice Hall Inc (New Jersey).

Hearn, D. and Baker, M. P. (1997). Computer Graphics, C Version. 2nd Ed. Prentice Hall (New Jersey).

Hershenson, M. (1999). Visual Space Perception. MIT Press (Cambridge, MA).

Hydro International. (2002). Product Survey: Hydrographic Navigation Software. Hydro International. November 2002, Vol. 6 (9). (pp. 39–41).

IHO (1994). Hydrographic Dictionary Part I Volume I, English. Special Publication No. 32 (5th Ed), IHO (Monaco).

Interactive Visualisation Systems (2004). World Wide Web Page accessed June 2004; http://www.ivs.unb.ca/products/fledermaus/index.html.

Javidi, B. and Okano, F. (2002). Three-Dimensional Television, Video and Display Technologies. Springer Verlag (Berlin).

Kjersaal, N (2002). Elektronisk og Akustiske Navigasjonsystemer for Maritime Studier. Tapir Akademiske Forlag (Trondheim, Norway).

Klein Associates Inc. World Wide Web page accessed February 2003; http://www.kleinsonar.com/sonar/3000/gloreck2.html.

Kongsberg Norcontrol AS (2002). Sea Map 10 ECDIS Operators Manual. KMSS CN-JZ7o GA9-Jan02.

Lavender, S. (2001). The Application of Remote Sensing to Hydrography. *The Hydrographic Journal*, No. 99, January 2001. (pp. 9–13).

Lillesand, T.M. and Kiefer, R.W. (2000). Remote Sensing and Image Interpretation. 4th Ed. John Wiley & Sons (New York).

Lipton, L. (1997). Stereo-Vision Formats for Video and Computer Graphics. *Proceedings of SPIE*, Volume 3012, Stereoscopic Displays and Virtual Reality Systems IV.

MacDonald, L.W. and Lowe, A.C. (1997). Display Systems, Design and Applications. John Wiley & Sons (New York).

Moe, H., Ommundsen, A. and Gjevik, B. (2002). A High-resolution Tidal Model for the Area around The Lofoten Islands, Northern Norway. *Continental Shelf Research* 22, (2002) (pp. 485–504).

National Aeronautics and Space Administration (NASA). World Wide Web page accessed in August 2002: http://mars.jpl.nasa.gov/MPF/ops/TwinPeaks_glyph_md.gif

National Center for Supercomputing Applications (NCSA) World Wide Web page accessed June 2004. http://cave.ncsa.uiuc.edu/index.html

Okoshi, T. (1976). Three-Dimensional Imaging Techniques. Academic Press Inc. (New York).

Ostnes, R., Abbott, V. and Lavender, S. (2004). Visualisation Techniques: An Overview – Part 1. *The Hydrographic Journal*, No. 113, July 2004.

Pastoor, S. and Wöpking, M. (1997). 3-D Displays: A review of Current Technologies. *Displays*, 17 (1997), (pp. 100–110).

Petrie, G. (2001). 3D Stereo-Viewing of Digital Imagery. Is Auto-Stereoscopy the Future for 3D Display in Geoinformatics. December 2001. (pp. 24–29).

Quality Positioning Services BV (QPS) (2003). QINSy A hydrographic Software Package brochure. Available in the World Wide Web page: http://www.qps.nl/Eng/Pages/QINSy.htm.

Shibata, T. (2002). Head Mounted Display Displays, 23 (2002), (pp. 57–64).

Sinclair, M. (1999). Laser Hydrography Commercial Survey Operations. Paper presented at the US Hydro 1999, Mobile, Alabama April 27–29.

Stereographics Corporation. World Wide Web page accessed in August 2002: http://www.stereographics.com/index.htm.

Trottin, T. (1997). Qualitative Aspects of Chromo Stereoscopy for Depth Perception. *Photogrammetric Engineering & Remote Sensing* (PE&RS), Vol. 63, No. 2, (pp 193–203).

University of Oslo, Department of Mathematics. World Wide Web page accessed March 2003; http://math.www.uio.no/~hjoungst/decannson/delfer/ademod.html.

Wahl, T. (1998). Integrated Use of Radar Satellites for Fisheries Enforcement Operations. Proceedings of 27th International Symposium of Remote Sensing, (pp. 123–126), Tromsø, Norway.

Wei, S. K., Huang, Y. F. and Klette, R. (1998). Colour Anaglyphs for Panorama Visualizations. Technical Report, CITR-TR-19, Computer Science Department of the University of Auckland (New Zealand).

Wearcam, University of Toronto, Department of Electrical Engineering. World Wide Web page accessed August 2002: http://wearcam.org/head-mounted-displays.html.

Wolf, P.R. and Dewitt, B. A. (2000). Elements of photogrammetry with applications in GIS. 3rd Ed, McGraw Hill (Boston, MA).

biographies

Runar Ostnes works as a lecturer in Nautical Science at Aalesund University College in Norway, and is also a PhD Student at the University of Plymouth in the UK. He has a Masters of Science degree in Nautical Science from the Norwegian University of Science and Technology and a Masters of Science degree in Defence Geographic Information from Cranfield University. During his career he has worked both as a Navigator in the Royal Norwegian Air Force and later as the Military Geographer of the Air Force He has also worked as a Hydrographic Surveyor in the North Sea.

Victor Abbott spent eleven years surveying and has lectured at the University of Plymouth since 1989. He has undertaken various activities for The Hydrographic Society (currently joint-organiser of Hydro4), the RICS (Surveying Courses Board) and IMarEST (currently Chairman of the local Branch). Victor manages the University's postgraduate surveying degrees and is supervising two PhDs. Recent research work includes correlation of remote sensing and swathe bathymetry in Morecambe Bay, UK, and the provision of precise heights along a redundant (possibly to be refurbished) canal route.

Samantha Lavender is a Senior Lecturer in Geomatics at the University of Plymouth and has over 9 years of postgraduate research experience and co-ordinates the multidisciplinary Geomatics Research Group (including coastal zone management, hydrography, geodesy, GIS, GPS, meteorology, navigation and remote sensing). Her research includes: the application of Earth Observation (EO) data to climate change and biological variability as part of the Atlantic Meridional Transect cruise programme and Centre for observation of Air-Sea Interactions and fluXes (CASIX); and the integration and application of modern technology within coastal zone management, including operational applications of EO data. She is a member of several societies, co-ordinates the RSPSoc special interest groups and sits on international satellite/grant peer review committees.

Appendix 2

OpenGL, GLU and GLUT implementation to Microsoft Windows XP and Visual C++ . NET

Text and files downloaded from:
http://www.css.tayloru.edu/~btoll/resources/graphics/opengl/xp/visualc.html

If you are compiling from the CSS labs, the library, dll, and header files are installed properly.

To create a Visual C++ project for an OpenGL program using the GLUT or GLUI toolkits:

1. Select "New" from the "File" menu
2. Select "Win32 Console Application" and give your project a name/location
3. Select "Empty Project"
4. Add the source code for the application to the "Source Files" section of the project

The necessary .lib, .dll, and .h files are available below. The suggested installation locations are valid for a default installation of Visual C (VC6). All files are installed correctly on the CSS lab machines. If you wish to compile on your own machine, only the glut and glui files need to be copied as outlined below. If you wish to compile only glut applications, the glui files are not needed. If you wish to compile glui applications, the glut files are needed as glui is based on glut.

HEADER FILES

glut.h installed in ..\Microsoft Visual Studio\VC98\Include\Gl

glui.h installed in ..\Microsoft Visual Studio\VC98\Include\Gl

The following files should already exist in the proper location:

glu.h installed in ..\Microsoft Visual Studio\VC98\Include\Gl

gl.h installed in ..\Microsoft Visual Studio\VC98\Include\Gl

glaux.h installed in ..\Microsoft Visual Studio\VC98\Include\Gl

LIBRARY FILES

glut32.lib installed in ..\Microsoft Visual Studio\VC98\Lib

glui32.lib (VC6) installed in ..\Microsoft Visual Studio\VC98\Lib

glui32.lib (VC7) - VisualStudio.Net

Zip file of complete GLUI project for VisualStudio.Net

The following files should already exist in the proper location:

glu32.lib installed in ..\Microsoft Visual Studio\VC98\Lib

glaux.lib installed in ..\Microsoft Visual Studio\VC98\Lib

Opengl32.lib installed in ..\Microsoft Visual Studio\VC98\Lib

DLL FILES

glut32.dll installed in C:\WINDOWS\system32

There is no glui dll file.

The following files should already exist in the proper location:

glu32.dll installed in C:\WINDOWS\system32

Opengl32.dll installed in C:\WINDOWS\system32

NOTE:

In order to make your application link properly, the following modification needs to be made to your project.

1. Select "Settings..." from the "Project" menu
2. Select the "Link" tab
3. Scroll to the end of the "Object/library models:" text box and add the following additional libraries: glu32.lib glut32.lib opengl32.lib glaux.lib glui32.lib

Your program should now find all the code it needs from the libraries included in the settings, and remain portable to the UNIX environment.

Visual Studio .Net

Zip file of complete GLUI project for VisualStudio.Net

Appendix 3

3ds Import library with documentation

L3DS documentation.

This is a L3DS documentation. It can only be distributed as a part of L3DS package, which includes the library itself(source code), this documentation and example programs.

Reference.

Introduction, basic usage
Simple data types, structures and enumerations
LMaterial class reference
LLight class reference
LMesh class reference
L3DS class reference

What is L3DS and how to use it?

L3DS is a set of classes that implement a loader for .3ds files. The classes are quite easy to use and have no external dependencies. Basic usage:
To use the library you have to include the file l3ds.h and add the file l3ds.cpp in your project.
This piece of code shows the basic functionality:

L3DS loader;

loader.LoadFile("scene.3ds);
Now the file is loaded and you can access the data:

printf("Number of meshes in the file %u\n", loader.GetMeshCount());
printf("Number of lights in the file %u\n", loader.GetLightCount());
printf("Number of materials in the file %u\n", loader.GetMaterialCount());

To access the mesh, light or material data, there are 3 classes: LMesh, LLight and LMaterial.

In addition to the normals, also tangents and binormals are computed, they can be used for tangent space lighting.

Known problems.

There are some known problems with the 3ds loader:
Normals are not computed correctly of there are triangles that are assigned to more than 1 smoothing group
Some meshes may be placed incorrectly.
Depending on the mesh, tangents and binormals are either useable or not. There's nothing I can do about it.

Simple data types and structures

This file describes simple data types and basic structures that are used by l3ds.

enum LShading {sWireframe, sFlat, sGouraud, sPhong, sMetal};

This is an enumerate for shading types of a material.

```
struct LVector4
{
    float x;
    float y;
    float z;
    float w;
};
```

```
struct LVector3
{
    float x;
    float y;
    float z;
};
```

```
struct LVector2
{
    float x;
    float y;
};
```

```
struct LColor3
{
    float r;
    float g;
    float b;
};
```

This structures defines a 4 component vector(used for vertices), 3 component vector(used for normals), 2 component vector(used for texture coordinates) and a 3 component RGB colour

```
struct LTriangle
{
    unsigned short a;
    unsigned short b;
    unsigned short c;
};
```

This is a triangle, a, b and c are the indices of the actual vertices, normals etc. in the corresponding arrays.

```
struct LTriangle2
{
```

```
    LVector4 vertices[3];
    LVector3 vertexNormals[3];
    LVector2 textureCoords[3];
    LVector3 faceNormal;
    uint materialId;
};
```

This is another triangle structure. The difference to LTriangle is that LTriangle2 provides vertices, normals and texture coordinates directly, and not as indices in an array. faceNormal is a triangle normal which could be used for flat shading. materialId is a number of a material used for this face.

```
struct LMap
{
    float strength;
    char mapName[255];
    float uScale;
    float vScale;
    float uOffset;
    float vOffset;
};
```

This is a structure that represents a "map". Maps are a part of a material. A material has a diffuse map, a specular map etc.
Here's a description of members:

strength - the opacity of the map, it is 1 for opaque maps and 0 for completely translucent maps.
mapName - this is a name of texture file that should be used with the map.
uScale, vScale - the scaling factors of the texture coordinates.
uOffset, vOffset - the translation of the texture coordinates.

LMaterial reference

const std::string& GetName()
This method returns the name of the material.

uint GetID()
This method returns the material ID associated with the material.

LMap& GetTextureMap1()
This method returns a reference to the first texture map.

LMap& GetTextureMap1()
This method returns a reference to the second texture map.

LMap& GetOpacityMap()
This method returns the reference to the opacity map.

LMap& GetSpecularMap()
This method returns the reference to the specular map.

LMap& GetBumpMap()
This method returns the reference to the bump map.

LMap& GetReflectionMap()
This method returns the reference to the reflection map.

LColor3 GetAmbientColor()
GetAmbientColor returns the ambient colour of the material.

LColor3 GetDiffuseColor()
This method returns the diffuse colour of the material.

LColor3 GetSpecularColor()
This method returns the specular colour of the material.

float GetShininess()
This method returns the shininess of the material.

float GetTransparency()
This method returns the transparency of the material, ranging from 1(transparent) to 0(opaque)

LShading GetShadingType()
This method returns the shading type of the material.

LLight reference.

const std::string& GetName()
This method returns the name of the light.

LVector3 GetPosition()
Returns the position of the light source.

LColor3 GetColor()
Returns the colour of the light source.

bool GetSpotlight()
This method returns true if the light is a spotlight and false if a light is a point light.

LVector3 GetTarget()
Returns the position of the target of the spotlight, only makes sense if GetSpotlight returned true.

float GetHotspot()
This method returns the hotspot value.

float GetFalloff()
This method returns the falloff value.

LMesh reference.

const std::string& GetName()

This method returns the name of the mesh.

uint GetVertexCount()
This method returns the number of vertices in the mesh. This is also the number of normals, texture coordinates, tangents and binormals.

uint GetTriangleCount()
This method returns the number of triangles in the mesh.

const LVector4& GetVertex(uint index)
This method returns the reference to the vertex with a given index. Index must be smaller than a value returned by GetVertexCount.

const LVector3& GetNormal(uint index)
This method returns the reference to the normal with a given index. Index must be smaller than a value returned by GetVertexCount.

const LVector2& GetUV(uint index)
This method returns the reference to the texture coordinates with a given index. Index must be smaller than a value returned by GetVertexCount.

const LVector3& GetTangent(uint index)
This method returns the reference to the tangent with a given index. Index must be smaller than a value returned by GetVertexCount.

const LVector3& GetBinormal(uint index)
This method returns the reference to the binormal with a given index. Index must be smaller than a value returned by GetVertexCount.

const LTriangle& GetTriangle(uint index)
This method returns the reference to the triangle with a given index, index must be smaller than a value returned by GetTriangleCount.

LTriangle2 GetTriangle2(uint index)
This method returns a triangle with a given index, index must be smaller than a value returned by GetTriangleCount.

uint GetMaterialCount()
This method returns the number of materials that are assigned to the mesh.

uint GetMaterial(uint index)
This method returns the material ID of the material with a given index, index must be smaller than a value returned by GetMaterialCount.

L3DS reference

bool LoadFile(const std::string &ampfilename)
This method loads a 3ds file. Call it before you call any other method.

uint GetMeshCount()
This method returns the number of meshes in the loaded 3ds file.

uint GetLightCount()

This method returns the number of lights in the 3ds file.

uint GetMaterialCount()
This method returns the number of materials in the 3ds file.

LMesh& GetMesh(uint index)
This method returns the reference to the mesh with a given index, index must be smaller than a value returned by GetMeshCount.

LLight& GetLight(uint index)
This method returns the reference to the light with a given index, index must be smaller than a value returned by GetLightCount.

LMaterial& GetMaterial(uint index)
This method returns the material with a given index, index must be smaller than a value returned by GetMaterialCount.

Appendix 4

Header files used in the CS application

stdafx.h – This header file is used to build a precompiled header file as an include file for standard system include files and for project-specific include files that are used frequently but are changed infrequently.

l3ds.h – This header file is used to implement the 3ds file import library.

windows.h – The Windows.h header file is the one essential include file required in all Windows source code. The reason for this is simple: Windows.h contains all of the definitions for Windows messages, constants, flag values, data structures, macros, and other mnemonics that permit the programmer to work without having to memorize thousands of hexadecimal values and their functions.

The #ifdef _WIN32 and #endif specifies that the windows header file shall be included if the Windows 32 bit API is used.

GL/glut.h – This is the header file for the GL utility toolkit (GLUT).

stdlib.h – This header file was developed as a file to declare certain standard library functions. These include the memory management functions, communication with the environment and others.

stdio.h – This is the header file for the standard Input/Output devices such as keyboard, mouse and display. The file contains the prototypes and macros needed to use the I/O library.

math.h – This is the header file for the Windows Math library, it defines math subroutines and constants for floating point arithmetic.